ORNL/TM-2017/146
IEA HPT Annex 41

IEA HPT Annex 41 – Cold Climate Heat Pumps: US Country Report

Van Baxter
Eckhard Groll

August 2017

OAK RIDGE NATIONAL LABORATORY
MANAGED BY UT-BATTELLE FOR THE US DEPARTMENT OF ENERGY

ORNL/TM-2017/146
IEA HPT Annex 41

Building Technologies Program
Energy and Transportation Science Division

IEA HPT ANNEX 41 – COLD CLIMATE HEAT PUMPS: US Country Report

Van Baxter, Oak Ridge National Laboratory
Eckhard Groll, Purdue University
Co Operating Agents

Date Published: August 2017

Prepared by
OAK RIDGE NATIONAL LABORATORY
Oak Ridge, Tennessee 37831-6283
managed by
UT-BATTELLE, LLC
for the
US DEPARTMENT OF ENERGY
under contract DE-AC05-00OR22725

U.S. Team Final Country Report

IEA HPT 41
"Cold Climate Heat Pumps"

Submitted by:

Ray Herrick Laboratories, Purdue University
Lead: Eckhard A. Groll (contact: groll@purdue.edu)
Contributors: Christian K. Bach (contact: cbach@okstate.edu)
Stephen L. Caskey (contact: scaskey@purdue.edu)
Alejandro C. Lavernia (contact: alaverni@purdue.edu)
Nicholas Salts (contact: nsalts@purdue.edu)

Oak Ridge National Laboratory
Lead: Van Baxter (contact: vdb@ornl.gov)
Contributors: Bo Shen
Omar Abdelaziz
C. Keith Rice
Gerald Groff, consultant
Gannate Khowailed, CSRA International
Karen Sikes, CSRA International

August 2017

Contents

LIST OF FIGURES

LIST OF TABLES

EXECUTIVE SUMMARY

In 2012 the International Energy Agency (IEA) Heat Pump Programme (now the Heat Pump Technologies (HPT) program) established Annex 41 to investigate technology solutions to improve performance of heat pumps for cold climates. Four IEA HPT member countries are participating in the Annex – Austria, Canada, Japan, and the United States (U.S.). The principal focus of Annex 41 is on electrically driven air-source heat pumps (ASHP) since that system type has the lowest installation cost of all heat pump alternatives. They also have the most significant performance challenges given their inherent efficiency and capacity issues at cold outdoor temperatures. Availability of ASHPs with improved low ambient performance would help bring about a much stronger heat pump market presence in cold areas, which today rely predominantly on fossil fuel furnace heating systems.

During the mid-1970s, following the first oil embargo, interest in use of heat pumps to provide space heating began to increase in many of the Organization for Economic Co-operation and Development (OECD) countries. Many northern U.S. electric power companies began experiencing increasing peak kilowatt (kW) demands during the heating season as shortages of natural gas and oil led to increased usage of direct electric heating. In response they began investigating the use of ASHPs as a means of mitigating the increased peak electric demands. ASHPs are almost universally applicable to buildings in all parts of the world and, given that they were the primary type available, were of main interest as an alternative electrical heating system at that time. However, as noted above, they suffer both heating capacity (output) and efficiency (coefficient of performance or COP) degradation as the outdoor ambient temperature drops while at the same time the building heat demand is increasing. As such, ASHPs require a supplemental heating source – usually direct electric resistance heating elements – to bridge the gap between the building heat demand and the ASHP heating output. This feature causes lower seasonal performance and limits peak electric demand reduction potential leading to limited acceptance of ASHPs in areas that experience large numbers of hours at cold temperatures (loosely defined as ≤ -7°C for purposes of Annex 41). In addition typical heat pump compressors fail to work at extremely low ambient temperatures due to the significantly high pressure ratio and discharge temperatures. A primary criterion for ASHPs to achieve good seasonal performance in cold areas is, therefore, achieving high heating output (capacity) at low ambient temperatures so as to minimize reliance on supplemental heat sources and maximize the overall system heating seasonal performance factor (HSPF in Btu/Wh or SPF_h in kW/kW).

For the reasons noted above, ASHPs are the primary heat pump type of interest for Annex 41. However, the Annex is open to ground source heat pumps (GSHP) and natural gas (engine or sorption) driven ASHPs as well at the participants' discretion. A primary technical objective of the Annex is to define pathways to enable ASHPs to achieve an "in field" $SPF_h \geq$ 2.63 W/W (HSPF ≥9.0 Btu/Wh), the minimum level necessary in order to gain recognition as a renewable technology in the European Union.

As stated in the 27 February 2013 legal text for the Annex, the work was originally divided into four main tasks:

- Task 1: Critical literature survey - Undertake a literature review and review of results from prior related research to identify candidate ASHP system design possibilities for further evaluation and study.
- Task 2: System design and application studies - modeling and/or laboratory-controlled measurements - The focus is on detailed analyses of promising component/system concepts considering the system performance and cost implications as well as design and control issues. Laboratory prototype and field prototype testing may be included in this task as well.

- Task 3: Simulations of energy savings impacts of prototype advanced ASHP design - This task will involve seasonal/annual performance simulations based on the prototypes developed in Task 2 to estimate energy and emissions savings potential.
- Task 4: Report and information dissemination - Each participant will provide a final country report addressing the results of the tasks above. These final country reports will be assembled into a final Annex report by the Operating Agent. This report will also suggest further areas for study and equipment development.

World energy consumption is projected to increase by 53% from about 530 EJ (505 quads) in 2008 to 810 EJ (770 quads) in 2035 (Conti et al., 2011). Energy consumption by OECD member countries is projected to increase by only 18% while that by non-OECD countries is projected to increase by 85% over this time span. Due to the increase in demand from non-OECD countries, it is expected energy prices will continue to increase from 2008 levels in spite of new developments in extraction methods such as fracking for natural gas or unconventional reserves such as oil tar sands. For the United States, current forecasts project the increase of energy prices (in 2011 dollars); Brent spot oil from $111 per barrel in 2011 to $163 per barrel in 2040, Henry Hub spot natural gas below $4 per million BTU through 2018 to $7.83 per million BTU in 2040, and mine mouth price of coal from $2.04 per million BTU in 2011 to $3.08 per million BTU in 2040 (EIA, 2013). In percentages, the predicted increase in the cost of energy is 47% for oil, roughly 90% for natural gas, and 51% for coal. These projected increases in fossil fuel prices could lead to increases in electricity prices of similar magnitude as well. With increases in consumption and costs of this magnitude, the urgency for reductions in U.S. energy consumption becomes evident.

The buildings sector in the United States accounted for about 42 EJ (40 quads) of primary energy consumption (~41% of the U. S. total) in 2010, making it the sector accounting for the largest consumption. The U.S. Energy Information Administration (EIA) projects this will increase by 17% by 2035. Space heating is responsible for ~22.5%, or roughly 9.5 EJ (9 quads) of this consumption (DOE, 2011). Fossil fuels account for about 6.7 EJ (6.3 quads) or 70% of the space heating energy consumption leaving a large potential for alternative heating methods employing electricity. Offsetting the consumption of fossil fuels on-site with electricity presents an opportunity to utilize renewable sources for power generation. Heat pumps are efficient technologies that employ electricity to achieve space heating where the heat output is a multiplier of the power consumption.

U.S. HEAT PUMP SHIPMENTS & TRENDS

U.S. heat pump shipments, along with most HVAC shipments, were significantly impacted by the economic recession and associated housing market decline, beginning in 2007 and intensifying over the next few years. When new single-family home construction drops (63 percent reduction in four years), the demand for new heat pumps is also depressed. The resulting steep drop in heat pump shipments between 2007 and 2009 is seen in Figure ES-1 (AHRI, 2010-2017; AHRI, 2012).

Since construction of new houses fell considerably during this time period, only 22% of heat pumps sold were installed in new homes during 2009; this indicates growing heat pump sales for add-on and replacement applications that usually require lower investments (Lapsa and Khowailed, 2011). Furthermore, high energy prices led some consumers and businesses to make upgrades by replacing inefficient equipment, including older heat pumps, which assisted sales. The heat pump market has shown somewhat more resilience to the housing crisis and economic downturn compared to competing space heating technologies. Figure ES-2 displays how heat pump shipments compared to those of gas- and oil-fired warm air furnaces for the period 1990 to 2015. Compared to the market peaks in 2005-2006, heat pump shipments dropped by ~17% during the 2009-2012 period while

combined gas and oil furnace shipments fell by ~35%. ASHP shipments rebounded starting in 2013 and exceeded the 2005-2006 levels in 2014-2015.

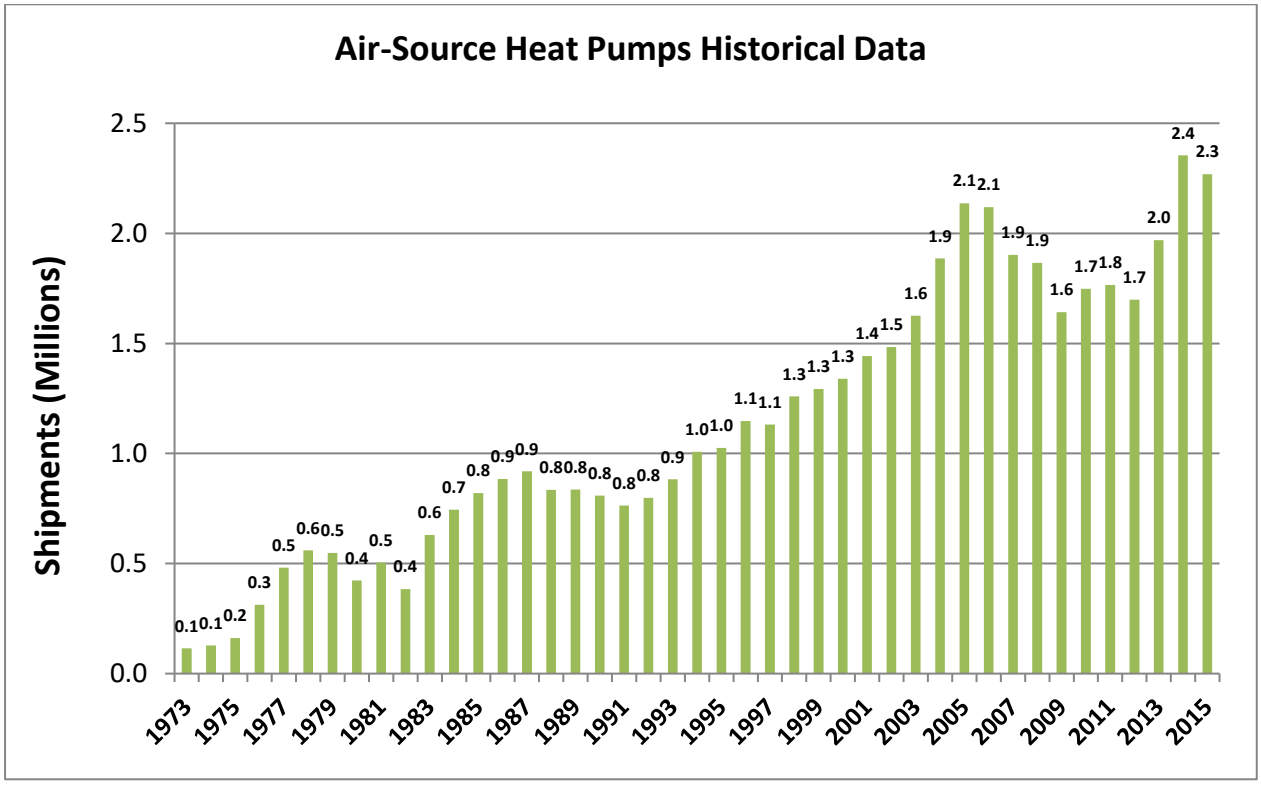

Figure ES-1: U.S. air source heat pump shipments (AHRI, 2010-2017)

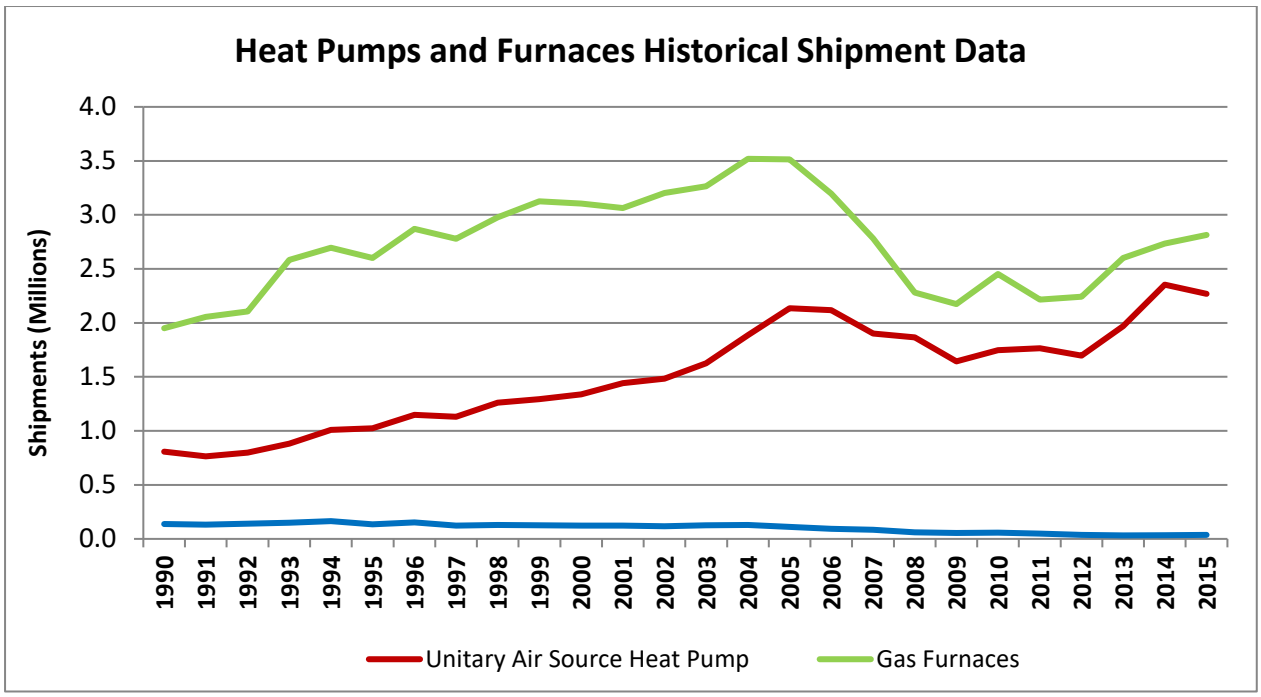

Figure ES-2: Unit shipments of heating equipment in the United States

PRELIMINARY CCHP MARKET ESTIMATE - 2010

As described by Khowailed et al. (2011), Cold climate heat pump (HP) technology is relevant to a substantial portion of the U.S. population, especially with more than one-third of U.S.

housing stock concentrated in colder regions of the country (blue-shaded areas in Figure ES-3, below) and another 31% in the mixed-humid climate region (green-shaded area).

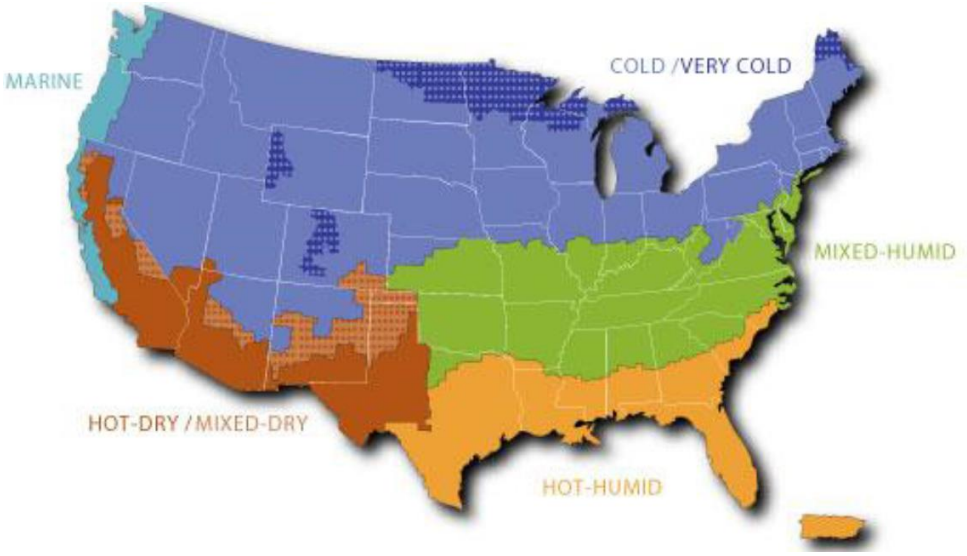

Figure ES- 3: Building America Climate Regions adopted in RECS2009 (U.S. EIA, 2011)

The primary target market for CCHPs is the 2.6 million U.S. homes using electric warm air furnaces and HPs in the cold/very cold regions (U.S. EIA, 2011). Secondary markets for CCHPs are comprised of 1) homes in the mixed-humid region of the country with conventional ASHPs or electric furnaces, and 2) homes in the cold/very cold region and the mixed-humid region that use fossil fuel fired warm air furnaces (propane, fuel oil, or natural gas) - albeit the fuel-fired furnace market is more challenging. The combined total of homes in these three secondary markets is 46 million (U.S. EIA, 2011). Khowailed, et al (2011) estimated that total potential annual shipments of CCHPs could reach ~275,000 assuming 1) the technology demonstrates consistent and reliable energy savings vs. the alternatives, and 2) a product rollout at a competitive price by a credible market leader. If CCHPs fully replaced the existing ASHPs and electric furnaces in the primary market they could yield annual primary energy savings of about 0.106 EJ (0.1 Quads), equivalent to about 5.4 million MT (5.9 million tons) of annual CO_2 emissions reduction.

CYCLE CONCEPT EVALUATION SUMMARY

The U.S. Department of Energy's Building Technology Office (DOE/BTO) established space heating capacity targets for CCHPs, listed in Table ES-1.

Table ES-1: U.S. Air-Source CCHP heating capacity targets – 2013

Outdoor Temperature	Heating Capacity
8.3°C (47°F)	9-21 kW (2.5-6 tons), nominal rating
-25°C (-13°F)	≥75% of nominal rating

U.S. CCHP R&D efforts described in the Task 1 and Task 2/3 reports focused on analyses and experimental (lab and field) investigation of several advanced VC cycles for ASHPs. Vapor injection (VI) cycle concepts, two-capacity compressors, variable speed (VS) compressors, parallel compressors, two-stage cycles with economizers, a liquid-flooded compressor cycle concept, and several other advanced cycle approaches have been investigated. Based on early stage analyses, three CCHP cycle concepts were identified as among the most promising for meeting the goals noted in Table ES-1 – two-stage

economizer cycle, an oil-flooded compressor cycle concept, and a single-stage cycle concept using parallel compressors.

Two-Stage Economizer System Concept

A field test of an advanced two-stage ASHP designed for cold climate operation has been completed at Camp Atterbury, a U.S. Army base outside Edinburgh in Indiana (Caskey et al., 2013). The heat pump is a two-compressor (two-stage) system with an economizer VI loop, similar to the concept analyzed by Bertsch et al. (2008). It featured a large tandem scroll compressor (two parallel compressors) for capacity boosting during low ambient temperature heating operation and a variable speed scroll compressor for cooling operation and moderate ambient temperature heating. The test was conducted under the US Department of Defense's (DOD) Energy Security Technology Certification Program (ESTCP). Two identical military barracks from available buildings located at Camp Atterbury were selected for the field demonstration. The originally installed HVAC system was a natural gas furnace with a split system A/C. A side-by-side performance comparison between the originally installed HVAC systems and the two pre-commercial heat pump units developed at Purdue University was conducted during the 2012-2013 heating season. Only commercially available components were selected for all parts of the heat pump units with help from three industrial partners, namely Ingersoll Rand - The Trane Company, Emerson Climate Technology, and Danfoss. The heat pump units had a design heating capacity of 18.34 kW (62,580 BTU/h) at an ambient temperature of -20^{o}C (4^{o}F).

The heat pump performance was compared to the existing HVAC system. For the monitored period at the Army site the ASHP system achieved approximately 19% source energy savings vs. the baseline gas furnace system but utility costs were higher due to the low price the Army pays for natural gas at the site. Using average Indiana residential electricity and gas prices, the utility costs for the ASHP and baseline furnace would have been comparable. This operation cost equivalence despite the energy savings of the ASHP is because the price for natural gas in Indiana is about one-third that of electricity per unit of energy delivered, which is true of most locations in the United States. The ASHP used no electric backup heating during the test period. Using ASHRAE Standard 55 (ASHRAE, 2010) to evaluate the thermal comfort indicated that the heat pump was able to maintain comfort levels throughout the heating season. Furthermore, while the first cost of the two-stage ASHP will be higher than that of a conventional single-stage ASHP, the installation and maintenance costs are estimated to be comparable.

Two-Port Vapor Injected Compression with Regeneration Concept

Additional research at Purdue University's Herrick Labs focused on the experimental investigation conducted with a commercially available 5-ton heat pump that was retrofitted with a two-port vapor injected scroll compressor. The injection ports within the two compression pathways were located in the fixed scroll with different distances from the suction chamber. The vapor at the two injection pressure levels was generated using two flash tank separators in a cascade configuration. This configuration made it necessary to not only control the superheat but also the liquid levels in the separators and subcooling of the refrigerant leaving the condenser.

Baseline performance data of the heat pump without vapor injection was obtained and compared with that of the two-port vapor injection system. For the baseline, the injection lines to the compression pockets were plugged within the fixed scroll to reduce dead volume and re-expansion losses. Also, the vapor-separator section was shut off and bypassed. In the second step, the plugs were removed and a staged expansion process was performed using the separator section. The generated vapor from each separator was injected into the respective compressor port causing an intercooling effect on the compression process.

With identical compressor speed, a 28% improvement in capacity was achieved at the 8.33°C design point, when compared to the baseline without vapor injection. When the baseline and vapor injected system capacity were matched by adjusting compressor speed, the COP increased by up to 6% at -8.33°C. Results of a bin-type analysis of the experimental results predict an improvement in the heating seasonal performance factor (HSPF) of 6% for Minneapolis and nearly 7% for ANSI/AHRI 210/240 cold climate region V.

Oil-flooded Compressor System Concept

Further research at Purdue University's Herrick Labs focused on the experimental investigation conducted with a commercially available 5-ton heat pump that was retrofitted with oil flooded compression and regeneration. The indoor coil face area was kept unchanged while an additional heat exchanger was added as the oil cooler in the air flow path. In addition, a counter-flow plate heat exchanger with low pressure drops was used as the regenerator.

The results show that by injecting oil in the compression process and using internal regeneration, the improvements in COP and heating capacity range from 4% to 15% and from 1% to 19%, respectively, depending on the oil mass fraction and operating temperatures compared with a conventional heat pump (without regenerator and without oil injection).

Single-Stage Cycle with Parallel Compressors

Research at ORNL investigated several different ASHP cycle configurations to identify those with potential to meet the heating capacity degradation target limit listed in Table ES-1. Two-capacity compressor, variable speed compressor, and dual, equal parallel single speed compressor (tandem compressor) systems were investigated. Nine of the system options investigated are listed in Table ES-2 along with the baseline conventional single speed compressor ASHP used for relative performance comparison.

Table ES-2: ASHP design and sizing options

#	Equipment Sizing Scenarios
1	Single speed heat pump having a rated HSPF of 9.6: sized such that rated cooling capacity matches building design cooling load [BASELINE].
2	Single heat pump, having a two-stage scroll compressor: sized such that rated high-stage (100%) cooling capacity matches building design cooling load.
3	Single heat pump, having a two-stage scroll compressor: sized such that rated low-stage (67%) cooling capacity matches building design cooling load.
4	Single heat pump, having a variable speed scroll compressor: sized such that rated cooling capacity at 2700 rpm matches building design cooling load.
5	Single heat pump, having a variable speed scroll compressor: sized such that rated cooling capacity at 3600 rpm matches building design cooling load.
6	Single heat pump, having a variable speed scroll compressor: sized such that rated cooling capacity at 4500 rpm matches building design cooling load.
7	Single heat pump, having a two-stage scroll compressor: sized such that 80% of rated cooling capacity matches building design cooling load.
8	Single heat pump, having a tandem scroll compressor pair: sized such that rated cooling capacity with one compressor matches building design cooling load.
9	Single heat pump, having a single speed VI scroll compressor: sized such that rated cooling capacity matches building design cooling load.
10	Two identical single speed heat pumps with rated HSPF of 9.6: sized such that rated cooling capacity of one unit matches building design cooling load; both units used for heating.

Note: All variable speed compressor system options have a speed range of 1800 - 7200 rpm; option 8, tandem compressor pair contains two identical compressors; the two-stage compressor options include one compressor having two capacity levels, i.e. 100%/67%.

Table ES-3 lists the heating capacity ratio and the heating COPs at 8.3°C and -25°C for each of the systems in Table ES-2. Four of the options (4, 5, 8, and 10) have estimated capacity ratios near the target level noted in Table ES-1 (≥75%). COPs at -25°C for these options range around 45-55% of the nominal COPs at 8.3°C. Estimated HSPF ratings are calculated based on the method prescribed in AHRI Standard 210/240 (AHRI, 2008) for U.S. region IV (mildly cold climate). The VS compressor-based designs offered somewhat greater low temperature capacity capability while the tandem compressor designs were somewhat less complex and had almost as much capacity capability.

Table ES-3: Predicted ASHP system performance indices

Options	COP @ 8.3°C (47°F)	Heating Capacity Ratio @ -25°C (-13°F)	COP @ -25°C (-13°F)	Region IV HSPF Rating (per AHRI Standard 210/240)
	[W/W]	[-]	[W/W]	[W/W (Btu/Wh)]
1.	3.58	40%	1.92	2.80 (9.55)
2.	3.79	42%	2.09	2.92 (9.96)
3.	3.78	57%	2.09	2.92 (9.98)
4.	4.30	94%	1.89	3.40 (11.61)
5.	4.14	74%	1.89	3.43 (11.71)
6.	3.80	61%	1.89	3.40 (11.59)
7.	3.79	52%	2.09	2.95 (10.05)
8.	4.38	75%	1.98	3.31 (11.31)
9.	3.75	43%	2.12	2.96 (10.09)
10.	3.58	80%	1.92	N/A

Based primarily on its relatively simple cycle concept (Figure ES-4), the tandem approach appeared to offer a more cost-effective approach compared to VS-compressor-based approaches so this concept was chosen for in-depth laboratory and field evaluation. A laboratory prototype test system was built by modifying a 17.5 kW (~60,000 Btu/h or 5-ton) rated cooling capacity, single-speed, conventional ASHP and replacing its original compressor with a pair of equal size, single-speed compressors providing 10.6 kW (~36,000 Btu/h or 3 tons) of rated cooling capacity. Parallel compressor CCHP systems using three different scroll compressor designs were evaluated in the lab: 1) conventional scroll compressor optimized for space cooling operation; 2) scroll compressors optimized for space heating operation; and 3) VI scroll compressors. The cycle concept in Figure ES-4 was used in the case of the cooling-optimized and heating-optimized compressors and is considered a ‘more cost effective’ concept. For the VI compressor system the cycle design is more complex (Figure ES-5) and is considered a ‘premium design’ concept. For all cases, the compressors were insulated and placed outside the outdoor air flow stream to minimize the compressor shell heat losses.

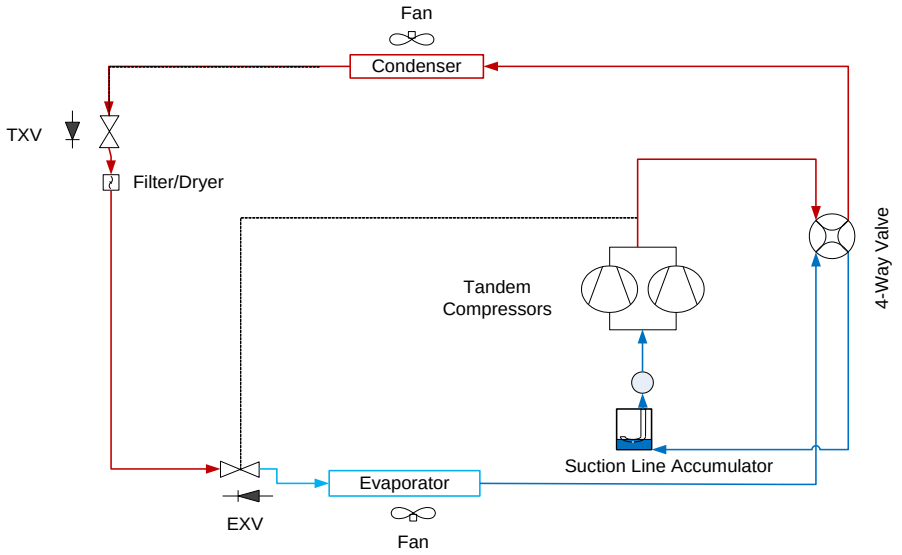

Figure ES-4: Cycle schematic for tandem, single-speed compressor CCHP with electronic expansion valve (EXV) to optimize discharge temperature in heating mode

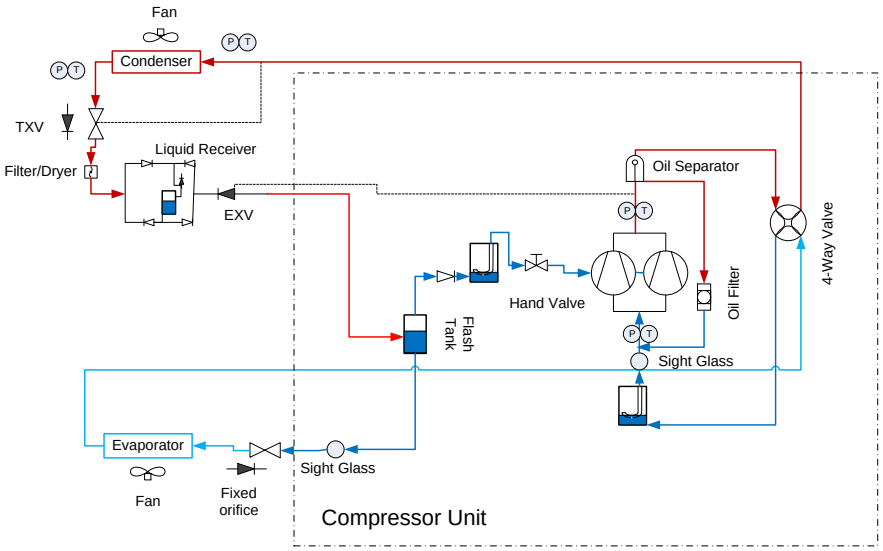

Figure ES-5: Cycle schematic for CCHP using tandem VI compressors and an EXV for heating mode refrigerant flow control

Tables ES-4 and ES-5 summarize the lab tested performance results for the parallel compressor lab breadboard with all three compressor types. Table ES-4 shows the lab-measured performance indices at 8.3°C, -8.3°C, and -25°C (47°F, 17°F and -13°F) outdoor temperature conditions with one or two compressors. Table ES-5 compares relative seasonal heating COP ratings (SCOPhs) [heating seasonal performance factors (HSPFs)] as calculated per AHRI Standard 210/240 in Region IV and V climates for the parallel compressor systems and a high efficiency baseline ASHP. The DHR_{min} building load level is generally representative of a very well insulated house (exceeding the 2015 U.S. code minimum insulation levels: Rice et al, 2015). DHRmax on the other hand is representative of an existing home with insulation levels below 2006 code minimum levels. The dropoff in seasonal efficiencies going from Region IV to the colder Region V climate is about 10.5% and 15.5% for the DHRmin and DHRmax load lines, respectively. Space heating performance was somewhat better at all ambient temperature test conditions for the heating-mode-optimized tandem compressor pair vs. the cooling-mode-optimized pair. It is also notable that the drop in SCOPh for the heating optimized and VI parallel tandem designs

between the min and max heating load lines is 1.3% or less in Region IV. This indicates that these designs maintain their seasonal performance well over the full range of house performance levels. By comparison, the single-speed baseline loses 23% in seasonal performance in Region IV between the DHRmin (rated) and DHRmax heating load lines. The SCOPh robustness of the tandem designs is also in contrast to recently tested variable-speed designs which lose 10 to 20% SCOPh in Region IV for representative heating loads approximately halfway between DHRmin and DHRmax levels (Rice et al, 2016). A similar performance robustness advantage is realized in Region V at higher heating load lines for the parallel tandem design, due to the boosted performance at -8.3°C (17°F) and below.

Table ES-4: Lab measured performance indices of parallel compressor CCHPs

	Ambient/Comp(s)	8.3°C, 1 Comp	-8.3°C, 2 Comp	-8.3°C, 1 Comp	-25°C, 2 Comp
Cooling mode optimized compressors	COP [-]	4.09	2.76	2.89	1.85
	Capacity, kW (Btu/h)	11.1 (37,960)	14.8 (50,455)	7.6 (25,860)	8.8 (30,040)
	Capacity Ratio -25°C vs. 8.3°C	100%	133%	68%	79%
	Discharge Temperature, °C [°F]	50.0 (122)	83.4 (183)	55.0 (131)	125.0 (257)
Heating mode optimized compressors	COP [-]	4.24	2.80	2.97	1.94
	Capacity, kW (Btu/h)	11.6 (39,717)	14.9 (50,921)	7.6 (25,917)	8.9 (30,245)
	Capacity Ratio -25°C vs. 8.3°C	100%	128%	65%	76%
	Discharge Temperature, °C [°F]	51.1 (124)	82.8 (181)	51.1 (124)	100.6 (213)
VI compressors	COP [-]	4.44	2.95	3.20	1.98
	Capacity, kW (Btu/h)	11.6 (39,720)	17.4 (59,362)	7.9 (26,918)	10.2 (34,913)
	Capacity Ratio -25°C vs. 8.3°C	100%	149%	68%	88%
	Discharge Temperature, °C [°F]	(52.2 (126)	70 (158)	52.8 (127)	84.4 (184)

Table ES-5: Heating Seasonal Performance Ratings of CCHPs using tandem single-speed compressors (per AHRI Standard 210/240)

Load	SCOPh (HSPF, Btu/Wh) Baseline	SCOPh (HSPF, Btu/Wh) cooling optimized	SCOPh (HSPF, Btu/Wh) heating optimized	SCOPh (HSPF, Btu/Wh) VI compressors
	Heating Season Ratings, Region: IV			
DHRmin	2.80 (9.55)	3.24 (11.04)	3.29 (11.21)	3.47 (11.84)
DHRmax	2.15 (7.35)	3.19 (10.90)	3.21 (10.95)	3.46 (11.80)
	Heating Season Ratings, Region: V			
DHRmin	2.47 (8.42)	2.90 (9.90)	2.94 (10.03)	3.13 (10.68)
DHRmax	1.96 (6.68)	2.69 (9.18)	2.71 (9.26)	2.96 (10.10)

The tandem VI compressor system configuration achieved 2 to 7% better COPs than the tandem, single-speed heating-optimized system configuration. It achieved an 88% heating capacity ratio with ~2.0 COP at -25°C, and ~4.4 COP and 11.7 kW capacity at the 8.3°C nominal rating condition. Figure ES-6 compares the heating capacities of the tandem single-speed compressors (heating optimized) and the tandem VI compressors, at two speed levels, as a function of the ambient temperature. DHRmax and DHRmin house load lines for the DOE Region V climate are overlaid on the VI prototype capacity data. These indicate

the potential for the CCHP prototypes to eliminate supplemental electric heat use in tight and well-insulated homes (aka DHRmin heating loads).

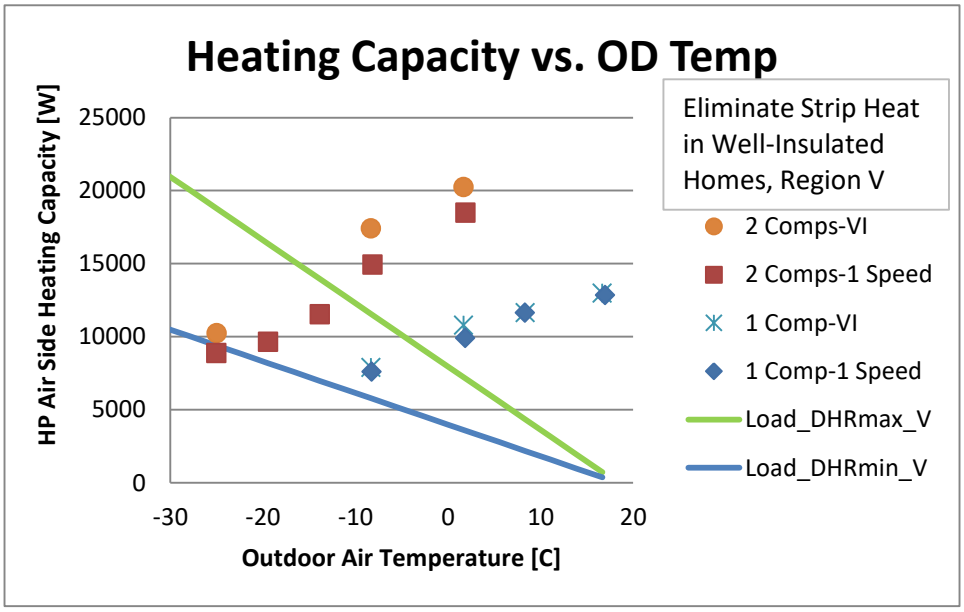

Figure ES-6: Heating capacity vs. ambient temperature, for tandem single-speed compressors and tandem VI compressors

A prototype CCHP using parallel heating-optimized scroll compressors was constructed and installed in an occupied, single-story ranch home in central Ohio in January 2015 for field testing. The prototype replaced the original home HVAC system – a conventional single-speed ASHP with rated cooling capacity of ~10.0 kW (34000 Btu/h) at 35°C (95°F) and heating capacity of ~10.3 kW (35000 Btu/h) at 8.3°C (47°F), equipped with a 19.5 kW supplemental resistance heater for second stage and full back up heating.

The field test prototype was built by modifying a two-capacity ASHP of nominal 17.6 kW (5-ton) cooling capacity - its original 2-capacity compressor was replaced with a heating-optimized tandem scroll compressor pair and controls added to stage the compressors. For the field test, the original 2-capacity ASHP control was retained but re-wired with a relay to enable calling the second compressor for second stage heating. Supplemental resistance heating elements were used for a third heating stage as needed. For defrosting, the CCHP prototype used a demand defrost control and operated both compressors to minimize defrost time.

A slightly different refrigerant schematic (Figure ES-7) was used in the field prototype for two primary reasons. First the lab testing showed that the system low temperature heating with heating-optimized compressors was much less sensitive to compressor discharge temperature than with the cooling-optimized compressors. Secondly, after installing the tandem compressor pair in the outdoor section it became difficult to find room for the EXV components required for the discharge temperature control scheme. So it was decided to simplify the refrigerant flow control to more conventional suction superheat control using a TXV with optimized system charge for heating mode. Figure ES-8 shows the outdoor unit of the prototype as installed at the test home, where one can see the compressors were wrapped by a thermal insulation layer.

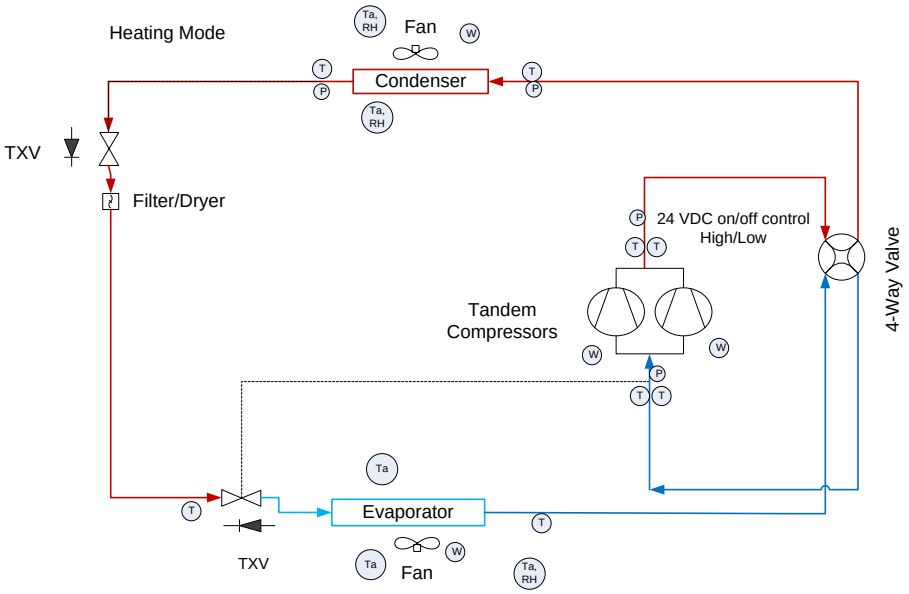

Figure ES-7: Field test prototype CCHP refrigerant schematic

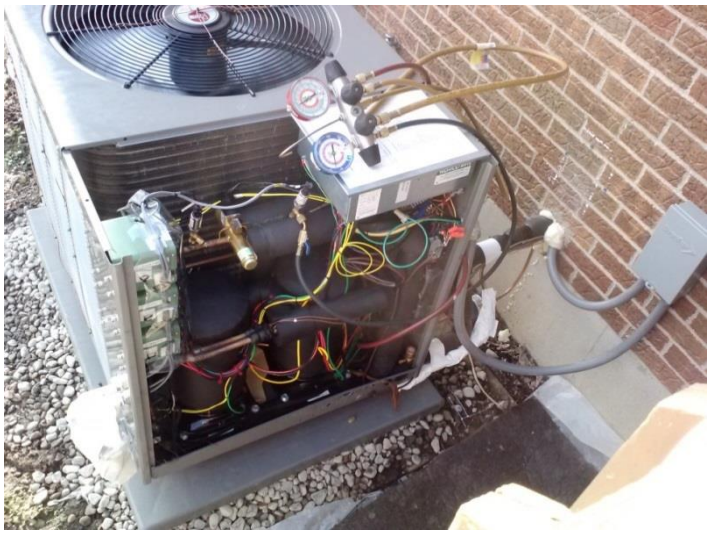

Figure ES-8: Outdoor unit of parallel compressor CCHP field test prototype

Field performance was monitored during three periods: 1) February through April, 2015 heating; 2) June through August, 2015 cooling; and 3) December, 2015 through January, 2016 heating. During the Feb.-Apr. 2015 period the minimum outdoor temperature experienced was 25°C (-13°F).

Figure ES-9 illustrates runtime fractions for two compressor operation and total compressor run time (either one or two compressors operating) versus ambient temperature bins for the first heating test period. At the lowest (rightmost) temperature bin, total compressor run time was 100% but the second compressor still cycled at an 80% rate. This indicates that the CCHP prototype still had some extra heating capacity capability even at this extreme condition.

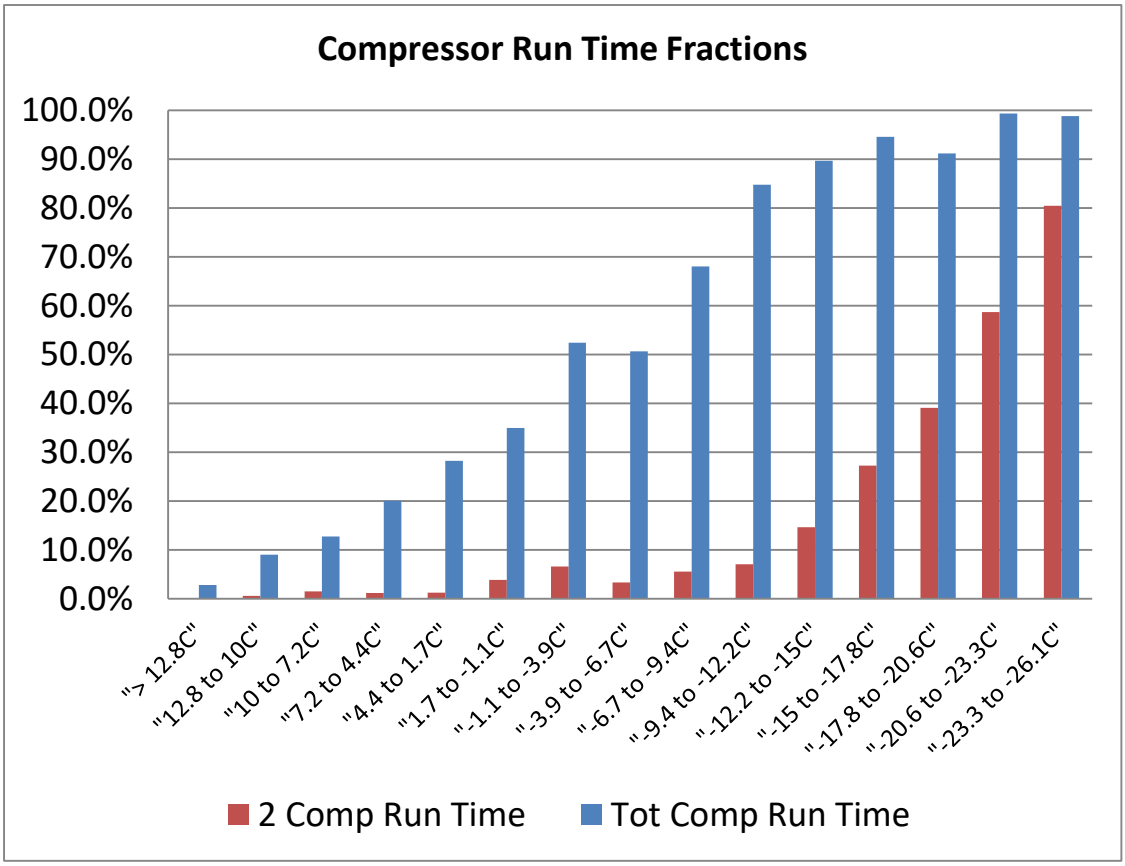

Figure ES-9: Compressor run time fractions, February-April, 2015

Figure ES-10 shows delivered heating capacities for one- and two-compressor operation and the measured delivered building heating load line. It can be seen that the second compressor was needed when the ambient temperature fell below -12.2°C (10°F). At the -25°C (-13°F) condition, the CCHP delivered 8.9 kW of heating, which is 75% of the lab-measured capacity of 11.6 kW at 8.3°C.

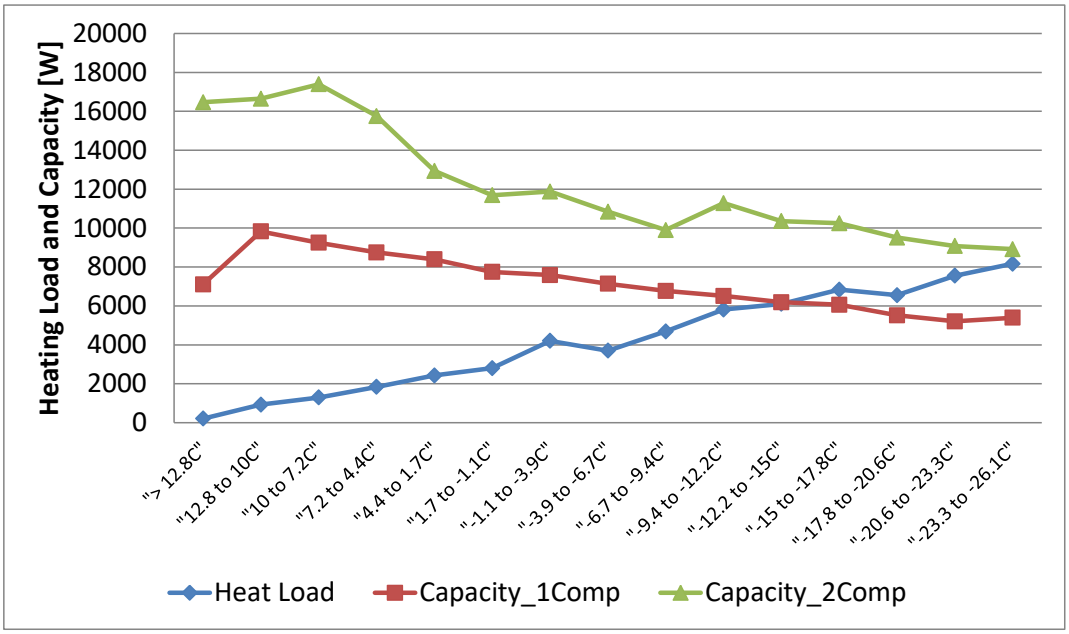

Figure ES-10: Delivered heating by CCHP and building load line, February-April, 2015

Overall, supplemental resistance heating (third stage) operation was minimal in the first heating test period, with most of the usage traceable to either system control issues or occupant behavior. (No defrost tempering resistance heat was used at the engineer homeowner's request.) At -25°C, the resistance energy use was 3.2% of the total even though the second compressor still cycled at 80%. This means that the heat pump responded slower than needed at this condition allowing space temperature to fall below the 1.1 °K dead band limit and activate the supplemental heater. Much of the resistance heat use seen during low outdoor temperatures could have been eliminated by changing the control to require two-compressor operation below a certain ambient temperature. Some 3rd stage operation was seen even at moderate ambient temperatures (between about 7.2°C to -10.0°C) but was mainly due to the thermostat setback operation by the homeowner. When the homeowner left for extended periods the thermostat set point would be lowered and then set back up when the homeowner returned. At times this resulted in the setup being high enough to trigger brief periods of 2nd and 3rd stage operation when they ordinarily would not be needed. Modifying the control to lock out the supplemental heater above a set outdoor temperature could eliminate most of this inadvertent 3rd stage operation.

Figure ES-11 shows field-measured COPs by outdoor temperature bin for single-compressor and two-compressor operation as well as a "total" COP. The total COP was calculated by the total energy delivery divided by the total energy consumed and includes the impacts of cycling losses, supplemental resistance heat use, frosting/defrosting losses, and losses due to switching between one- and two-compressor operation. For the 7.2°C to 10°C bin, the single-compressor COP was 4.05 while the total COP was 3.83 (lower because of cycling losses and occasional two-compressor operation). A control modification to prevent two-compressor operation above a set outdoor temperature would allow the total COP at mild outdoor temperatures (higher than about 2°C or so) to much more closely follow the single compressor COP curve.

It is encouraging to see that, at -25°C, the total COP was 2.2 i.e. 120% more efficient than resistance heating. The field COP at -25°C is higher than that measured in the lab (1.94 given in Table ES-4) mainly because the field return air temperature is 1.1 to 2.2°C lower than the controlled value in the lab.

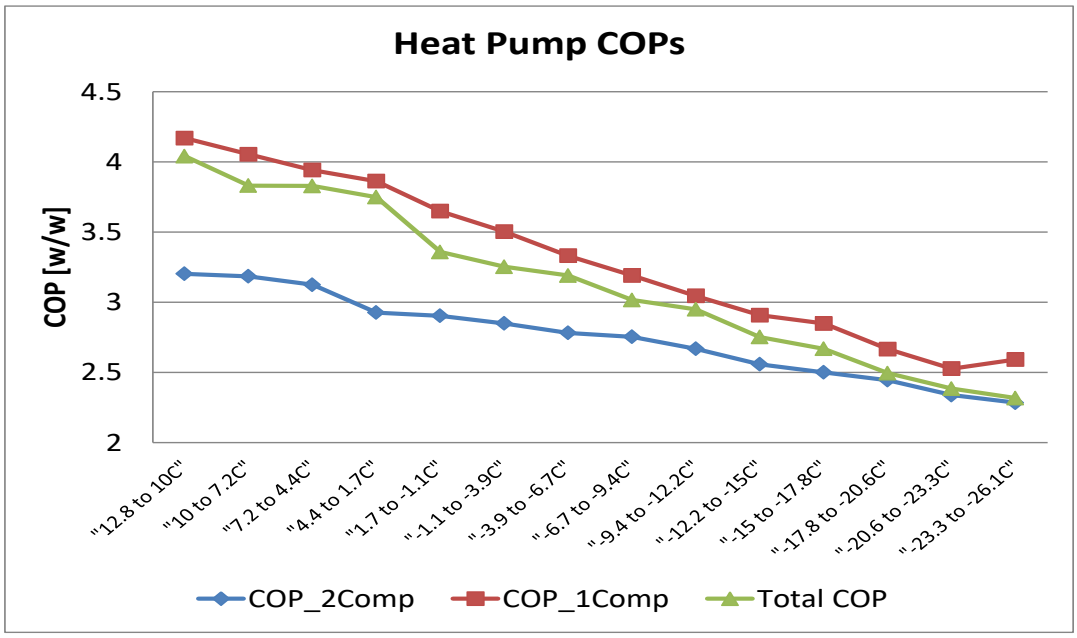

Figure ES-11: Field COPs in heating mode, February-April, 2015

In the first heating operation test period, the overall average field-measured COP was 3.16.

Cooling season data for the CCHP prototype was recorded from June through August of 2015. Prior to the start of the cooling season the control board was adjusted to allow only single compressor operation. In this case, the indoor and outdoor heat exchangers, sized for the base 17.5 kW ASHP, were oversized for single compressor operation, thus leading to superior cooling performance. The averaged field measured COP over the test period was 5.2, with an average ambient temperature of 25.6°C. Figure ES-12 below shows the field measured average COPs per temperature bin. The dropoff in COP at the lowest temperature bin is most likely due to increased cycling losses at the low cooling loads in this temperature bin offsetting the higher steady-state COPs from lower ambient temperatures.

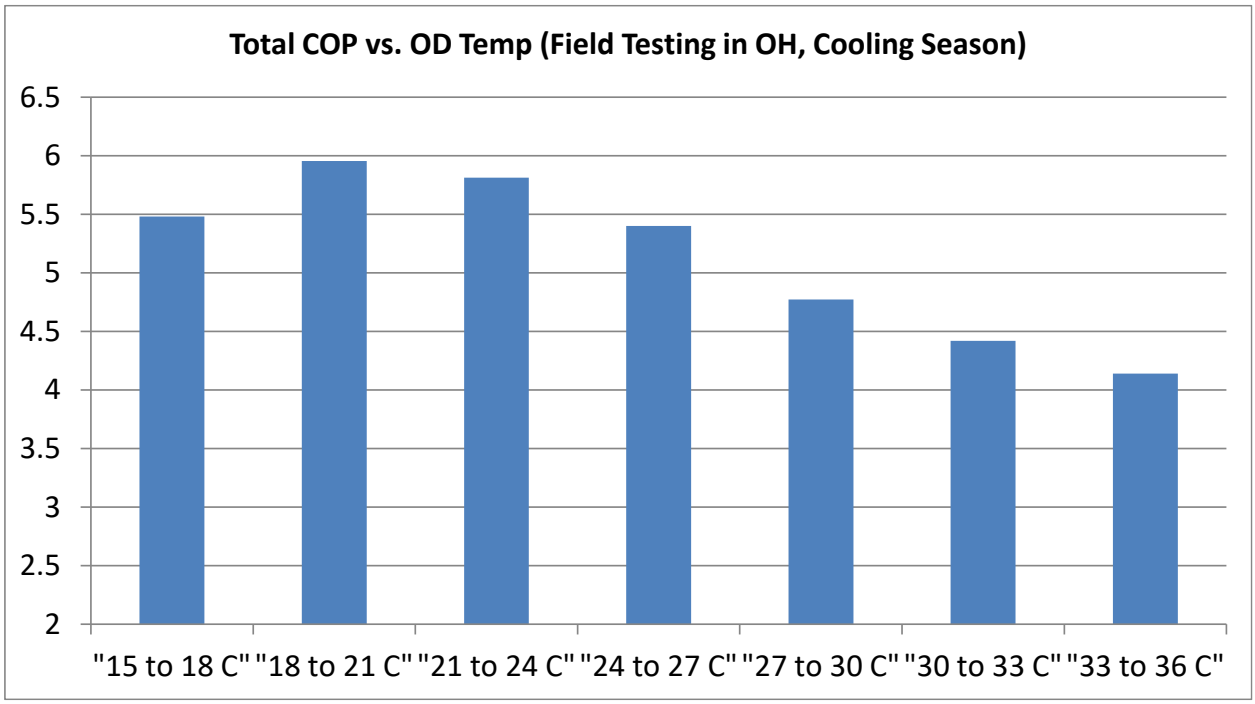

Figure ES-12: Field COPs in cooling mode

Figure ES-13 shows monthly electricity billing data for the field test home from June 2012 to November 2015 (about two years before installation of the prototype CCHP and for a year afterward). Note here that the kWh from the electric bills has had 800 kWh in “base” consumption (due to lights, water heater, appliances, etc.) subtracted so that it represents the heat pump usage only. In comparison to the previous single-speed ASHP in the same house, >40% HVAC energy reduction was achieved by the CCHP during the coldest months with similar monthly average temperatures (around -6 to -7°C). It can be seen that there are no apparent energy savings in the 2015 cooling months. This was due to a change in the family --- the homeowners had a new baby in the 2015 summer. So they set the thermostat to a lower temperature than they had used in previous summers and the heat pump ran more frequently offsetting the better efficiency of the CCHP prototype.

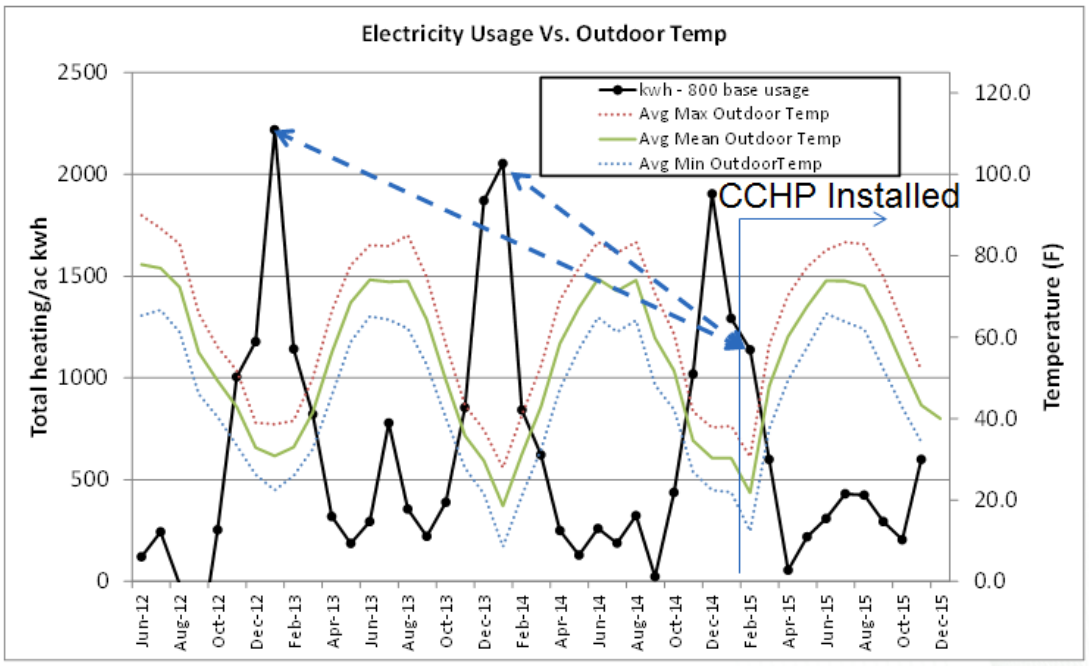

Figure ES-13: Monthly electric bills for field test home before/after installing the prototype CCHP

Before the project ended it was possible to collect another set of heating data from December 2015 through January 2016. Before data collection began, an outdoor temperature controller was added to the CCHP system to prevent the second compressor from running when the ambient temperature is above -12.2°C. However, the homeowner also adopted a higher thermostat setting of 21.7°C, about 1.7°C higher than the previous heating seasons due to the new family member. Due to the higher thermostat setting, the return air temperatures to the CCHP in 2016 were consistently about 2.2°C higher than those in 2015 leading led to a higher heating demand in 2016. Consequently, the second compressor ran more frequently in 2016. Figure ES-14 compares the average heat pump COPs per temperature bin for both heating test periods. Because of the higher temperature setting and the ~2.2°C higher return air temperature to the CCHP, the average heat pump heating COPs per temperature bin during the 2nd test period were 10% to 15% lower than those during the 1st period. The field measured, averaged COP for the 2nd period was 2.84, or about 10% lower than the 1st period average of 3.16. Overall average measured SCOPh for the test system combined for both test periods was about 3.00.

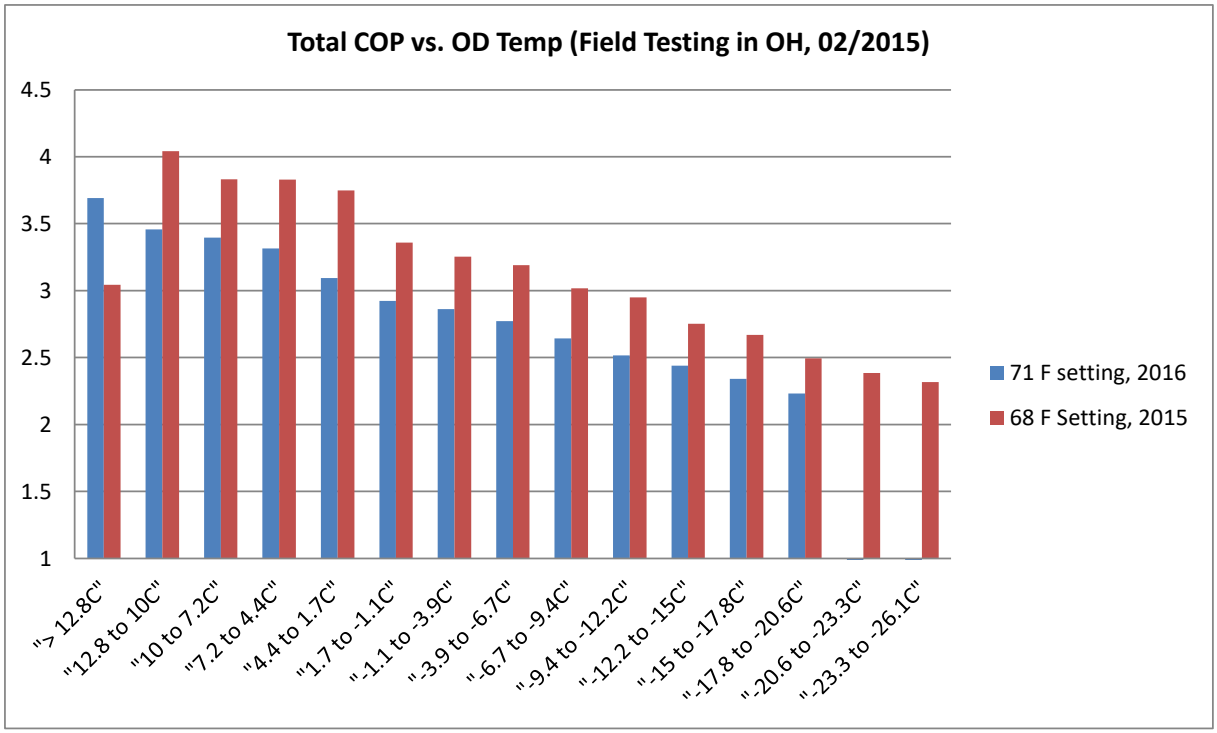

Figure ES-14: Average bin COPs for the two heating test periods

A second CCHP field test prototype system has been constructed based on the tandem VI compressor lab prototype design of Figure ES-5. It was installed at the Cold Climate Housing Research Center in Fairbanks, AK in May 2016 and field testing began in June 2016. Results will be reported after the planned one-year field test is concluded.

TASK 1 REPORT – LITERATURE AND TECHNOLOGY REVIEW

1 INTRODUCTION

During the mid-1970s, following the first oil embargo, heat pumps became of greater interest to northern U. S. electric power companies, particularly for those experiencing large peak demands during the heating season, as shortages of natural gas and oil led to increased usage of direct electric heating. Air-source heat pumps (ASHP), given their wider market presence relative to other heat pump types, almost universal applicability, but with inherent efficiency and capacity issues at cold outdoor temperatures were of primary interest for improvement as an electrical heating system alternative at that time. ASHPs based on the simple vapor compression cycle suffer both heating capacity (output) and efficiency (coefficient of performance or COP) degradation as the outdoor ambient temperature drops. At the same time, building heat demand is increasing so ASHPs require a supplemental heating source – usually direct electric resistance heating elements - to bridge the gap between the building heat demand and the ASHP heating output. These characteristics result in lower seasonal performance and limits peak electric demand reduction potential leading to limited acceptance of ASHPs in areas that experience large numbers of hours at cold temperatures (loosely defined as ≤-7°C for purposes of Annex 41). A primary criterion for ASHPs to achieve good seasonal performance in cold areas is achieving high heating output at low ambient temperatures so as to minimize reliance on supplemental heat sources and maximize the overall system heating seasonal performance factor (HSPF or SPF_h).

With increasing concern for technology options that can result in reduced CO_2 emissions, it is appropriate to revisit research and development work undertaken in different countries on heat pump systems for cold climates and to examine technology improvements that could lead to expanded usage of electric heat pumps for applications in cold regions. Accordingly, in 2010 the U. S. Department of Energy's Building Technology Office (DOE/BTO) solicited R&D proposals focused on advancing heat pump technology for cold climate applications. The performance targets specified in the solicitation are listed in Table 1 below.

Table 1: U. S. DOE cold climate heat pump performance targets, 2010

Outdoor Temperature	Heating COP	Heating Capacity
8.3°C (47°F)	4.5, nominal rating	14 kW (48,000 Btu/h), nominal rating
-25°C (-13°F)	≤50% reduction from nominal	≤25% reduction from nominal

At the same time, the U. S. proposed to the IEA Heat Pump Programme (IEA HPP) that a new Annex be established to collaborate with other HPP members to improve performance of heat pumps for cold climates. Annex 41 was officially approved in May of 2012. The principal focus of Annex 41 is on electrically driven ASHPs since that system type has the biggest performance challenges given its inherent low ambient temperature performance problems alluded to above. However, the Annex is open to ground source heat pumps and natural gas (engine or sorption) driven ASHPs as well at the Participants' discretion. Availability of heat pump systems with improved low ambient performance would help bring about a much stronger heat pump market presence in cold areas which today rely predominantly on fossil fuel furnace heating systems. A primary technical objective of the Annex is to define pathways to enable ASHPs to achieve an "in field" heating $SPF_h \geq 2.63$ W/W (HSPF ≥9.0 Btu/Wh), the minimum level necessary in order to gain recognition as a renewable technology in the EU.

The U. S. Department of Defense (DOD) has estimated that buildings accounted for 24% of its energy consumption in 2007 (U.S. DOD WSTIAC, 2009). Several mandates, including Executive Order 13514, "Federal Leadership in Environmental, Energy, and Economic

Performance" (EO 13514, 2009), calling for the improvement on the efficiency of federal buildings are affecting the current and future stock of DOD buildings. The use of heat pumps designed for cold climates is a promising approach to improve the HVAC efficiencies to aid compliance with these mandates. The goals are to create a clean energy economy that the Federal Government will lead by example. One significant goal is mandatory energy reductions to reach net-zero-energy buildings by 2030 (EO 13514). The Energy Independence and Security Act of 2007 includes Section 315, "Improved Energy Efficiency for Appliances and Buildings in Cold Climates" specifically addressing advancements for cold climates. One requirement of the act is the reduction of fossil fuels in new or renovated buildings, 55% by 2010 then 100% by 2030 (EISA, 2007).

In May of 2006, the Secretary of Defense commissioned an Energy Security Task Force, ESTF, to develop a roadmap to reduce the fossil fuels requirement for the DOD. A heat pump designed for cold climates has the ability to replace fossil fuel heating methods with an efficient, electricity based system. CO_2 emission reductions can be very substantial compared to fossil fuel heating systems in areas where the electricity is predominantly produced from renewable energy sources.

2 BACKGROUND – ENERGY USE AND INCREASING ENERGY PRICES

World energy consumption is projected to increase by 53% from about 530 EJ (505 quads) in 2008 to 810 EJ (770 quads) in 2035 (Conti et al., 2011). Energy consumption by Organization for Economic Co-operation and Development (OECD) member countries is projected to increase by only 18% while that by non-OECD countries is projected to increase by 85% over this time span. Due to the increase in demand from non-OECD countries, it is expected energy prices will continue to increase from 2008 levels in spite of new developments in extraction methods such as fracking for natural gas or unconventional reserves such as oil tar sands. For the United States, current forecasts project the increase of energy prices (in 2011 dollars); Brent spot oil from $111 per barrel in 2011 to $163 per barrel in 2040, Henry Hub spot natural gas below $4 per million BTU through 2018 to $7.83 per million BTU in 2040, and mine mouth price of coal from $2.04 per million BTU in 2011 to $3.08 per million BTU in 2040 (EIA, 2013). In percentages, the expected increase in the cost of energy is 47% for oil, roughly 90% for natural gas, and 51% for coal. These projected increases in fossil fuel prices could lead to increases in electricity prices of similar magnitude as well. With increases in consumption and costs of this magnitude, the urgency for reductions in U.S. energy consumption becomes evident.

The buildings sector in the United States accounted for about 42 EJ (40 quads) of primary energy consumption (~41% of the U. S. total) in 2010, making it the sector accounting for the largest consumption. The U. S. Energy Information Administration (EIA) projects this will increase by 17% by 2035. Space heating is responsible for ~22.5%, or roughly 9.5 EJ (9 quads) of this consumption (DOE, 2011). Fossil fuels account for about 6.7 EJ (6.3 quads) or 70% of the space heating energy consumption leaving a large potential for alternative heating methods employing electricity.

Offsetting the consumption of fossil fuels on-site with electricity presents an opportunity to utilize renewable sources for power generation. Heat pumps are efficient technologies that employ electricity to achieve space heating where the heat output is a multiplier of the power consumption. Heat pumps specifically designed for cold climates were one of 15 technologies selected for the refined study of the reduction of primary energy consumption of HVAC systems in commercial buildings (Roth et al., 2002). Business case analyses conducted by Oak Ridge National Laboratory predict a cumulative energy savings potential of 0.53 EJ (0.5 quads) from 2015 to 2030 for a cold climate heat pump assuming a 25% penetration rate when compared to conventional electric heat pump and electric resistance units (Khowailed et al., 2011).

3 BRIEF U. S. HEAT PUMP MARKET HISTORY

3.1 National Shipments & Trends

Since heat pump sales first emerged as a significant alternative for space heating and cooling of buildings during the 1950s, market sales have experienced significant volatility originating from:

- Government efficiency regulations and test methods
- Government and utility incentives for heat pumps
- Modifications to international trade barriers
- Technological breakthroughs
- Major swings in the housing market
- Economic recessions
- Availability, cost and rate structures of electricity and natural gas
- Favorable customer and utility experiences with certain models

The section below provides a high level overview of how the heat pump market has evolved in the U.S. since its inception, accompanied by explanations of the underlying market drivers.

3.1.1 1950-1969

Early growth of heat pumps was very rapid following the wide-scale acceptance of residential forced-warm air heating systems and central air conditioning, in addition to the potential for abundant, low-cost electricity that nuclear power could supply. However, sales were soon slowed substantially due to poor product reliability resulting from inexperience or inadequate product testing on the part of many manufacturers who attempted to capitalize on the emerging market opportunity (Groff and Ertinger, 1984).

3.1.2 1970 – 1989

Despite the negative experiences mentioned above, heat pump sales grew at modest rates, mostly in mild climate zones with low electric rates, up until 1973 when the first oil embargo occurred. From 1973 to 1978, heat pump sales (or shipments) grew from ~100,000 to over 560,000 annually, as shown in Figure 1, and heat pumps began to gain traction in the colder northern climate areas where natural gas and heating oil dominated. In the same period, the fraction of heat pump sales to northern areas of the U. S. rose from 15% to over 35%. The rise is significant because these areas accounted for 75% of U. S. space-heating energy use at the time (Groff and Ertinger, 1984).

A recession from 1979-1981 together with greater-than-expected availability of natural gas dampened the heat pump sales growth rate considerably. But by 1983, sales had reached ~700,000 per year, and projections indicated that by 1990 they should reach 1,000,000 units annually (Groff and Ertinger, 1984). Continued availability of adequate natural gas supplies and relatively low gas prices vs. electricity generally dampened heat pump sales growth so that the 1,000,000 annual sales level was not reached until the mid-1990's.

3.1.3 1990 – 2009

The United States experienced a relatively small economic downturn in 2001. A surge in heat pump sales is seen in 2005, which analysts believe is directly tied to the government regulation to increase the minimum seasonal energy efficiency ratio (SEER) for heating and cooling equipment from 10 to 13 – a 30% improvement. The change, which went into effect in 2006, caused an increase in equipment costs, and as a result, manufacturers in many

cases chose to ship out as much inventory as possible in 2005 since this stock would not meet the new standard. The lasting impact of this change on the heat pump market continues to be felt since some manufacturers were unable to produce at full capacity in 2006 while still meeting the new standard.

Heat pump shipments, along with most HVAC shipments, were also significantly impacted by the economic recession as well as the associated housing market decline, beginning in 2007 and intensifying over the next couple of years. When new single-family home construction drops (63 percent reduction in four years), the demand for new heat pumps was also depressed. The resulting steep drop in heat pump shipments between 2007 and 2009 is seen in Figure 1 (AHRI, 2010-2017; AHRI, 2012).

Since construction of new houses fell considerably during this time period, only 22% of heat pumps sold were installed in new homes during 2009. This indicates growing heat pump sales for add-on and replacement applications that usually require lower investments (Lapsa and Khowailed, 2011). Furthermore, high energy prices led some consumers and businesses to make upgrades by replacing inefficient equipment, including older heat pumps, which assisted sales.

3.1.4 2010 to date

The heat pump market has shown resilience to the aforementioned housing crisis and economic downturn, with 2014-2015 shipments recovering to somewhat exceed the previous 2005-2006 peak. Furthermore heat pump shipments appear to be recovering faster than gas furnaces, increasing their market share. Figure 2 displays how heat pump shipments compared to those of competing heating technologies for the period 1990 to 2012. Compared to the market peaks in 2005-2006, heat pump shipments dropped by ~17% during the 2009-2012 period while combined gas and oil furnace shipments fell by ~35%. ASHP shipments rebounded starting in 2013 and exceeded the 2005-2006 levels in 2014-2015.

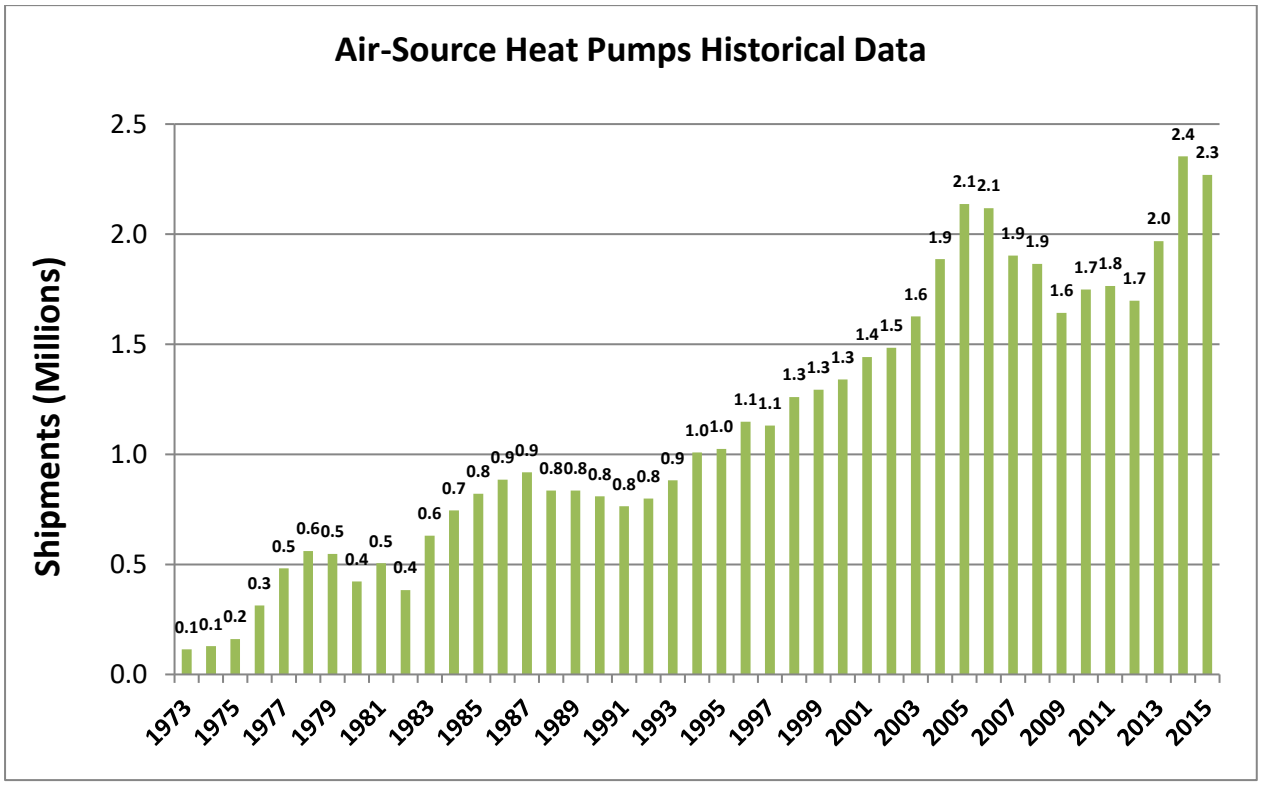

Figure 1: U.S. air source heat pump shipments (AHRI, 2010-2017)

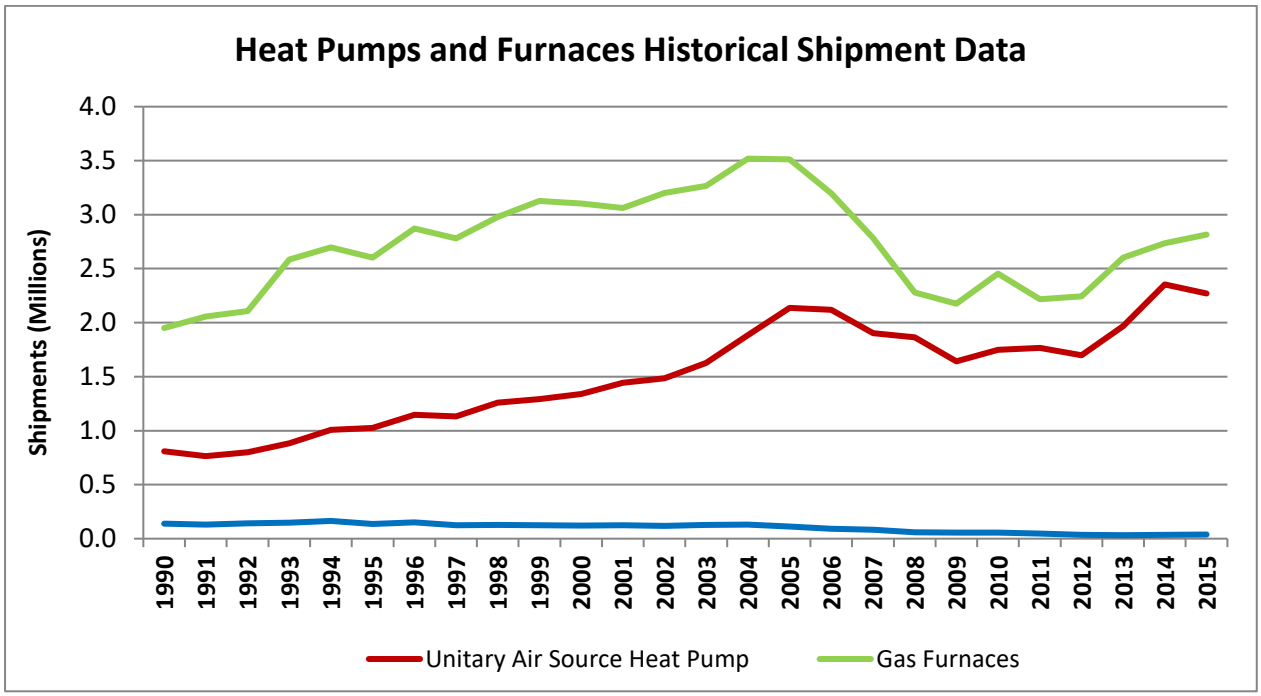

Figure 2: Unit shipments of heating equipment in the United States (AHRI, 2010-2017)

3.2 Regional Shipments & Trends

The South U. S. census region has been best suited for heat pumps due to relatively lower electricity prices and moderate weather presenting a favorable market for ASHPs. The 2009 Residential Energy Consumption Survey (EIA, 2009) data highlights the primary heating equipment used in homes across the country. As of 2009, 9.8 million U.S. homes relied on heat pumps for their primary heating equipment, representing about 8.6% of the 114 million homes in the United States. A majority are in the South region with 7.5 million of the region's homes using heat pumps as their primary heating equipment (about 18% of the total 42 million homes located here).

Figure 3 provides a visual display of heat pump presence across the United States as of 2009. As indicated by the greener shades, the South clearly has the highest overall share of heat pump of all U.S. census regions. Within this region, the South Atlantic division shows the most penetration, with Virginia having the largest share of heat pump technologies among all the states (36% of its 3 million homes use heat pumps as the primary heating technology). Heat pump penetration is not as high in the West South Central division of the South region, with only 4% of homes in Texas, Arkansas, Louisiana, and Oklahoma relying on heat pumps for their heating purposes. Only 2% of homes in the Northeast region use heat pumps, largely driven by 400,000 homes in Pennsylvania. Similarly, only 2% of homes in the Midwest region use heat pumps. The West region shows a somewhat stronger presence of heat pump technologies with about 5% of the homes currently using them as their primary heating system, mainly driven by 600,000 homes in Arizona. The relatively wider availability of natural gas to residential areas in the West South Central division and Northeast, Midwest, and West regions is at least partially responsible for the lower market share of electric heat pumps in those areas. It should be noted that the 18 states shaded grey in Figure 3 had insufficient data, either because no cases were in the reporting sample, data was withheld due to a Relative Standard Error (RSE) of the sample being greater than 50 percent, or fewer than 10 households were sampled. Based on the overall regional data described above however, the heat pump share of homes in these states is estimated at <2%.

The lower market presence of heat pumps in northern areas of the U. S. is not due to any inadequacy of heat pump performance or reliability. One of the authors of this report (Groff) has personal knowledge of individual electric heat pumps operating successfully in locales with winter temperatures reaching extremes as low as -50°C (-58°F). Heat pump life studies sponsored by the Electric Power Research Institute (EPRI) covering heat pump installations in parts of nine U. S. states (Alabama, northern Illinois, Indiana, Kentucky, Michigan, Ohio, Tennessee, Virginia, and West Virginia) showed median heat pump service lifetimes ranging from ~20.5 years in southern locations to ~15-16 years in northern locations (Lovvorn and Hiller, 2002; Lovvorn et al, 2001; Bucher et al, 1989; Pientka, 1987). Median life for the compressor from these studies was estimated at ~13.5 years in the Alabama studies indicating that no more than one compressor replacement was typically required during the service life of the heat pump installations surveyed (Lovvorn et al, 2001). Bucher et al, (1989) noted that for the heat pumps that required compressor replacement in their study, only 4.6% required more than one compressor replacement during their service lifetime.

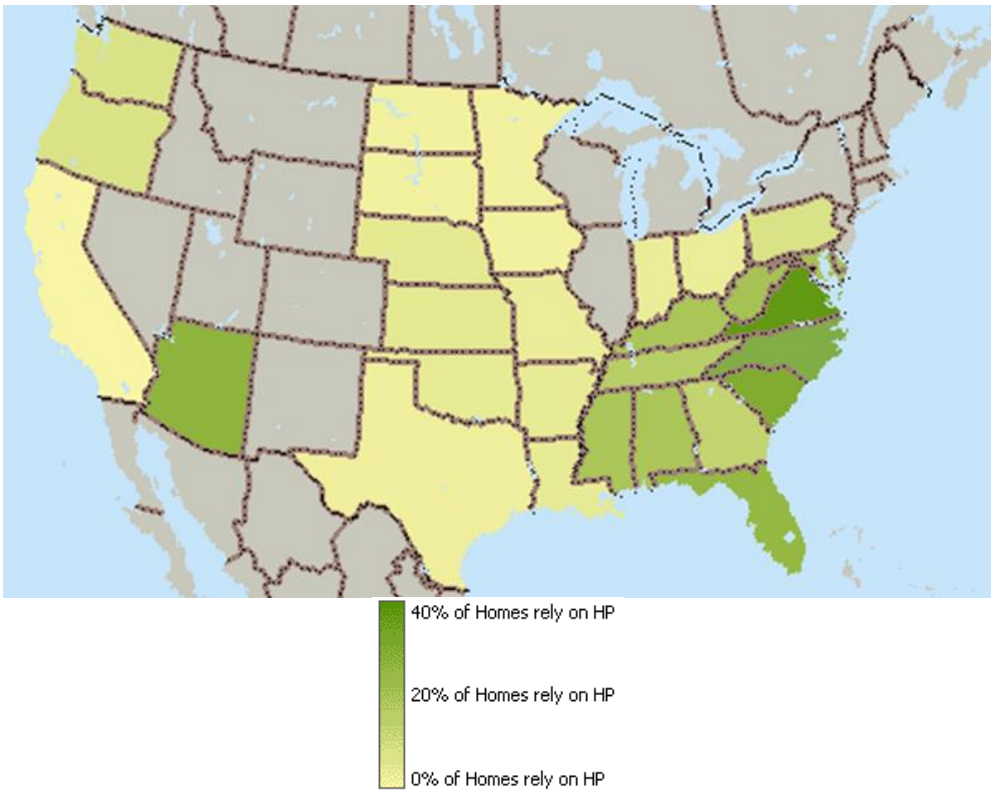

Figure 3: Percentage of homes using heat pump technology as the main heating equipment, as of 2009 (EIA, 2009)

As shown in Figure 4, heat pumps have increased in market share (relative to other heating systems) in the United States for approximately the past 12 years, maintaining close to 40% of the national market over the past couple of years. A closer look at how heat pumps fare in the four individual census regions, however, shows mixed performance. As of 2012, heat pumps accounted for well over half of all heating systems installed in new single-family houses in the South, with significant boosts beginning around 2002 (U.S. Census Bureau, 2013). A U.S. population shift from colder to warmer climates (U.S. EIA, 2013), like the South, is believed to have an overall positive impact on heat pump sales given that region's favorable market for ASHPs as noted above. More houses built in this region likely means more heat pumps installed over time, and this population shift is anticipated to continue through 2030.

The Midwest region experienced a similar boost in shipments starting in 2002, capturing approximately 20% of the market by 2009-2010, but this gain has started to tail off in recent years. The West demonstrated its highest market share back in the early 1980s, but has since lost ground to competing technologies. Finally, the Northeast has experienced rather steady, although minimal, market share at roughly 10% (U.S. Census Bureau, 2016).

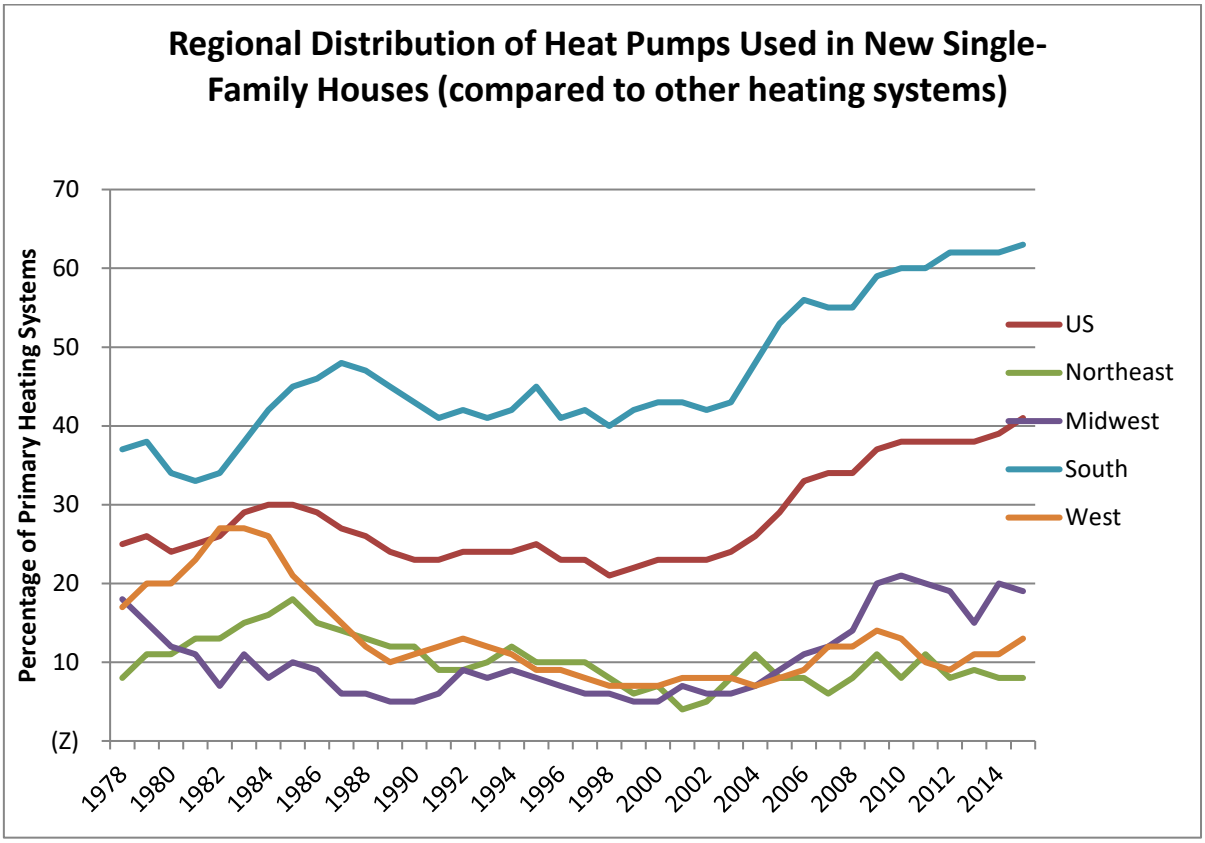

Figure 4: Heat pump market share by region

The introduction of cold climate heat pumps (CCHP) and other improved technologies is expected to aid in the expansion of the heat pump market beyond the Sunbelt areas into the colder regions traditionally dominated by gas furnaces. The Residential Energy Consumption Survey (RECS) heating stock data in 2001, 2005, and 2009 for cold / very cold regions of the country shows that gas furnaces are slowly losing traction within the market and that electric furnaces and HPs are gaining momentum, showing promise for the future penetration of cold climate heat pumps. Furthermore, regional standards for gas furnaces are expected to become stricter in the near future, requiring an increase in the minimum efficiency to an annual fuel utilization efficiency (AFUE) rating of 90% in the cold / very cold (northern) part of the country, which will increase the initial equipment cost, potentially leading to new trends in heating equipment (Khowailed et al., 2011).

3.3 Preliminary CCHP Market Estimate – 2010

As described by Khowailed et al. (2011), cold climate heat pump (HP) technology is relevant to a substantial portion of the U.S. population, especially with more than one-third of U.S. housing stock concentrated in colder regions of the country (blue-shaded areas in Figure 5, below) and another 31% in the mixed-humid climate region (green-shaded area).

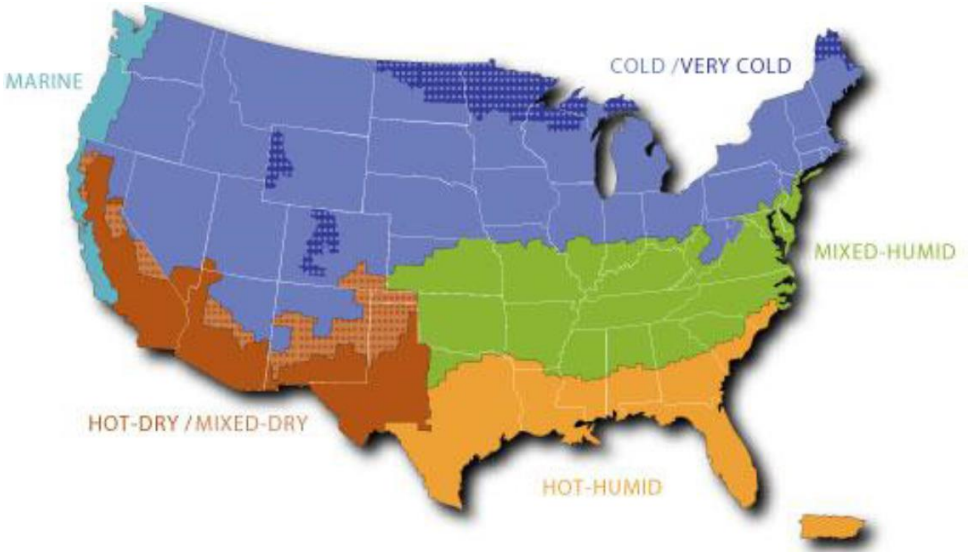

Figure 5: Building America Climate Regions adopted in RECS2009 (U.S. EIA, 2011)

The primary target market for CCHPs is the 2.6 million U.S. homes using electric warm air furnaces and HPs in the cold/very cold regions (U.S. EIA, 2011). Secondary markets for CCHPs are comprised of 1) homes in the mixed-humid region of the country with conventional ASHPs or electric furnaces, and 2) homes in the cold/very cold region and the mixed-humid region that use fossil fuel fired warm air furnaces (propane, fuel oil, or natural gas) - albeit the fuel-fired furnace market is more challenging. The combined total of homes in these three secondary markets is 46 million (U.S. EIA, 2011). Khowailed, et al (2011) estimated that total potential annual shipments of CCHPs could reach ~275,000 assuming the technology demonstrates consistent and reliable energy savings vs. the alternatives, and a product rollout at a competitive price by a credible market leader. If CCHPs fully replaced the existing ASHPs and electric furnaces in the primary market they could yield annual primary energy savings of about 0.106 EJ (0.1 Quads), equivalent to about 5.4 million MT (5.9 million tons) of annual CO_2 emissions reduction.

4 LITERATURE REVIEW

A review of previous and current literature was performed to examine the results of earlier cold climate specific ASHP R&D activities and to identify candidate heat pump technology advances that could achieve sufficient heating capacities and desirable efficiencies while operating at low outdoor temperatures. Ultimately, the goal of the literature review is to highlight the development status of technologies that could lead to greater heating seasonal efficiency for heat pumps (particularly ASHPs) in colder climate locations. Much of the current literature review summarized in this section is taken from a Master's Thesis by Caskey (2013).

4.1 Pre-1990 Cold Climate Heat Pump R&D in the United States

Considerable research and development activity was begun in the U. S. in the late 1970's and early 1980's to improve the performance of ASHPs, resulting in higher efficiency and more reliable products for northern U. S. applications (Groff and Reedy, 1978; Groff et al., 1978, Groff et al., 1979; Bullock et al., 1980). A great deal was learned about the technology needs to enable heat pumps to become more attractive for colder climate applications. In intervening years, advanced heat pump designs have been pursued (and some have been brought to the market) that incorporate design concepts or features for improved cold climate performance (see for instance Hadley et al., 2006). While many of these improved heat pump designs have been technically successful, market opportunities were limited due to the

continuing relatively low cost of fossil fuels vs. electricity and to the higher initial cost of these products and systems.

In the mid-1970s electric utility companies were motivated to sponsor research into alternative electrically operated heating products as an alternative to direct electric heaters and gas or oil furnaces. Notable programs launched during this period were undertaken by EPRI, EESERCO (a consortium of Northeastern U.S. utilities) and Niagara Power Corporation (now National Grid). Westinghouse's research group was awarded a contract by EPRI to identify heat pump design concepts (including in combination with solar energy utilization) that would be effective in the colder climates. EESERCO and Niagara Mohawk sponsored similar projects that were focused on more practical design solutions (i.e. that could be carried to actual product development). These latter studies (as undertaken by the Carrier Corporation Research Division), included field monitoring of ASHPs in residences in four northern U. S. cities with varying climate conditions – Boston, MA; Syracuse, NY; Minneapolis, MN; and Seattle, WA. All of these locations experienced at least 2800 °C-days (5,000 °F-days) of heating. In addition a detailed seasonal performance (SPF) simulation model was developed, calibrated using data from the field monitoring, and used for parametric studies (Groff and Reedy, 1978; Groff et al., 1978). The heat pumps used in the field studies were single-speed ASHPs typical of those available in the 1960s and 1970's, applied to residences and one commercial building – see Figure 6 for two examples.

Figure 6: Sample outdoor sections of heat pumps field tested from 1976-1978: left, ca 1960's unit installed in Seattle residence (note semi hermetic compressor); right, ca 1970's unit originally installed in Minneapolis residence (note - unit was undersized)

Field measured SPFs for the tested heat pumps ranged from 1.20 in the coldest location (Minneapolis), to 1.5-1.6 (Boston and Syracuse), to 2.2 in the mild Seattle location. These values were impacted by the fact that the 1976 winter experienced much lower outdoor temperatures than average for the three coldest locations. Using the calibrated SPF model it was projected that for average weather at these locations, the SPFs would have been slightly higher, ranging from about 1.3 to 2.3 (Groff and Reedy, 1978; Groff et al., 1978). The heat pump tested in Minneapolis was undersized for the house and location, so a subsequent year of testing was undertaken using a larger and more efficient ASHP (30% increased capacity and 19% higher COP at the 8°C (or 47°F) rating point). The field measured heating season results showed an increase in SPF of 24% (1.49 vs. 1.2 the previous year) (Groff et al., 1979). This illustrates the inherent advantage of increasing the heat pump size (heating capacity) for improving SPF in colder locations.

Bullock et al. (1980) described a more detailed heat pump sizing study based on ranges of heat pump capacity levels, house load (e. g. thermal envelope) characteristics, climatic conditions (e.g. locations) and economic factors (operating and maintenance costs, fuel

costs, and fuel cost escalation rates). A metric called the size ratio (SR) was defined as shown in Figure 7 to characterize the heating capacity of a heat pump relative to its heating load at the standard rating temperature of 8.33°C (47°F). Four local climate levels were considered, denoted as A-D with A the mildest and D the most severe (highest heating degree-days). Three house thermal envelope levels were considered – 3 being the most insulated, least infiltration (with lowest heating requirement) and 1 the lowest (with highest heating requirement). Three different fuel cost escalation rate (I_{ESC}) assumptions were considered as well – 0-10%. Figures 8 and 9 illustrate typical results generated for a mild and severe climate, respectively. It can be seen that for the more severe climate (Figure 8), the SR is much more dependent on the range of house load levels and fuel cost factors. Generally, higher values for I_{ESC} favor larger SR values. More heavily insulated houses (aka house level 3) also tend to favor higher SR values – however the absolute heat pump size for more efficient homes would generally be smaller due to the smaller absolute heating requirement. Figure 10 illustrates the range of optimum SR values vs. heating degree days. For this figure, the "upper" boundary would be typical for better insulated homes with a high I_{ESC} assumption. Conversely, the "lower" boundary would pertain to less insulated dwellings and a low I_{ESC} assumption.

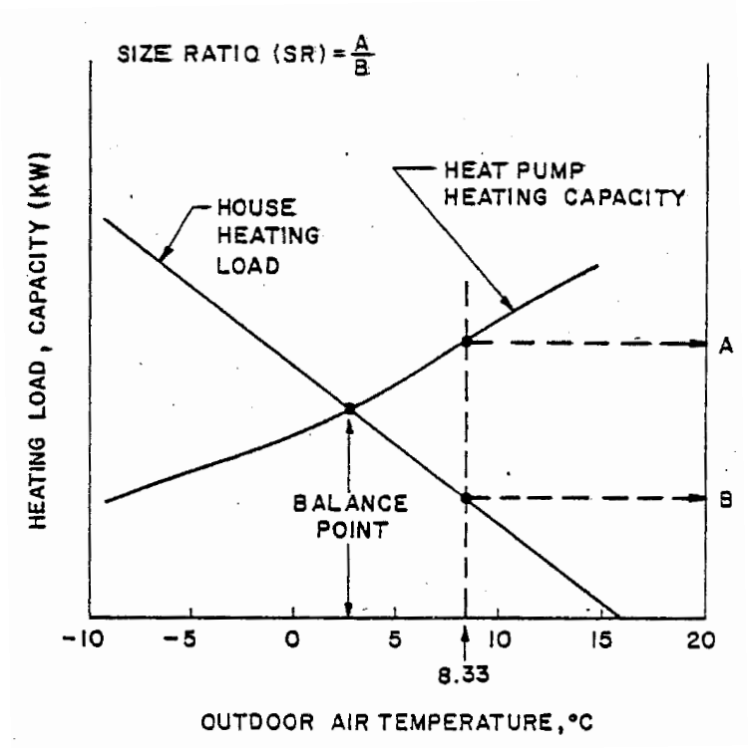

Figure 7: Size Ratio (SR) definition (from Bullock et al., 1980)

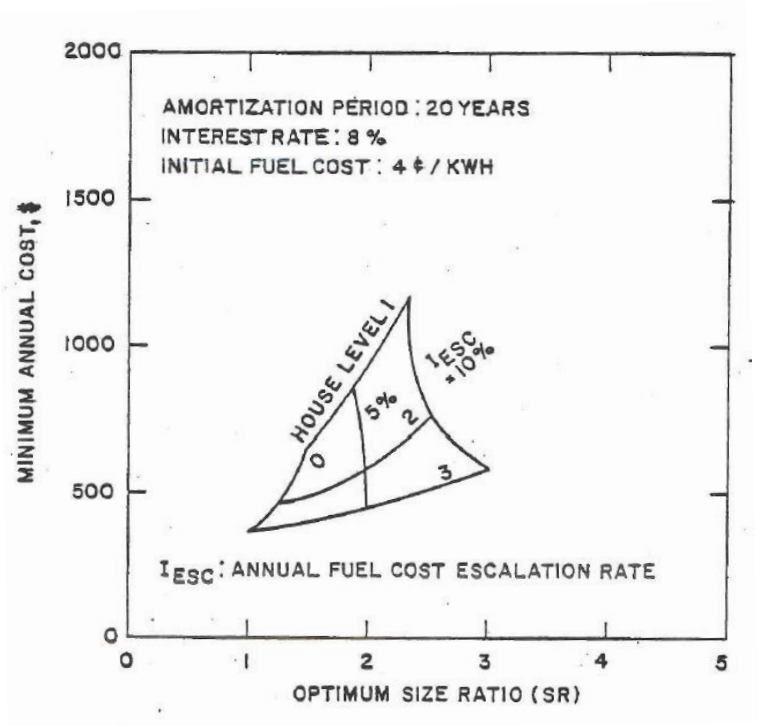

Figure 8: Heat pump minimum annual cost vs. Size Ratio for mild location - climate A (from Bullock et al., 1980)

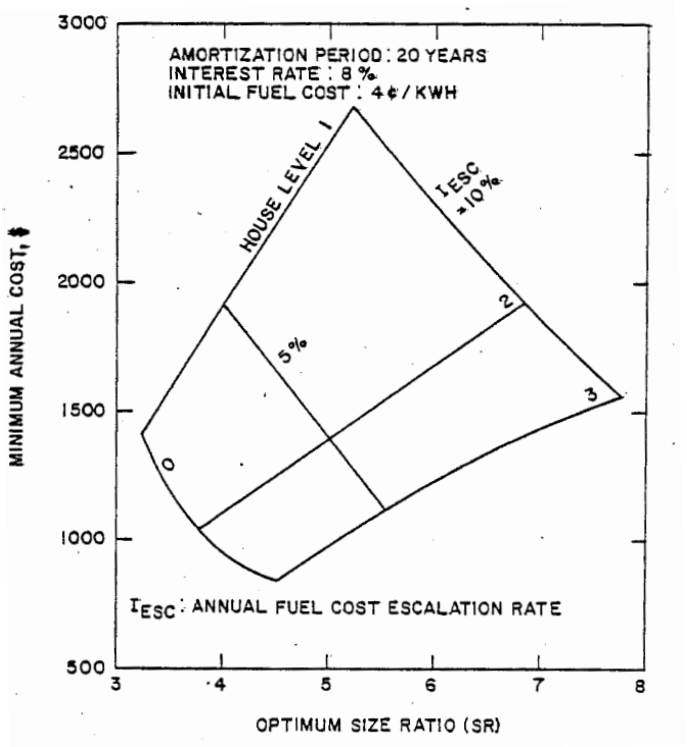

Figure 9: Heat pump minimum annual cost vs. Size Ratio for severe location - climate D (from Bullock et al., 1980)

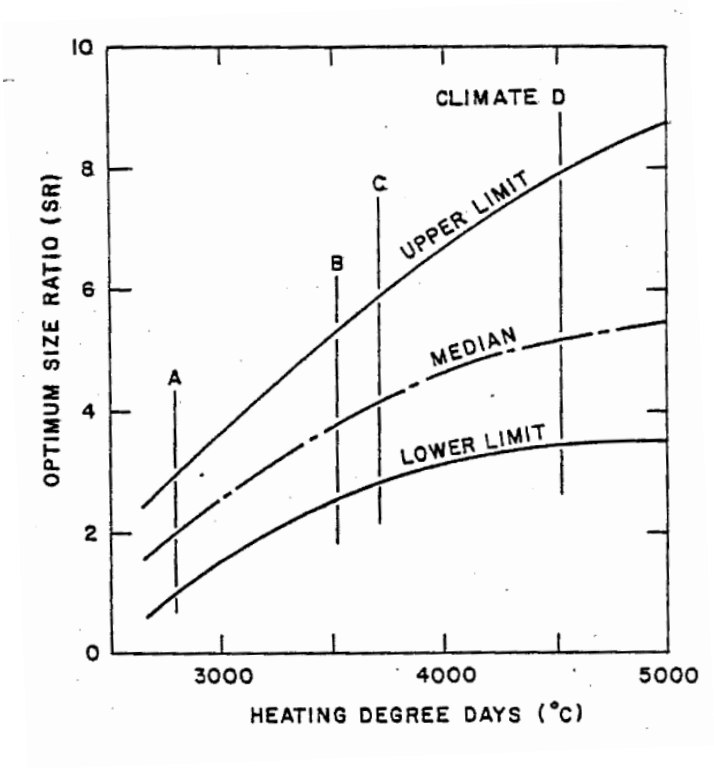

Figure 10: Optimum Size Ratio (SR) vs. heating degree-days (from Bullock et al., 1980)

It is important to note, as pointed out in Bullock et al. (1980), the curves in Figure 9 are not "general" but are tied to the particular set of assumptions about the house and cost parameters used. Also note that the foregoing information was developed for single-speed ASHP equipment of circa 1970 design, far less efficient than current models being marketed in the United States.

From the field testing and computer studies, new product designs were formulated by the Carrier Research group, leading to prototype models that were also tested in the field over the following years. Among the most important features for good cold climate performance included in the prototypes were demand defrost systems, application of properly sized receivers, and minimization of reversing valve thermal losses.

In parallel with the field studies above, the Carrier group also analytically examined the energy savings potential of thermostat night setback control. Results indicated that use of night setback with heat pumps in colder climates could yield modest improvements in heating SPF. But careful system control (especially of the electric supplemental heaters) would be critical. The study concluded that night set back was not recommended for existing heat pump technology at the time (see Bullock, 1978).

The Carrier group was also invited to join Électricité de France (EdF) in a program to investigate electric ASHPs (both air-to-air and air-to-water types) for heating in the French climates. Field tests were conducted on several residences with various existing heating system types and for two large commercial buildings. These studies were reported in papers by Groff et al. (1984) and by Groff and Moreau (1983). From these studies, two prototypes with functions and features for improved cold climate performance were designed and fabricated. These units were installed in U.S. and French homes and were monitored to determine actual performance. A number of the design elements developed for these prototypes were utilized in later Carrier products including a 3 piece heat pump for cold climate applications (pictured in Figure 11) that incorporated an outdoor fan-coil unit, an

indoor fan-coil unit and an indoor compressor box (to enable capture of compressor heat to the indoor environment).

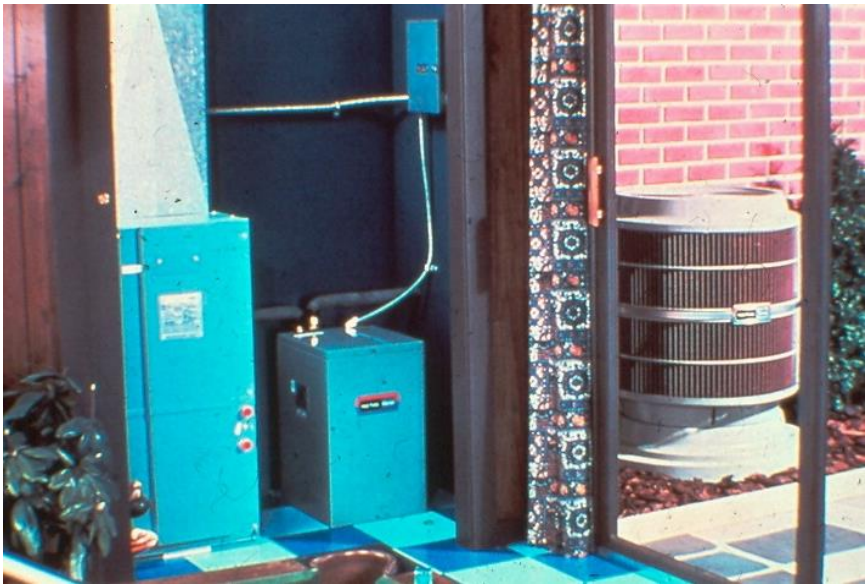

Figure 11: Early 1980's 3-piece ASHP design for northern climate applications

More advanced designs incorporating various approaches for capacity modulation (multiple compressors, multiple speed or displacement compressors, inverter-driven system technology, etc.) can be and have been developed (Lannus, 1993; Hadley et al., 2006) with varying degrees of market success. Variable capacity systems also have an advantage in that they can operate at lower capacity or lower compressor speed in the cooling season, thus avoiding cooling performance penalties that typically accrue from oversizing. Modifications to the vapor compression cycle itself (incorporation of ejectors, multiple stage cycles, etc.) can also be used to boost low temperature capacity and efficiency. The following section discusses some of the more recent developments.

4.2 Recent U. S. R&D Efforts and Developments - Low Outdoor Temperature Air-Source Heat Pumps

4.2.1 Multi-stage compressor system investigation

A conference paper by Bertsch et al. (2006) investigated in detail three heat pump technologies for use in cold climates. The authors first identified the four principle problem areas faced by ASHPs when operating at low outdoor temperatures. The first issue is a lack of heating capacity caused by lower refrigerant flow rates at the low temperatures when the heating load is the largest – which leads to significant need for a backup heating source, usually provided by electric resistance heaters, to supplement the heat pump output. The second issue is that the discharge temperature of the compressor reaches high levels due to the low suction pressures and high compressor pressure ratio experienced at low ambient temperature operation. The third issue is that the heat pump COP decreases quickly under low outdoor temperature operation. The last main problem involves sizing the heat pump capacity. If the heat pump capacity is sized to meet house design heating loads at a very low outdoor temperature, this leads to oversizing for cooling, resulting in frequent cycling and degraded cooling seasonal performance.

Six different heat pump technologies were identified that have the potential to solve some of these issues by varying degrees. Table 2 provides a side-by-side comparison between these

six technologies and a conventional heat pump and shows the number of heating modes, efficiency, output, and discharge temperature of each technology.

Table 2: Comparing different heat pump technologies to a single-stage baseline (Bertsch et al., 2006)

#	Concept	Preferred Compressor*)	Number heat output steps	Relative Efficiency	Relative Heat output	Discharge temperature
1	1-stage cycle	LT	1	100%	100%	High
2	2-stage w. intercooler	2-stage	1	130%	100%	Acceptable
		Sc, Recip, Rot	3	130%	140%	Acceptable
3	2-stage w. economizer	2-stage	1	130%	100%	Low
		Sc, Recip, Rot	3	130%	150%	Low
4	Cascade cycle	Sc, Recip, Rot	1	140%	140%	Low
5	Refrigerant injection	Sc, Screw	2	Comparable	115%	High
6	Oil cooling	Recip, Rot	1	Comparable	Comparable	Acceptable
7	Mechanical subcooling	LT + Sc	2	110%	120%	High

*) Sc…Scroll, Recip…Reciprocating, Rot…Rotary, LT…Low temperature

Three of these technology options were selected for detailed comparison - the two-stage using an intercooler, the two-stage using an economizer and the cascade cycle. It can be seen from Table 2 that these three technologies have the highest relative efficiency and relative heat output with low or acceptable discharge temperatures. The schematic for each of these three technologies is shown in Figure 12.

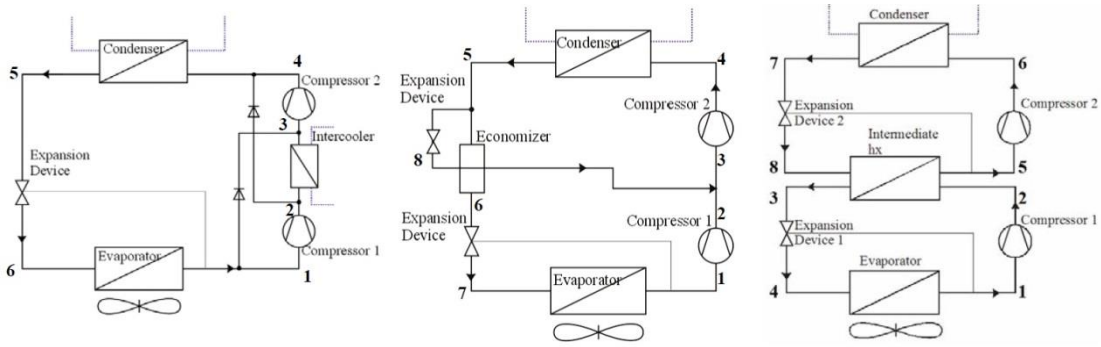

Figure 12: Heat pump schematic - Intercooler (Left) - Economizer (Middle) - Cascade (Right) (Bertsch et al., 2006)

System simulation models were created for each of the three technologies to simulate the heating capacity and performance for comparison. The supply temperature for each was fixed to 50°C (122 °F) which is somewhat higher than typical for single-stage heat pumps (≤100°F). A plot of the COP versus outdoor temperature for each heat pump technology is shown in Figure 13 and is compared to a second law efficiency of 50%. The intercooler and economizer cycles show similar performance at temperatures above 0°C (32°F) while the cascade cycle performs relatively better at colder temperatures. All cycles show COPs above 2 at the low outdoor temperatures indicating reasonably good efficiency during these extremes.

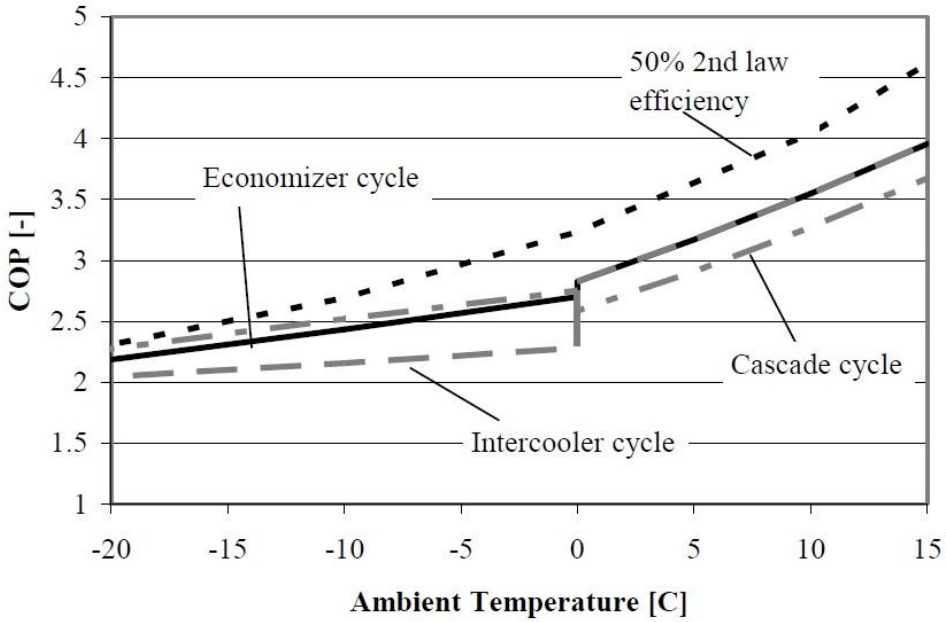

Figure 13: Comparison of the COP for the three technologies compared to a 50% second law efficiency (Bertsch et al., 2006)

The heating capacity compared to a linear heating demand of a building is plotted versus the outdoor temperature for all three technologies in Figure 14. All three cycles have similar capacities at the low ambient temperatures. The only noticeable difference between these technologies is at the warmer ambient temperatures. The cascade cycle COP is considerably lower than that of the economizer and intercooler cycles, and this is most likely due to the sizing selected for the high stage cycle. Bertsch et al. assumed the cascade cycle has an additional outdoor heat exchanger to allow for the high side cycle to operate without the low side cycle. Overall, all three cycles are predicted to be able to satisfy the heating load. The conclusion made from these results and the equipment required is that the two-stage economizer cycle would be the best choice for an ASHP in colder climates.

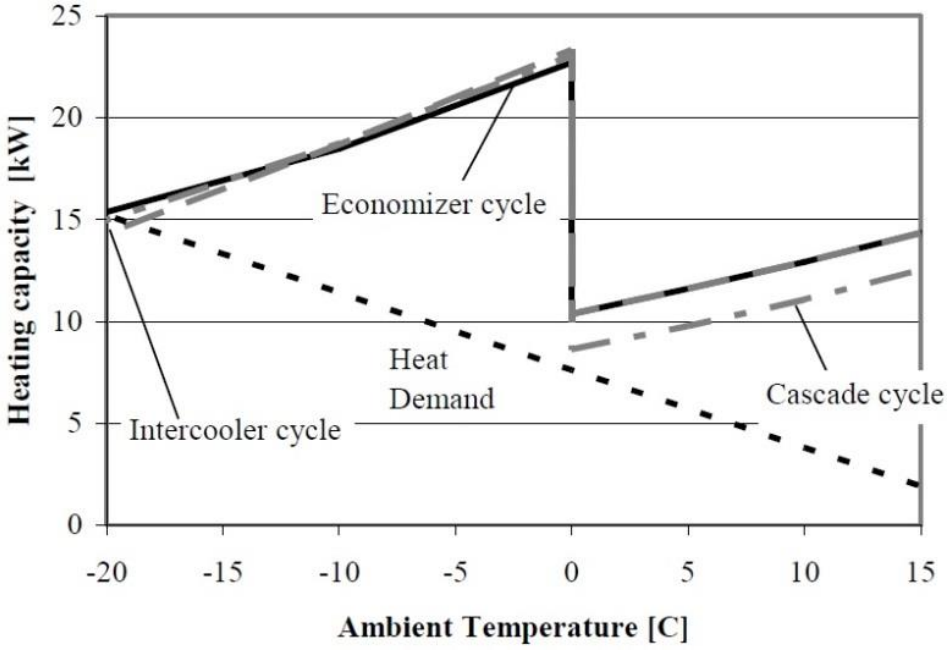

Figure 14: Comparison of the heating capacity for the three technologies (Bertsch et al., 2006)

4.2.2 Vapor injection (VI) heat pump

Heat pumps with compressor vapor injection (VI) can be classified into two fundamental configurations. One utilizes a flash tank also known as an open economizer and the other uses a heat exchanger economizer or closed economizer. Figure 15 shows a schematic of each system. The flash tank cycle uses an expansion valve before a fixed volume tank to separate the liquid and vapor refrigerant at an intermediate pressure. The saturated vapor is drawn from the top of the tank and enters an injection port on the compressor. The saturated liquid is expanded further to the evaporation pressure. For the economizing heat exchanger cycle, the subcooled liquid leaving the condenser is separated into two streams; one is expanded to an intermediate pressure and heated by subcooling the other refrigerant stream through the heat exchanger. The superheated refrigerant enters the injection port on the compressor. If the phase separation process in the flash tank was perfect and the superheat entering the injection port of the compressor from the economizer heat exchanger was zero, the ideal cycles of both systems would be thermodynamically identical (Wang et al., 2009).

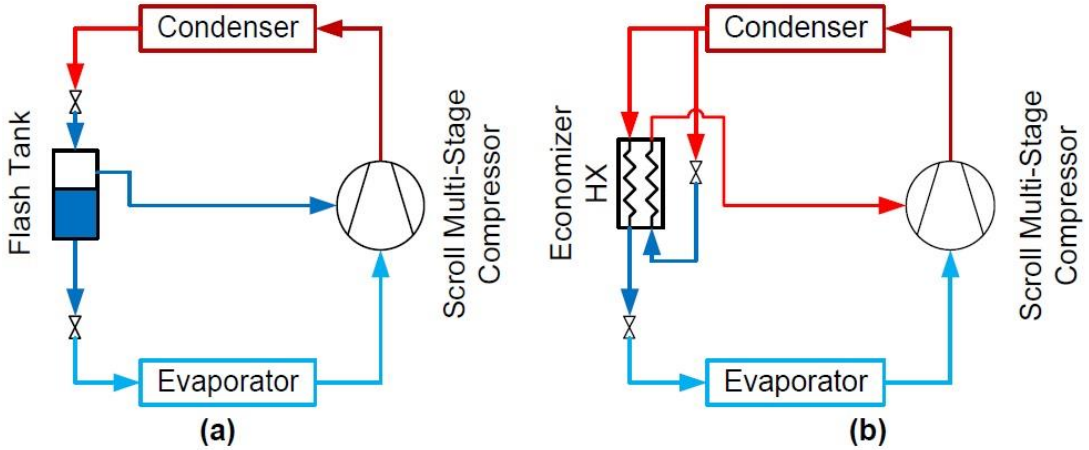

Figure 15: Schematic of two VI cycles with (a) flash tank (b) economizer heat exchanger (Abdelaziz et al., 2011

These systems create a multi-stage compression process within one compressor by mixing the superheated vapor in the compressor with saturated or a smaller degree of superheated vapor. As the number of injection ports is increased to approach continuous injection, the compression process will follow the refrigerant vapor saturation curve. One model predicts that continuous injection will improve the system COP between 18% and 51% for common air-conditioning and refrigeration applications, where higher temperature lift cycles benefit most significantly (Mathison et al., 2011). Abdelaziz and Shen (2012) conducted an optimization analysis of the two cycles in Figure 15. Optimizations were conducted to 1) minimize heat exchanger (HX) area subject to prescribed capacity and COP at rating conditions (47°F or 8.3°C) followed by 2) analysis to maximize system efficiency subject to a minimum capacity constraint at a low temperature operation condition (-15°F or -26.1°C). Their results suggested that the flash tank cycle of Figure 15(a) offers both lower system HX sizes and better performance at the low ambient condition.

Experimental results on an 11 kW R410a heat pump with flash tank VI showed about 30% heating capacity improvement with 20% COP gain at the ambient temperature of −17.8°C (0°F) when compared to a conventional system having the same compressor displacement volume (Wang et al., 2009). The system capacity for both heating and cooling compared to the conventional system is shown in Figure 16 as a function of the outdoor temperature. The system heating and cooling capacity increases when vapor injection is used compared to the conventional system.

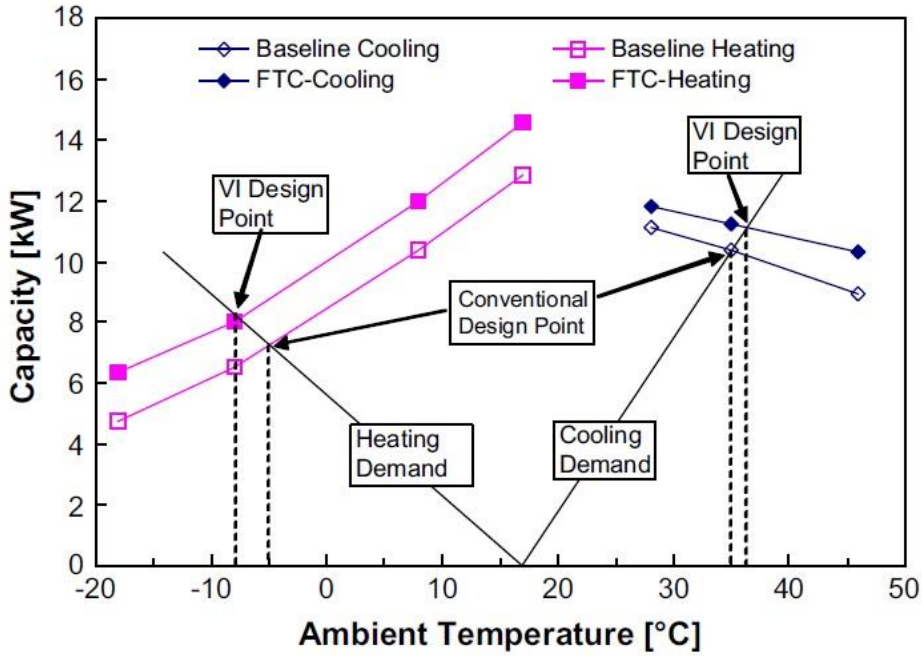

Figure 16: Flash tank VI cycle (FTC) compared to conventional (baseline) heat pump (Wang et al., 2009

When comparing the two types of VI cycles, experimental results have shown the flash tank cycle to have a heating capacity and COP of 10.5% and 4.3% higher, respectively, than the economizing heat exchanger cycle (Ma and Zhao, 2008). A literature review of VI cycles concluded that the flash tank cycle is more favorable in terms of the performance improvement and cost while the economizing heat exchanger has the advantage of wider VI operating range (Xu et al., 2011). For R-410A, there have been some experimental and theoretical investigations of the air-source, vapor injection heat pump, but additional experimental results are needed to fully understand the various VI cycle options (Rohm et al., 2011).

VI cycle concepts utilizing multi-port compressors (one implementation of multi-stage VI compression) have also been investigated (Song, 2013; Ramaraj, 2012; Mathison et al., 2011). Figure 17 illustrates the cycle concept (a) and an example implementation in a scroll compressor (b). Previous theoretical and experimental work has shown that economizing holds significant potential to improve the performance of vapor compression equipment. Mathison et al. (2011) predicted that the maximum performance improvement with economizing can be achieved by continuously injecting two-phase refrigerant to maintain a saturated vapor state in the compressor. For an R-410A cycle evaporating at 5°C and condensing at 40°C, the cycle model predicts that economizing will improve the COP by approximately 18% in this limiting case. The benefits are even greater for a larger temperature lift application, such as a cold climate heat pumps; the model predicts that economizing can provide up to a 51% improvement in COP for a cycle using R-404A with an evaporation temperature of -30°C and a condensing temperature of 40°C. However, continuously injecting refrigerant is not only beyond the capabilities of current compressors, but also requires the development of equipment to continuously supply refrigerant to the compressor at the desired pressure and quality. In addition, injecting a two-phase mixture introduces the possibility for damage to the compressor if the evaporation process within the compressor is not well-understood.

Mathison (2011) demonstrated that using a finite number of injection ports and saturated vapor in place of a two-phase mixture provides a practical means for approaching the

limiting cycle performance. For the R-410A cycle evaporating at 5°C and condensing at 40°C, the model predicted that injecting saturated vapor through three ports will provide a 12% improvement in COP, which is approximately 69% of the maximum benefit provided by economizing with continuous injection of two-phase refrigerant. Therefore, the development of the economized cycle currently focuses on using saturated vapor injection with two or three ports.

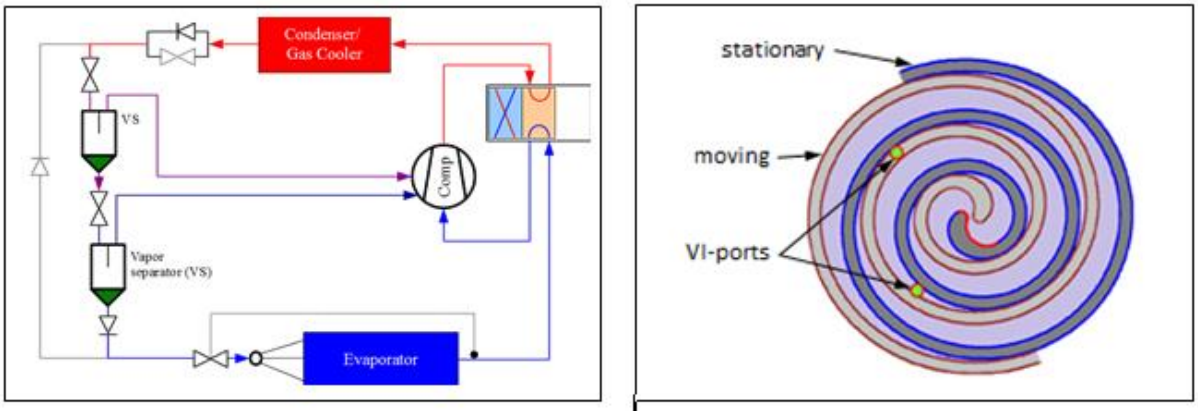

Figure 17: Multi-port VI compressor concept

4.2.3 Two-stage ASHPs with economizing

The only difference between a two-stage economizer (see schematic in Figure 12 (middle)) and VI cycle is two individual compressors are used with a mixing chamber in between instead of directly injecting vapor into a compressor chamber of the compressor. By compressing the refrigerant in stages, a second-law-based thermodynamic analysis shows the increase in irreversible losses at high-temperature differences can be minimized. A two-stage R-134a refrigeration system operating at -30°C evaporating and 60°C condensing has a 24% improvement in performance compared to a single-stage system (Zubair et al., 1996). Analysis on a cascade system highlights the reduction of entropy generation when compressing in stages. Going from 1 to 2 stages reduced the superheat losses significantly from 94 kJ/K-hr to 0.106 kJ/K-hr to reach an overall reduction of desuperheating entropy generation of 78% (Ratts et al., 2000).

An R-134a two-stage heat pump with both an economizing heat exchanger and a flash tank was used for heating water from a waste energy source. In spite of the higher source temperatures used, the experimental results demonstrated that the frequency control of the high-stage compressor to control the intermediate pressure resulted in an ability to improve the performance by as much as 5.2% as compared to the single-stage system without economizing under identical heat source conditions (Kwon et al., 2013). A normalized pressure was calculated using the three system pressures to identify the optimal operating point for fixed heat source temperatures. A plot of three different source temperatures for COP versus the normalized pressure is shown in Figure 18.

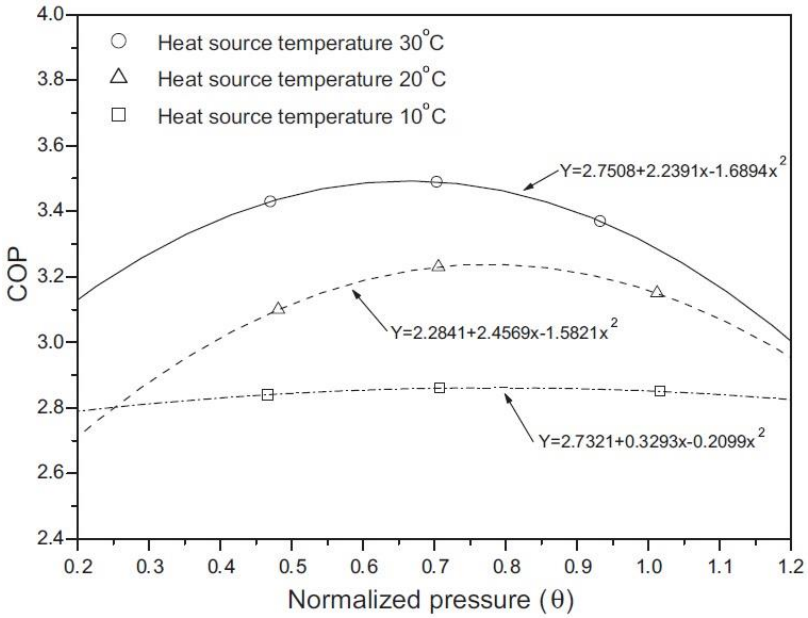

Figure 18: COP vs. normalized pressure of two-stage heat pump (Kwon et al. 2013

An R-410A two-stage heat pump with an economizing heat exchanger was lab tested down to ambient temperatures of -30°C (-22 °F), achieving a heating capacity and COP of roughly 11 kW and 2.1 respectively (Bertsch et al., 2008). The plots of the experimental results compared to the simulation of the system heating capacity and COP are shown in Figure 19. This capacity is about 85% of that measured for single-stage operation at the US rating condition of 8.3°C (47°F) vs. the ≥75% DOE goal listed in Table 1. The two-stage heat pump is shown to have much larger heating capacities than a conventional heat pump at low outdoor temperatures. Note that the system's measured space heating capacity in two-stage operation at ~-27°C (~-17°F) is very close to that at the standard U.S. rating condition of 8.3°C (47°F) when operating in single-stage mode. The system could also be easily built from off-the-shelf components with little modifications which identifies the commercialization potential of a two-stage heat pump with economizing heat exchanger. A field test prototype was built and tested in Indiana – results are discussed later in the Task2/3 part of this report.

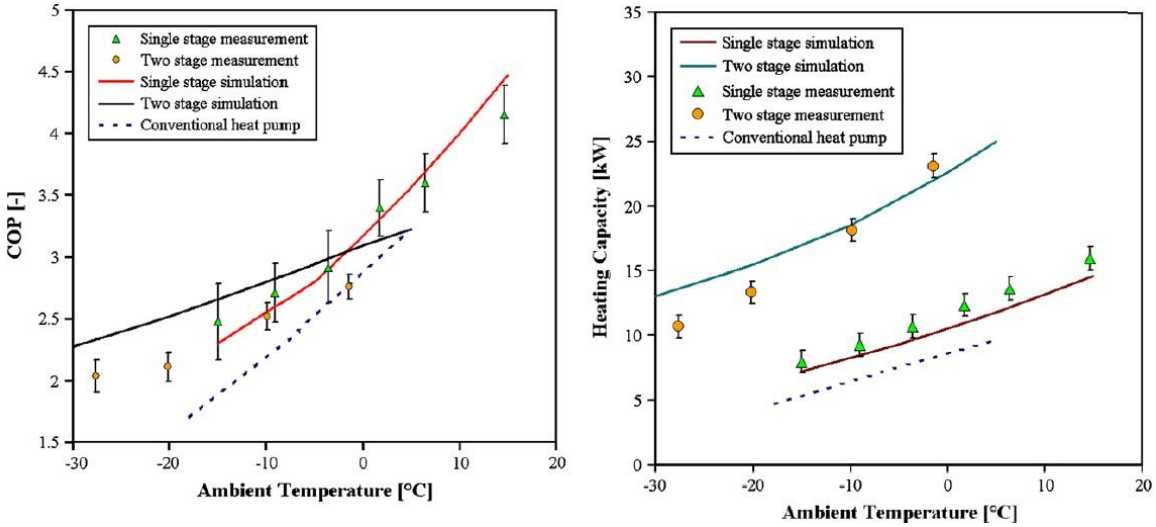

Figure 19: Experimental results of two-stage heat pump compared to simulation results; manufacturer's data was used to indicate performance of conventional HP (Bertsch et al. 2008

4.2.4 Oil-flooded compressor concept investigation

The oil flooding concept utilizes oil injection into the compressor suction port(s) to absorb the heat of compression (reducing discharge temperature) and approach an isothermal compression process (Bell, 2011). Figure 20 illustrates a cycle schematic and p-h diagram of the concept. The addition of compressor flooding with regeneration in vapor compression systems results in a more isothermal compression process that can have a significant beneficial impact on system efficiency for large temperature lifts. For refrigerants with large pressure differences across the compressor, the use of a hydraulic expander can also help to recapture some of the work of compression of the flooding liquid. The engineering challenges in implementation of this technology are reasonable, which suggests that it could be applied readily in new equipment. Analyses indicate this concept has both capacity and efficiency advantages over VI cycles for low-temperature applications (Bell et al., 2011). In particular, the injection of oil results in an increase in refrigerant mass flow rate and overall isentropic efficiency and a decrease in the compressor discharge temperature. The analyses conducted so far clearly suggest that designing an efficient scroll compressor with oil injection for application to a low-source-temperature ASHP application will be possible with respect to energy performance and manufacturability.

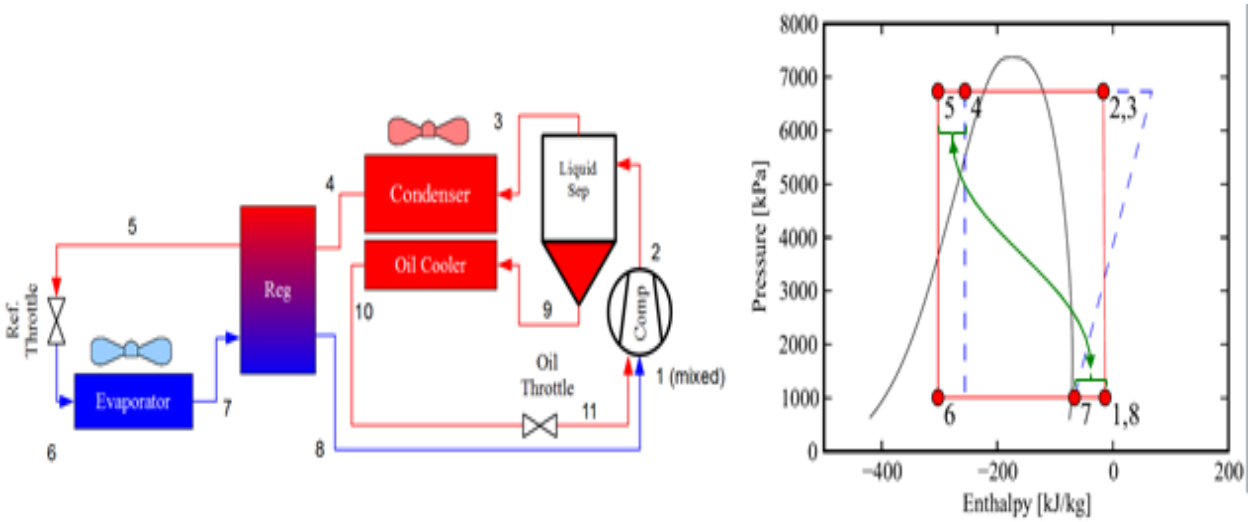

Figure 20: Schematic (left) and p-h cycle diagram (right) of flooded compressor cycle concept – from Bell (2011)

4.2.5 Cold climate field tests

A field test was performed in several northern U. S. locations on a commercially available, multi-capacity ASHP (Hadley et al., 2006) – *Note – product no longer manufactured today*. The manufacturer's data indicate a heating COP of 2.0 at -23.3°C (-10°F) for the heat pump, as shown in Table 3. Additional heating COPs at different ambient temperatures are compared to those of a standard ASHP.

Table 2: Manufacturer's heating COP data for field test ASHP designed for cold climates (CCHP) compared to a conventional air source heat pump (Std. ASHP) (Hadley et al., 2006)

Outdoor Air Temp.	-20°F	-10°F	0°F	10°F	20°F	30°F	40°F	50°F
CCHP	1.9	2.0	2.2	2.2	2.5	2.8	3.1	3.3
Std. ASHP	na	na	2.0	2.3	2.5	2.8	3.1	3.6

Five of the advanced heat pumps were monitored over a winter in Oregon and Idaho. Six months after the installation, one heat pump had a compressor failure that required

replacement. The reason for the failure was never determined. Another complication occurred where a booster compressor never engaged at another location. The measured average heating COP for outdoor temperatures between -23.3°C and -20.5°C (-10°F and -5°F) was 1.2, about 40% lower than the manufacturer's data indicated. The results for all five heat pumps at different temperature bins are shown in Table 4. Overall the average field-measured COPs are considerably lower than the manufacturer's published values.

Table 3: Experimental results of the measured heating COP for all 5 locations (Hadley et al., 2006)

Outdoor Temperature Bin	-15°F to -10°F	-10°F to -5°F	-5°F to 0°F	0°F to 5°F	5°F to 10°F	10°F to 15°F	15°F to 20°F	20°F to 25°F	25°F to 30°F	30°F to 35°F	35°F to 40°F	40°F to 45°F	45°F to 50°F	50°F to 55°F
Chiloquin	-	-	-	-	-	1.3	1.5	1.6	1.6	1.7	1.9	1.9	1.8	2.0
Burley	-	-	1.7	1.1	1.2	1.3	1.4	1.5	1.6	1.7	1.6	1.7	1.7	1.6
Paul	1.5	1.5	1.6	1.6	1.6	1.6	1.6	1.7	1.8	1.9	2.0	2.1	2.1	1.9
Rigby	1.3	1.2	1.2	1.3	1.3	1.3	1.4	1.4	1.5	1.6	1.6	1.6	1.5	1.4
Ashton	-	1.0	1.4	1.3	1.2	1.2	1.2	1.3	1.3	1.3	1.4	1.4	2.0	1.7
Average	**1.4**	**1.2**	**1.5**	**1.3**	**1.3**	**1.4**	**1.4**	**1.5**	**1.6**	**1.6**	**1.7**	**1.7**	**1.8**	**1.7**

4.2.6 Summary – Recent R&D studies

The simulation and experimental results of several different heat pump cycles were presented that showed sufficient capacity and performance at low outdoor temperatures for cold climates compared to conventional single-stage ASHPs. The two-stage cycle presents an easier commercialization path due to the use of off-the-shelf components. Additional field testing is required to further validate the technology as market ready due to complications seen in previous field testing.

4.3 Complementary CCHP Market Promotion Activities

The US Northeast Energy Efficiency Partnership (NEEP) established a voluntary specification for cold climate ASHPs to help promote wider use of heat pumps in the northern parts of the US and the Northeast area in particular. The specification was initially established in late 2014 with the most recent update effective January 1, 2017, and can be downloaded from the NEEP web site http://www.neep.org/initiatives/high-efficiency-products/emerging-technologies/ashp/cold-climate-air-source-heat-pump. It covers only air-to-air type variable-speed ASHPs (air-to-water ASHP and GSHPs are excluded). In order to be listed as complying with the NEEP specification, manufacturers' products must have a rated SCOPh ≥2.93 (US HSPF ≥10) for US climate region IV (moderate heating requirements) per AHRI Standard 210/240. In addition they must report space heating capacity and COP (from laboratory test data or engineering data) for at least 8.3 °C, -8.3 °C, and -15 °C (47 °F, 17 °F, and 5 °F) and at lower temperatures if available.

As of March 24, 2017, nearly 300 individual variable-speed ducted and ductless heat pump models were listed as complying with the latest NEEP CCHP specification V2.0. The list can be downloaded from the link above. Over 80% of the products listed are ductless types, either single-zone (2.6 to 9.4 kW nominal heating capacity) or multi-zone (2.9 to 14.1 kW nominal capacity). The remainder are centrally ducted (US type central air distribution systems) of about 6.5 to 16.5 kW nominal heating capacity.

The Electric Power Research Institute (EPRI) has also developed a specification for advanced ASHPs or Next Generation Heat Pumps (NextGen) (Domitrovic, 2017). This specification has two different levels or tiers. Under Tier 1 ASHP products must meet the

same SCOPh requirement as for the NEEP specification above (≥2.93) but must also have space heating capacity at -8.3 °C ≥80% of the rated capacity at 8.3 °C. Under Tier 2, products must have a rated SCOPh ≥3.81 (US HSPF ≥13) for US climate region IV and a space heating capacity at -15 °C ≥80% of the rated capacity at 8.3 °C. Only about 7% of the products listed on the NEEP website currently meet the more stringent Tier 2 requirements.

5 CONCLUDING REMARKS

All of the advanced ASHP system concepts discussed above can result in improved performance under extreme cold outdoor conditions. All address in one way or another the key challenge for electric-driven ASHPs under these conditions – to maintain or boost heating capacity and thereby reduce usage of backup electric resistance heating, thus yielding better heating SPFs. They also have another characteristic in common – all involve increased system complexity which will result in increased cost compared to conventional ASHPs. A number of viable ASHP products designed for cold climate applications now exist with rated performance that approaches the annual space heating efficiencies of GSHPs, gas-driven ASHPs, or other residential HVAC systems in cold climate locations.

6 ACKNOWLEDGEMENTS

The assembly of this report and the ORNL technical activities described herein are supported by the U. S. Department of Energy, Building Technologies Office (DOE/BTO) under Contract No. DE-AC05-00OR22725 with UT-Battelle, LLC. The official report number is ORNL/TM-2013/472.

The Purdue technical activities have been supported by the U. S. Department of Defense, Environmental Security Technology Certification Program (ESTCP), Energy and Water Projects, Cold Climate Heat Pump 201136, and by the U. S. Department of Energy under Award Number DE-EE0003842.

7 REFERENCES

Abdelaziz O. A., B. Shen, Z. Gao, V. D. Baxter, and I. Iu. 2011. “Development of a high performance air source heat pump for the US market.” Proceedings of the 10th IEA Heat Pump Conference, Tokyo, Japan. CD rom format only.

Abdelaziz O. A. and B. Shen. 2012. “Cold Climates Heat Pump Design Optimization,” *ASHRAE Transactions*, Vol. 112, Part 1.

Abdelaziz O. A. 2013. “ORNL Cold Climate – Experimental Investigations,” presentation at Annex 41, 1st Working Meeting, Purdue University, July 1.

AHRI 2008. ANSI/AHRI Standard 210/240-2008, “Performance Rating of Unitary Air-Conditioning and Air Source Heat Pump Equipment,” Air-Conditioning, Heating, and Refrigeration Institute, Arlington, VA, USA.

AHRI 2010-2017. Central Air Conditioners and Air-Source Heat Pumps Historical Data. Retrieved from AHRI website (www.ahrinet.org) in December 2010 and in January 2017).

AHRI 2012. “HVAC&R & Water Heating Industry Statistical Profile,” 2012 Edition.

ASHRAE 2010. ANSI/ASHRAE Standard 55-2010, “Thermal Environmental Conditions for Human Occupancy,” American Society of Heating, Refrigerating, and Air-Conditioning Engineers, Atlanta, GA, USA.

Bach C. K., J. A. Braun, E. A. Groll, and W. T. Horton. 2013. “Cold Climate Heat Pumps Performance improvement by modification of compression process and cycle,” presentation at Annex 41, 1st Working Meeting, Purdue University, July 1.

Bell I. H. 2011. “Theoretical and Experimental Analysis of Liquid Flooded Compression in Scroll Compressors,” PhD Thesis, Herrick Laboratories, Purdue University, West Lafayette, IN, USA.

Bell I. H., E. A. Groll, and J. E. Braun. 2011. “Performance of Vapor Compression Systems with Compressor Oil Flooding and Regeneration,” *International Journal of Refrigeration*, Vol. 34, No. 1, pp. 225-233.

Bertsch S. S. 2005. “Theoretical and experimental investigation of a two stage heat pump cycle for Nordic climates,” (Doctoral dissertation, Master’s thesis, Mechanical Engineering, Herrick Labs 2005-13P, Report).

Bertsch S. S. and E. A. Groll. 2006. “Air Source Heat Pump for Northern Climates Part I: Simulation of Different Heat Pump Cycles,” Proceedings of the 11th International Refrigeration and Air Conditioning Conference at Purdue.

Bertsch S. S. and E. A. Groll. 2008. “Two-stage air-source heat pump for residential heating and cooling applications in northern US climates,” *International Journal of Refrigeration*, Vol. 31(7), pp. 1282-1292.

Bucher M. E., C. M. Grastataro, and W. Coleman. 1989. “Heat Pump Life and Compressor Survival in Diverse Climates,” EPRI Report No. CU-6254, February 1989 (AEP).

Bullock C. E. 1978. “Energy Savings through Thermostat Setback with Residential Heat Pumps,” *ASHRAE Transactions*, Vol. 84, Part 1.

Bullock C. E., G. C. Groff, and W. R. Reedy. 1980. “Sizing of Air-to-Air Heat Pumps for Northern Climate Residential Heating Applications,” Proceedings of the International HVAC Congress, Berlin, Germany, April 17-18.

Caskey S. L., E. A. Groll, and W. J. Hutzel. 2013. “Cold Climate Heat Pump Field Demonstration of Air-Source Heat Pump with Two-Stage Compression and Economizing,” presentation at Annex 41, 1st Working Meeting, Purdue University, July 1.

Caskey S. L. 2013. “Cold Climate Field Test Analysis of an Air-Source Heat Pump With Two-Stage Compression and Economizing,” Master’s Thesis, Purdue University, Ray W. Herrick Laboratories, West Lafayette, IN.

Census Bureau, U.S. 2016. Census Bureau’s Characteristics of New Single-Family Homes Reports.

Conti, J., and P. Holtberg. 2011. “International Energy Outlook 2011,” Washington: Independent Statistics and Analysis of US Energy Information Administration.

Department of Defense, U.S., Energy Security Task Force, Office of the Under Secretary of Defense. 2009. The WSTIAC Quarterly, Vol. 9, No. 1.

Department of Energy, U.S. 2011. “Buildings Energy Databook,” Office of Energy Efficiency & Renewable Energy.

Domitrovic, R., 2017. Personal communication to Van Baxter, April 7.

Energy Independence and Security Act of 2007. Public Law, (110-140), 2.

Energy Information Administration, U.S. (EIA) 2009. “Residential Energy Consumption Survey,” Tables HC6.8, HC6.9, HC6.10, and HC6.11. Accessed September 2013.

Energy Information Administration, U.S. (EIA) 2013. “Annual Energy Outlook (AEO).” Early Release Overview, Release Date: December 5, 2012, Report Number: DOE/EIA-0383ER.

Energy Information Administration, U.S. (EIA) 2013. “Annual Energy Outlook 2013,” DOE/EIA-0383(2013), retrieved September 2013.

Executive Order. 2009. 13514. Federal Leadership in Environmental, Energy, and Economic Performance.

Groff G. C. and W. R. Reedy. 1978. “Investigation of Heat Pump Performance in the Northern Climate through Field Monitoring and Computer Simulation,” *ASHRAE Transactions*, Vol. 84, Part 1.

Groff G. C., C. E. Bullock, and W. R. Reedy. 1978. “Heat Pump Performance Improvements for Northern Climate Applications,” pp. 838-846 in Proceedings of the 13th International Energy Conversion Engineering Conference, San Diego, CA, USA, September. Society of Automotive Engineers. Paper no. 789455.

Groff G. C., W. R. Reedy, and C. E. Bullock. 1979. “Recent Investigation of Air-Source Heat Pump Performance in Cold Climates,” Paper E1-25 in Proceedings of the 15th International Congress of Refrigeration, Venice, Italy, September 23-29. International Institute of Refrigeration.

Groff G. C. and J. P. Moreau. 1983. “An Investigation of Air-to-Water Heat Pump Performance in New and Existing French Homes,” *ASHRAE Transactions*, Vol. 89, Part 1.

Groff G. C. and R. E. Ertinger. 1984. “Heat Pumps in the USA – Projections for the Future,” Published in the Proceedings of the 1st International Energy Agency Heat Pump Conference, Graz, Austria, May.

Groff G. C., C. E. Bullock, and R. E. Hough. 1984. “An Investigation of Electric Heat Pumps Applied to Commercial Buildings,” Published in the Proceedings of the 1st International Energy Agency Heat Pump Conference, Graz, Austria, May.

Hadley A., J. Callahan, and R. Stroh. 2006. “Without strip heat: In-Situ monitoring of a multi-stage air source heat pump in the Pacific Northwest,” Bonneville Power Administration.

Khowailed G., K. G. Sikes, and O. A. Abdelaziz. 2011. “Preliminary Market Assessment for Cold Climate Heat Pumps,” Oak Ridge National Laboratory report ORNL/TM-2011/422, August.

Kwon O., D. Cha, and C. Park. 2013. “Performance evaluation of a two-stage compression heat pump system for district heating using waste energy,” *Energy*.

Lannus A. 1993. “Expanding the Limits: Heat Pump Technology and markets in North America,” p. 373-380 in *Heat Pumps for Energy Efficiency and Environmental Progress*. Proceedings of the 4th International Energy Agency Heat Pump Conference, Maastricht, The Netherlands, April 26-29.

Lapsa M. and G. Khowailed. 2011. “The Evolution of the U.S. Heat Pump Market,” Proceedings of the 10th International Energy Agency Heat Pump Conference, Tokyo, Japan.

Lovvorn N., C. C. Hiller, and A. Bartolucci. 2001. “Heat Pump Life in Alabama—Revisited: A Follow-Up Survey 13 Years Later,” EPRI, Palo Alto, CA, and Alabama Power Company, Birmingham, AL: 2001. 1006265.

Lovvorn N. and C. C. Hiller. 2002. “Heat Pump Life Revisited,” *ASHRAE Transactions*, Vol. 108, Part 2.

Mahderekal I., B. Shen, E. A. Vineyard. 2012. “System Modeling of Gas Engine Driven Heat Pump,” Proceedings of 14th International Refrigeration and Air Conditioning Conference at Purdue, West Lafayette, IN.

Mathison M. M., J. E. Braun, and E. A. Groll. 2011. “Performance Limit for Economized Cycles with Continuous Refrigerant Injection,” *International Journal of Refrigeration*, Vol. 34, pp. 234-242.

Mathison M. M. 2011. “Modeling and Evaluation of Advanced Compression Techniques for Vapor Compression Equipment,” PhD Thesis, Purdue University, Ray W. Herrick Laboratories, West Lafayette, IN.

Pientka K. A. 1987. “Heat Pump Service Life and Compressor Longevity in a Northern Climate,” *ASHRAE Transactions*, Vol. 93, Part 1.

Ramaraj S. 2012. “Vapor compression enhancements for cold climate heat pumps,” Master Thesis, Herrick Laboratories, Purdue University, West Lafayette, IN, USA.

Rice, C. K., B. Shen, and S. S. Shrestha, 2015, *An Analysis of Representative Heating Load Lines for Residential HSPF Ratings*, ORNL TM-2015/281, UT-Battelle LLC, Oak Ridge National Laboratory, July.

Rice, C. K., B. Shen, and S. S. Shrestha, 2016. *Revised Heating Load Line Analysis: Addendum to ORNL/TM-2015/281*, ORNL/TM-2016/293, UT-Battelle LLC, Oak Ridge National Laboratory, July.

Ratts E. B. and J. S. Brown. 2000. “A generalized analysis for cascading single fluid vapor compression refrigeration cycles using an entropy generation minimization method,” *International Journal of Refrigeration*, Vol. 23(5), pp. 353-365.

Rohm C. W. and M. S. Kim. 2011. “Effects of intermediate pressure on the heating performance of a heat pump system using R410A vapor-injection technique,” *International Journal of Refrigeration*, Vol. 34(8), pp. 1911-1921.

Roth K. W., D. Westphalen, J. Dieckmann, S. D. Hamilton, & W. Goetzler. 2002. “Energy consumption characteristics of commercial building HVAC systems Volume III: Energy savings potential,” Report prepared by TIAX LLC for DOE Building Technologies Program.

Ryan J. D. and G. C. Groff. 2002. North American Market Overview. pp. 26-37 in *Heat Pumps – Better by Nature*. Proceedings of the 7th International Energy Agency Heat Pump Conference, Beijing, China, May 19-22.

Shen B. and C. K. Rice. 2012. “Multiple-Zone Variable Refrigerant Flow System Modeling and Equipment Performance Mapping,” Conference CD of ASHRAE 2012 Winter Conference, Chicago, IL.

Shen B., O. Abdelaziz, and C. K. Rice. 2012a. “Auto-Calibration and Control Strategy Determination for a Variable-Speed Heat Pump Water Heater Using Optimization,” *HVAC&R Research*, Vol. 18(5), pp. 904–914, 2012.

Shen B., C. K. Rice., and E. A. Vineyard. 2012b. “Development of 20 IEER Rooftop Units – A Simulation Study,” Proceedings of 14th International Refrigeration and Air Conditioning Conference at Purdue, West Lafayette, IN.

Shen B. 2013. “Cold Climate Heat Pump – ORNL System Modeling and Analysis,” presentation at Annex 41, 1st Working Meeting, Purdue University, July 1.

Shen, B., S. S. Shrestha, and O. A. Abdelaziz. 2013. “Assessment of Main Strategies for Achieving Performance Targets for Cold Climate Heat Pump,” draft ORNL Report (under review), February, 2013.

Song. 2013. “Modeling and experimental validation of multi-port vapor injected scroll compressor,” Master Thesis, Herrick Laboratories, Purdue University, West Lafayette, IN, USA.

Wang S. and A. Majumdar. 2004. “Digital Scroll Technology,” *ISHRAE Journal*, January-March, Issue 2004.

Wang X., Y. Hwang, and R. Radermacher. 2009. “Two-stage heat pump system with vapor-injected scroll compressor using R410A as a refrigerant,” *International Journal of Refrigeration*, Vol. 32(6), pp. 1442-1451.

Xu X., Y. Hwang, and R. Radermacher. 2011. “Refrigerant injection for heat pumping/air conditioning systems: literature review and challenges discussions,” *International Journal of Refrigeration*, Vol. 34(2), pp. 402-415.

Zubair S. M., M. Yaqub, and S. H. Khan. 1996. “Second-law-based thermodynamic analysis of two-stage and mechanical-subcooling refrigeration cycles,” *International Journal of Refrigeration*, Vol. 19(8), pp. 506-516.

TASKS 2 AND 3 – SIMULATION RESULTS AND PROTOTYPE LAB AND FIELD EXPERIMENTS

1 INTRODUCTION

In 2010 the U.S. Department of Energy's Building Technology Office (DOE/BTO) solicited R&D proposals focused on advancing heat pump technology for cold climate applications – i.e. CCHPs. DOE's CCHP performance targets provided in that solicitation are listed in Table 1 of the Task 1 report. In 2013, DOE modified those goals somewhat in light of analyses results highlighted in Task 4. The revised targets are in Table 5 below; very similar to the 2010 targets with some modification to the nominal heating capacity target and removal of specific COP targets. ASHPs continued to be the primary technology focus.

Table 4: U.S. CCHP performance targets – 2013

Outdoor Temperature	Heating Capacity
8.3°C (47°F)	9-21 kW (2.5-6 tons), nominal rating
-25°C (-13°F)	≥75% of nominal rating

U.S. CCHP R&D efforts described in the Task 1 report and this Task 2/3 report are focusing on analyses and experimental (lab and field) investigation of several advanced VC cycles for ASHPs. Vapor injection (VI) cycle concepts, two-capacity compressors, variable speed (VS) compressors, parallel compressors, two-stage cycles with economizers, a liquid-flooded compressor cycle concept, and several other advanced cycle approaches have been investigated.

In the sections that follow, current U.S. R&D results under Tasks 2 and 3 of Annex 41 are summarized for three cycle concepts identified in Task 1 as among the most promising for meeting the goals noted in Table 5.

2 TWO-STAGE ECONOMIZER SYSTEM

Research at Purdue University's Herrick Labs identified a number of cycle concepts that could be useful for ASHPs in cold climate applications (Bertsch et al., 2006). Of these, three were seen to have the highest relative efficiency and relative heat output with low or acceptable discharge temperatures and were selected for detailed comparison – the two-stage using an intercooler, the two-stage using an economizer, and the cascade cycle. Figure 21 illustrates the three cycles.

System simulation models were created for each of the three technologies to simulate the heating capacity and performance for comparison. The heating supply temperature for each was fixed to 50°C (122°F). Both the intercooler and economizer cycles showed similar performance at temperatures above 0°C (32°F) while the cascade cycle performed relatively better at colder temperatures. All cycles showed COPs above 2 at the low outdoor temperatures indicating reasonably good efficiency during these extremes. All three cycles had similar capacities at the low ambient temperatures. The only noticeable difference between these technologies is at the warmer ambient temperatures. The cascade cycle COP is considerably lower than that of the economizer and intercooler cycles, and this is most likely due to the sizing selected for the high-stage cycle. Bertsch et al. (2006) assumed the cascade cycle has an additional outdoor HX to allow for the high side cycle to operate without the low side cycle. Overall, all three cycles are predicted to be able to satisfy the heating load. The conclusion made from these results and the equipment required (relative

cycle complexity) is that the two-stage economizer cycle would be the best choice for an ASHP in colder climates.

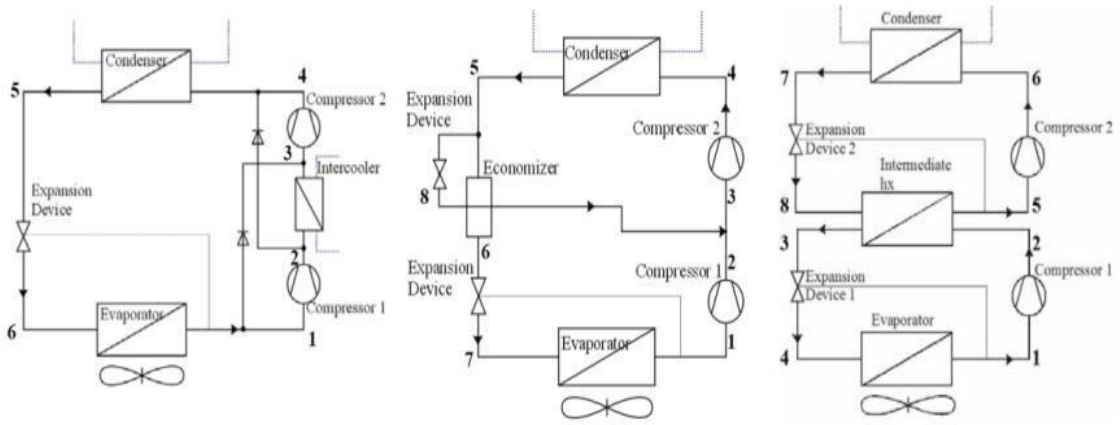

Figure 21: Heat pump cycle schematics - Intercooler (left), Economizer (middle), Cascade (right) (Bertsch et al., 2006

A two-stage, economizer system using R-410A was experimentally tested down to ambient temperatures of -30°C (-22°F), achieving a heating capacity and COP of roughly 11 kW and 2.1, respectively (Bertsch et al., 2008). The plots of the experimental results compared to the simulation of the system heating capacity and COP are shown in Figure 22. The two-stage heat pump is shown to have much larger heating capacities than a conventional heat pump at low outdoor temperatures. For an outdoor air temperature of about -29°C (~-20°F), the tested capacity was ~11kW or ~85% of the measured capacity at the U.S. nominal heat pump rating condition of ~8.3°C (47°F) compared to the desired target of 75% (Table 1). The lab test system was easily built using off-the-shelf components with little modification, showing promise for being manufacturable with relatively low cost premium compared to conventional ASHPs.

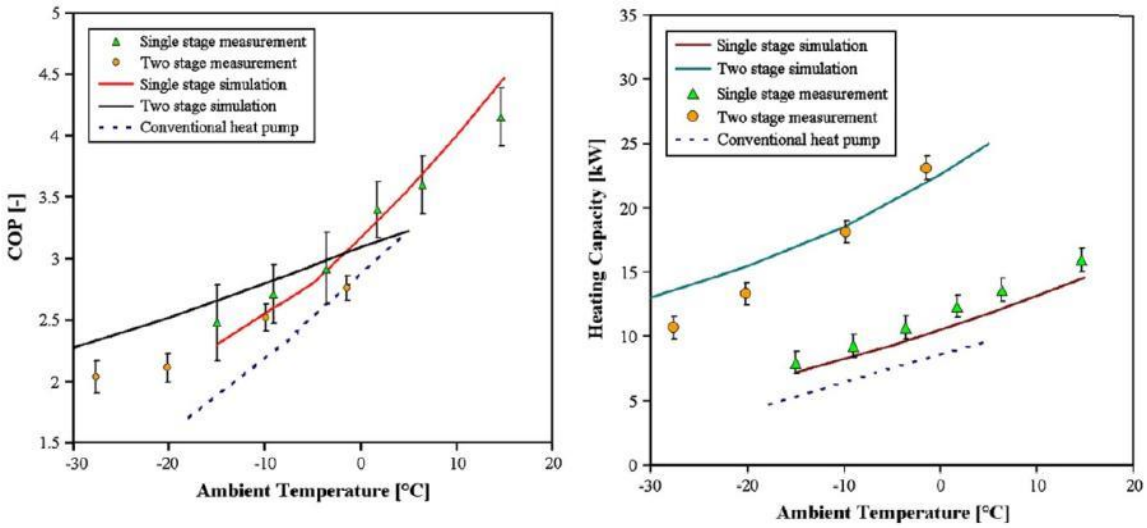

Figure 22: Experimental results of two-stage heat pump compared to simulation results; manufacturer's data was used to indicate performance of the conventional single-stage ASHP (Bertsch et al., 2008

A field test of an advanced two-stage ASHP designed for cold climate operation has been completed at Camp Atterbury, a U.S. Army base outside Edinburgh in Indiana (Caskey et al., 2013). The heat pump was a three-compressor (two-stage) system with an economizer VI loop, similar to the concept analyzed by Bertsch et al. (2008). It featured a large tandem

scroll compressor (two parallel, single-speed compressors) for capacity boosting during low ambient temperature heating operation and a variable speed scroll compressor for moderate ambient temperature heating and cooling operation. The test was conducted under the DOD's Energy Security Technology Certification Program (ESTCP). Two identical military barracks from available buildings located at Camp Atterbury were selected for the field demonstration. The originally installed HVAC system was a natural gas furnace with a split system A/C. A side-by-side performance comparison between the originally installed HVAC system and the two pre-commercial heat pump units developed at Purdue University was conducted during the 2012-2013 heating season. Only commercially available components were selected for all parts of the heat pump units with help from three industrial partners, namely Ingersoll Rand - The Trane Company, Emerson Climate Technology, and Danfoss. The heat pump units had a design heating capacity of 18.34 kW (62,580 BTU/h) at an ambient temperature of -20°C (4°F).

The heat pump performance was compared to the existing HVAC system using six performance objectives that are listed in Table 6. The objective of the project was to reach or surpass the success criteria listed for each performance objective.

Table 5: ESTCP project performance objectives of the cold climate heat pump

Performance Objective	Metric	Data Requirements	Success Criteria
Quantitative Performance Objectives			
1. Reduce primary energy for heating (Energy)	Therms or kW-hr	Electric and gas use metered	Reduce primary energy use by 25%
2. Reduce costs (Finances)	$	Base rates for electricity and fuel	10% reduction in heating costs
3. Reduce emissions (Environment)	Metric ton CO_2 equivalent	Conversions for fuels	Reduce CO_2 emissions by 15%
Qualitative Performance Objectives			
4. Ease of installation	Ability of a technician-level individual to install the heat pump	Feedback from the technicians on installation time	A field technician team is able to install the system
5. Maintenance	Ability of a technician-level individual to maintain the heat pump	Feedback from the technicians on maintenance calls	A field technician team is able to operate the system
6. Comfort	Maintain temperature within comfort range of building occupants	Indoor temperature readings and survey of occupants	80% of occupants satisfied with indoor conditions

Caskey et al. (2013) discussed results of the field test from the 2012-2013 heating season in general comparison with the criteria listed in Table 2. For the monitored period at the Army site, the ASHP system achieved approximately 19% source energy savings vs. the baseline gas furnace system but utility costs were higher due to the low price the Army pays for natural gas at the site. [NOTE – the choice of baseline system was dictated by the project sponsor, the U.S. Department of Defense.] Using average Indiana residential electricity and gas prices, the utility costs for the ASHP and baseline furnace would have been comparable. This operation cost equivalence, despite the energy savings of the ASHP, is because the price for natural gas in Indiana is about one-third that of electricity per unit of energy delivered, which is true of most locations in the United States. The ASHP used no electric backup heating during the test period. Using ASHRAE Standard 55 (ASHRAE, 2010) to evaluate the thermal comfort indicated that the heat pump was able to maintain comfort

levels throughout the heating season. Furthermore, while the first cost of the two-stage ASHP will be higher than that of a conventional single-stage ASHP, the installation and maintenance costs are estimated to be comparable.

3 TWO-PORT VAPOR INJECTED COMPRESSION WITH REGENERATION CONCEPT

An experimental investigation was conducted at Purdue University using a commercially available 5-ton heat pump that was retrofitted with a two-port vapor injected scroll compressor. The injection ports within the two compression pathways were located in the fixed scroll with different distance from the suction chamber. The vapor at the two injection pressure levels was generated using two flash tank separators in a cascade configuration. This configuration made it necessary to not only control the superheat but also the liquid levels in the separators and subcooling of the refrigerant leaving the condenser.

Baseline performance data of the heat pump without vapor injection was obtained and compared with that of the two-port vapor injection system. For the baseline, the injection lines to the compression pockets were plugged within the fixed scroll to reduce dead volume and re-expansion losses. Also, the vapor-separator section was shut off and bypassed. In the second step, the plugs were removed and a staged expansion process was performed using the separator section. The generated vapor from each separator was injected into the respective compressor port causing an intercooling effect on the compression process.

The heat pump is a split air-to-air system with an outdoor unit and indoor unit. The indoor unit contains the AC-mode expansion device, the heat exchanger, and the indoor blower. The outdoor unit contains the outdoor heat exchanger and blower motor, the compressor, vapor separators, and control valves necessary to facilitate the different operating modes of the system. Only heating mode operation was considered during the testing. The compressor is operated on a variable speed drive, allowing a closer match between heating requirement of the building and the capacity of the heat pump. For single stage operating mode, Figure 23 (B0), the vapor separators are bypassed by an electronic expansion valve (EXV). The refrigerant is evaporated and superheated in the outdoor heat exchanger, then passes through the 4-way valve and accumulator (acc) to the compressor suction. The refrigerant is compressed by the compressor and passes through discharge muffler (M) and the 4-way valve to the indoor heat exchanger, where it is condensed and subcooled. The subcooled refrigerant travels through the bypass valve in the thermostatic expansion valve (TXV) and the filter drier back to the EXV. In flash gas bypass operating mode (B0 FGB), Figure 24, the flash gas from the expansion process is taken off using the low pressure (LP) separator before the evaporator and bypassed through a control valve directly to the accumulator while the liquid refrigerant is drained to the evaporator.

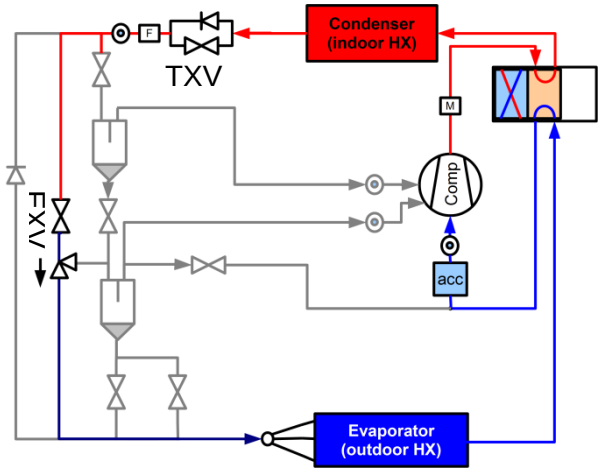

Figure 23: Single stage operating mode (B0)

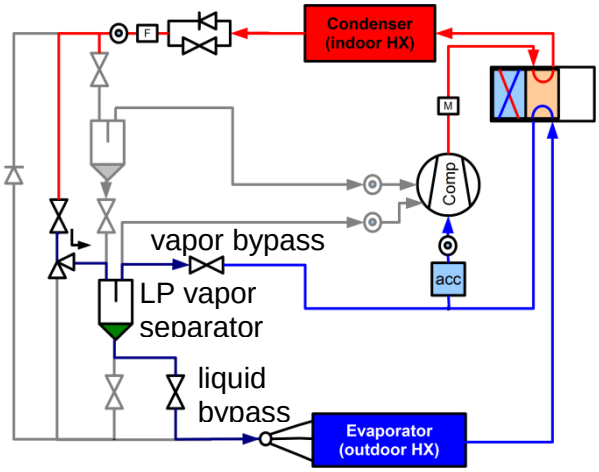

Figure : Flash gas bypass operating mode (B0 FGB

The injection ports of the compressor are internally plugged for both the B0 and B0 FGB configurations. This was done to reduce re-expansion losses. These plugs are removed for the vapor injected configuration (B1), Figure 25. In that configuration, the expansion process is split up into three stages, where the flash gas from the high pressure and intermediate pressure expansion is injected into the injection ports of the compressor. For the vapor injected mode with hybrid control, as indicated in Figure 26, the last expansion process is done using 5 balancing valves, where each valve controls the superheat of a neighboring circuit pair of the outdoor heat exchanger. This approach, named reduced hybrid control, reduces the number of balancing valves when compared to hybrid control as introduced by Kim *et al.* (2008) by 50% for an even number of circuits. The tested heat pump additionally used 2-step balancing valves, which are expected to be cheaper to produce than electronic expansion valves.

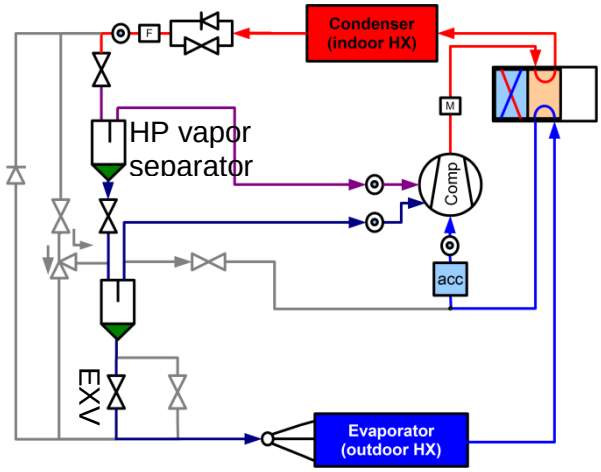

Figure 25: Vapor injection operating mode (B1)

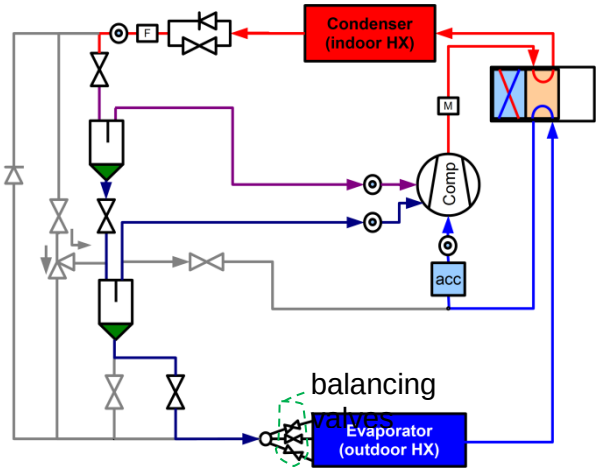

Figure 26: Vapor injection operating mode (B1H)

Refrigerant inlet and outlet temperatures were measured for all major components. Air inlet and outlet temperatures were measured using thermocouple grids for both indoor and outdoor units. Inlet dew point was measured for the indoor and outdoor units with the outlet dew point measured at the outdoor unit. Chilled mirror sensors were used for all dew point temperature measurements. The relative humidities at the air inlet of the indoor and outdoor units were measured as a backup in case of sensor failure. The air-side flow rate of the indoor unit was measured using an ASHRAE nozzle box that follows ASHRAE 41.2 (ASHRAE, 1987).

The different operating modes lead to different methods for controlling the system. For the B0 configuration, superheat was the only controlled variable; subcooling was between 4 and

5 K for clean coil operating conditions. For the B0 configuration with flash gas bypass, subcooling was additionally controlled. For the vapor injected configurations, liquid levels in the two separators were controlled to allow the charge in the system to balance. Superheat for the vapor injected system was either controlled by a single valve or, in case of the hybrid control scheme, by the balancing valves. The balancing valves were used to equalize the superheats and to move the overall superheat to the target value. The set point for both superheat and subcooling was 5 K for all system configurations. It was necessary to increase the superheat set point for some operating conditions to maintain stable operation of the system.

Test data was taken under steady state operating conditions, e.g. no or only small trend in discharge temperature and all other temperatures and pressures. The start of the steady state period was judged during system operation, after the start of that period, at least 30 minutes of steady state data was taken. This resulted in 30 minutes or more of steady state data after the final data selection. The average absolute mismatch between useful airside and refrigerant side capacity was 2.2 %, with the maximum occurring value being 3.7%. Reported values in this paper are based on the refrigerant side, due to the better accuracy of these measurements.

Figures 27 and 28 show the improvement in COP and capacity relative to the baseline system (B0). Vapor injection leads to significant improvement in capacity, with about 11% at high ambient temperature and 28% at -8.3°C ambient temperature. For the “fix capacity” case, compressor speed was reduced to match the baseline B0 capacity – with exception of the H1 test, where no further reduction of compressor speed was possible. The COP improvements are smaller – with identical compressor speed than for the baseline, up to 3.7% improvement is possible. If capacity is matched, more than 6% COP improvement is possible. COP improvement tends to increase towards lower ambient temperatures. One of the reasons for this is that the performance improvement due to vapor injection becomes more important than the re-expansion losses at the injection ports since the cooling effect of the injected vapor becomes more significant. The flash gas bypass only leads to a COP (3%) and capacity (7%) improvement for the H2 condition, but did not lead to any benefits for the other operating conditions.

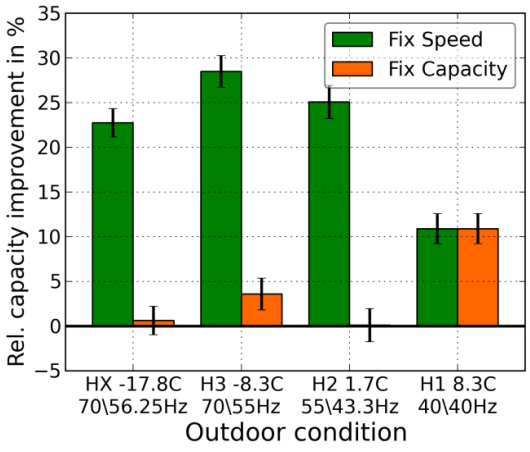

Figure 27: Relative capacity improvement, B1 vs. B0

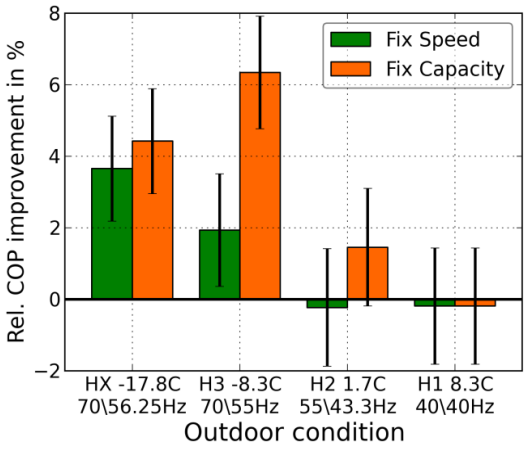

Figure 28: Relative COP improvement B1 vs. B0

One benefit of the vapor injection is that the capacity degrades less towards lower ambient temperature if the same compressor speed is used. Figure 29 shows that the capacity for the vapor injected system increases by nearly 7% as ambient temperature decreases from the H1 to the H3 test while compressor speed is increased from 40 to 70 Hz. For the same conditions, the B0 system capacity decreases by 2%. The differences in COP are less pronounced as shown in Figure 30. The COP for all tested system configurations – even at

the lowest ambient temperature – exceeds 2. COP decreases from the highest ambient temperature to the lowest ambient temperature. For the B0 system, the COP for HX conditions (i.e., with additional HX) is 70% of the COP for H1 conditions. For the vapor injected system, a relative COP of 72% of H1 conditions is maintained under HX conditions. Application of the hybrid control leads to additional improvement of COP and capacity over the vapor injected system with a standard distributor.

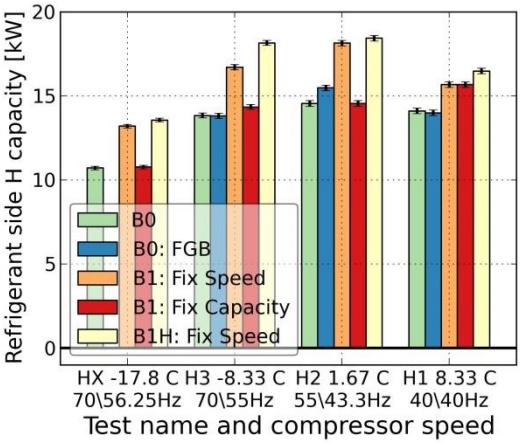

Figure 29: Relative capacity improvement, B1 vs. B0

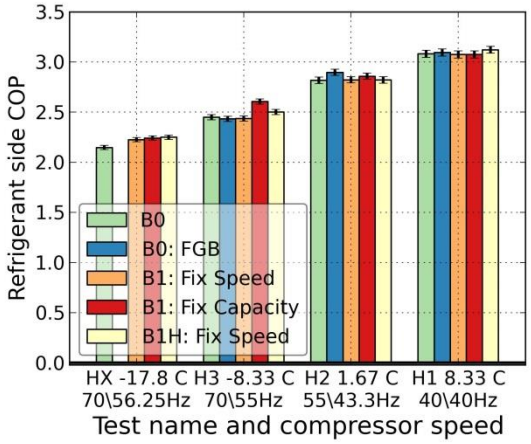

Figure 30: Relative COP improvement B1 vs. B0

4 OIL-FLOODED COMPRESSOR SYSTEM

The oil flooding concept utilizes oil injection into the compressor suction port(s) to absorb the heat of compression (reducing discharge temperature) and approach an isothermal compression process (Bell et al., 2011; Yang et al., 2014; Ramaraj et al., 2016). Figure 31 illustrates a cycle schematic and p-h diagram of the concept. The addition of compressor flooding with regeneration in VC systems results in a more isothermal compression process that can have a significant beneficial impact on system efficiency for large temperature lifts. For refrigerants with large pressure differences across the compressor, the use of a hydraulic expander can also help to recapture some of the work of compression of the flooding liquid. The engineering challenges in implementation of this technology are reasonable, which suggests that it could be applied readily in new construction. Analyses indicate this concept has both capacity and efficiency advantages over VI cycles for low-temperature applications (Bell et al., 2011). In particular, the injection of oil results in an increase in refrigerant mass flow rate and overall isentropic efficiency and a decrease in the compressor discharge temperature. The analyses conducted so far clearly suggest that designing an efficient scroll compressor with oil injection for application to a low-source-temperature ASHP application will be possible with respect to energy performance and manufacturability.

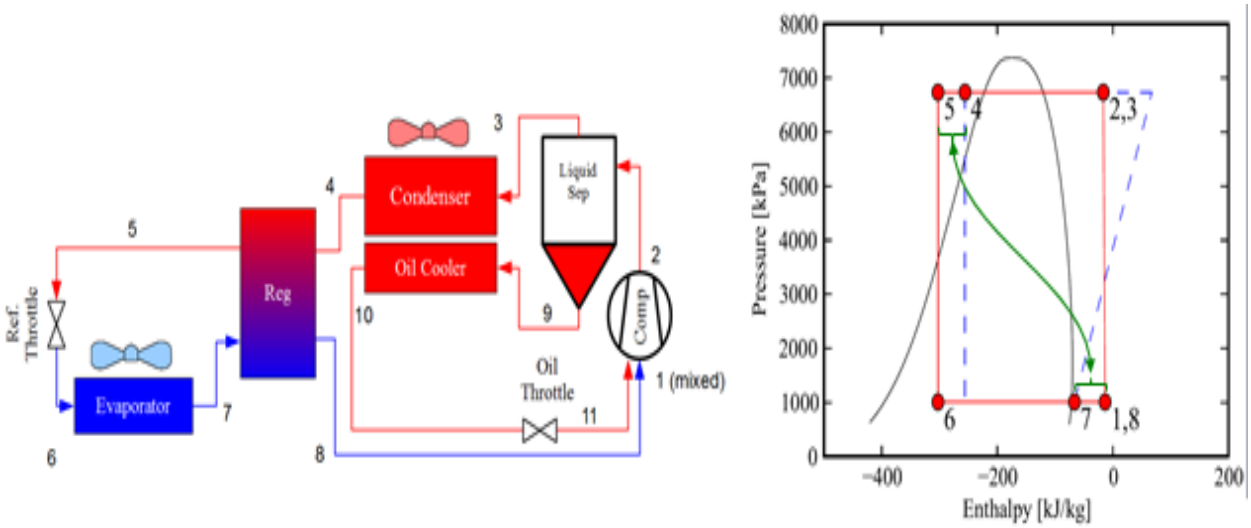

Figure 31: Schematic (left) and p-h cycle diagram (right) of flooded compressor cycle concept - from Bell et al. (2011)

As depicted in Figure 32, a commercial 5-ton (17.6 kW) R410A packaged heat pump system was retrofitted with an oil-flooded scroll compressor, an oil separator, a regenerator (internal heat exchanger), and an oil cooler. Although the reversible packaged heat pump is designed to run in heating mode as well as in cooling mode, it was decided to focus on the heating mode operation only. A schematic of the retrofitted heat pump can be found in Figure 33. The schematic can be divided into two separate loops: oil loop and refrigerant loop.

For the refrigerant loop, the superheated vapor is compressed from the evaporating pressure to the condensing pressure in the compressor. After compression, the two-phase mixture (oil and refrigerant) is separated inside the oil separator. Then, the refrigerant passes through the reversing valve and goes into the indoor unit where it rejects heat to the indoor air flow. At the outlet of the indoor unit, the refrigerant is subcooled and flows through the Thermostatic Expansion Valve (TXV), which works as a straight tube in heating mode. The fluid is then further subcooled in the regenerator before flowing through the mass flow meter and filter-dryer. Afterwards, the refrigerant is expanded to the evaporating pressure through an Electronic Expansion Valve (EXV2) and two parallel piston expansion valves (fixed orifice valves). Compared with the baseline system, this EXV2 has been added to the commercial packaged heat pump in order to control the superheat at the outlet of the evaporator. After the expansion devices, the low-pressure two-phase mixture is evaporated and superheated in the outdoor unit. At the outlet of the evaporator, the fluid passes through the regenerator to be further superheated by heat transfer with the subcooled liquid refrigerant flow. The flow then passes through the reversing valve and accumulator, and goes back to the compressor suction.

In the oil loop, the oil is injected into the scroll set at the inlet of both suction chambers. After compression, the oil is separated from the refrigerant in the oil separator (there is still a small amount of refrigerant in the oil due to the solubility of refrigerant into oil). Then, the oil is cooled down in the oil cooler by heat transfer with the indoor air flow. The liquid oil passes through the oil mass flow meter and is expanded in the Electronic Expansion Device (EXV1) before going back to the compressor.

As can be seen in Figure 13, a solenoid valve has been placed before the EXV1. It is directly connected to the power consumption of the compressor. If the compressor is running, the solenoid valve is open. Otherwise, it is closed. Its aim is to close the oil loop when the system is not running and to prevent the migration of oil from the top of the system to the bottom of the system by gravity.

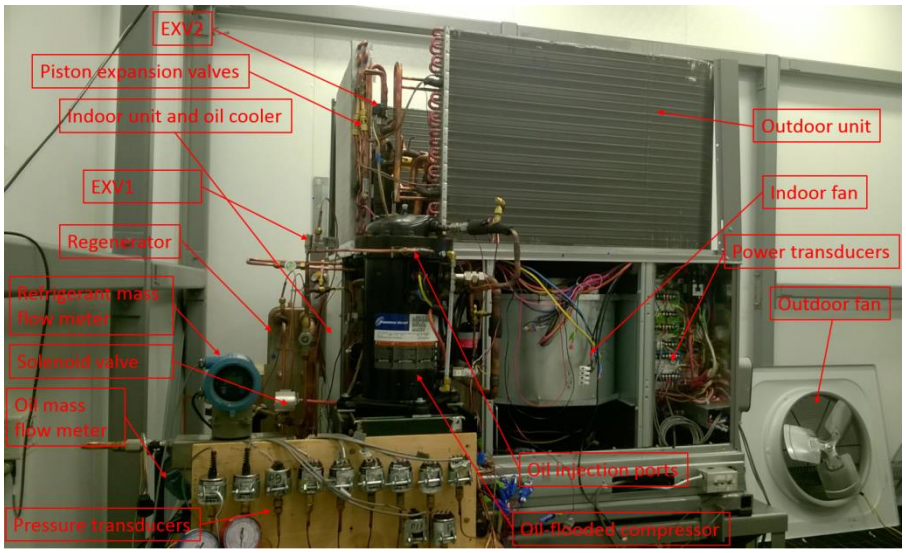

Figure 32: Experimental setup

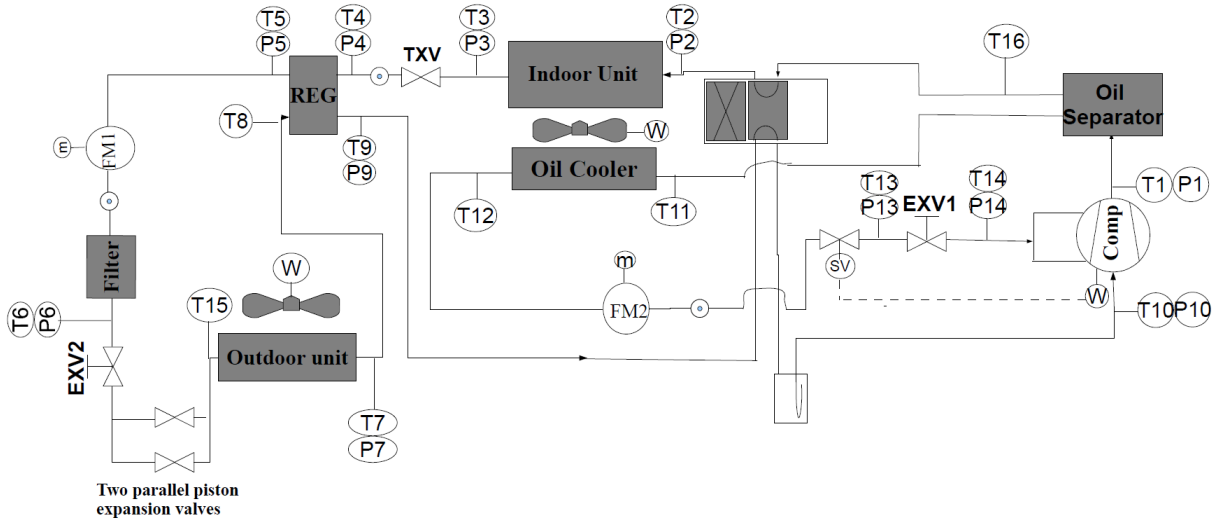

Figure 33: Schematic of a packaged heat pump using oil-flooded compression with regeneration technology

The modified heat pump was tested in psychrometric chambers in order to fully understand the effect of oil-flooded compression with regeneration on system performance in heating mode. The test matrix used for this test stand was inspired by the AHRI Standard 210/240. Since there is no standard for oil-flooded systems, a test matrix with different oil mass fractions was created and is presented in Table 7. In order to investigate the impact of oil mass fraction on the system performance, the oil mass fraction varies for each test from 0.0 to 0.3, in 0.05 intervals. The oil mass fraction is defined by:

$$x_o = \frac{\dot{m}_o}{\dot{m}_o + \dot{m}_r} \tag{1}$$

Table 6*:* Test matrix for oil-flooded heat pump in heating mode

Test *	Air entering the indoor unit			Air entering the outdoor unit			Indoor air flow rate	
	T [°F]	T [°C]	RH [%]	T [°F]	T [°C]	RH [%]	CFM	[m³/s]
H1	70	21.1	≤ 56.03	47	8.33	72.64	1750	0.826
H2	70	21.1	≤ 56.03	35	1.67	81.80	1750	0.826
H3	70	21.1	≤ 56.03	17	-8.33	69.41	1750	0.826

Test *	Air entering the indoor unit			Air entering the outdoor unit			Indoor air flow rate	
	T [°F]	T [°C]	RH [%]	T [°F]	T [°C]	RH [%]	CFM	[m³/s]
H4	70	21.1	≤ 56.03	0	-17.78	min	1750	0.826
* For every test in heating mode, the oil mass fraction varies from 0.0 to 0.30, in 0.05 intervals.								

The following comments about the test matrix can be made:

- In the AHRI Standard 210/240, the H4 test is missing. As oil-flooding is particularly interesting for low temperature applications, a very low temperature test (H4 test) has been added to the test matrix so as to evaluate the performance at these conditions.
- For the indoor unit, the relative humidity must be below 56.03%. Since the value is not imposed, a fixed set point of 50% has been chosen.
- For the H4 test, the relative humidity in the outdoor room is set to minimum.

To evaluate the performance of the heat pump equipped with the oil-flooded compressor and regenerator, steady-state experimental data were recorded for each test listed in the test matrix[1]. The superheat at the outlet of the evaporator was controlled by EXV2 at a value of 5°C for every test. Steady state was maintained for at least 30 minutes for every test condition. The recorded data were then processed in order to evaluate the performance of the system. A total of 33 experimental points were obtained: 23 for the test matrix, 6 additional points at higher superheat for evaluating the influence of superheat and the last 4 points for determining system performance both without the regenerator and oil injection.

Figures 34 to 39 show the performance of the oil-flooded compressor for different outdoor room temperatures, a fixed indoor room temperature (21.11°C) and a fixed superheat of 5°C at the outlet of the evaporator. The isentropic efficiency of the compressor must account for the effect of oil injection and is defined by:

$$\varepsilon_{is,cp} = \frac{\dot{m}_r \cdot \left(h_{r,ex,cp,is} - h_{r,su,cp}\right) + \dot{m}_o \cdot \left(h_{o,ex,cp,is} - h_{o,su,cp}\right)}{\dot{W}_{cp}} \quad (2)$$

where $\dot{m}_r$ and $\dot{m}_o$ are the mass flow rate of refrigerant and oil, respectively, $\dot{W}_{cp}$ is the compressor power consumption, $h_{r,ex,cp,is}$ and $h_{o,ex,cp,is}$ are respectively the enthalpies at the compressor discharge with an isentropic compression between suction and discharge. Figure 34 shows that the isentropic efficiency has a maximum for an oil mass fraction of approximately 0.1 at a given outdoor room temperature. The increase of the isentropic efficiency at low oil mass fraction is most likely due to reduced internal leakage and friction. The decrease at higher oil mass fraction might be due to different reasons: higher pressure drops through suction and discharge ports due to oil injection, higher pressure drops through the compression process due to the oil viscosity, higher power consumption used to pump the oil from low pressure to high pressure and more irreversibilities in the two-phase flow (such as non-homogeneous equilibrium). The isentropic efficiency is also higher at higher outdoor air (ambient) temperatures mainly because the refrigerant mass flow rate is higher, the electromechanical losses are lower and the built-in volume ratio is more suited to the pressure ratio of the system (lower over-compression at higher outdoor temperatures, i.e. the external pressure is too high at low outdoor room temperature).
The volumetric efficiency of the compressor is calculated according to the following expression (Ramaraj et al. 2014):

$$\varepsilon_{vol,cp} = \frac{\dot{m}_r + \dot{m}_o}{\rho_{m,su,cp} \cdot \dot{V}_{s,cp}} \quad (3)$$

[1] For tests H2, H3 and H4, the maximum oil mass fraction was limited to 0.25 by the system, therefore no data are available for an oil mass fraction of 0.3. For test H1, the oil mass fraction was limited to 0.2.

where the volume flow rate and the inlet mixture density are given by:

$$\dot{V}_{s,cp} = V_{s,cp} \,.\, N_{rot,cp} \tag{4}$$

$$\rho_{m,su,cp} = \frac{(1 - x_o) + S \,.\, x_o}{(1 - x_o) \,.\, v_r + S \,.\, x_o . v_o} \tag{5}$$

and where v_r and v_o are the specific volume of refrigerant and oil, respectively, and S is the slip ratio, which was taken to be 1 (i.e., a homogeneous two-phase flow). As can be seen in Figure 35, the volumetric efficiency increases with the oil mass fraction and seems to stabilize at higher oil mass fraction. This increase is probably due to lower internal leakage. For instance, the volumetric efficiency between $x_o = 0$ and $x_o = 0.25$ increases by 6.64% at $T_{out} = -17.78°C$.

As expected, the discharge temperature decreases when oil is injected as shown in Figure 36, the temperature difference between no oil injection and $x_o = 0.25$ is approximately 35-40°C depending on the outdoor room temperature. Moreover, at a given oil mass fraction, the discharge temperature increases slightly when the outdoor room temperature decreases. However, a higher increase could have been expected. This slight increase could be explained by two opposing effects. On one hand, the pressure ratio increases when the outdoor room temperature decreases, which tends to increase the temperature difference between suction and discharge temperature. On the other hand, the compressor suction temperature decreases at lower outdoor room temperature, which limits the discharge temperature. The lower suction temperature is mainly due to lower temperatures at the inlet of the regenerator (high pressure side, T4 in Figure 36) because of lower condensing temperatures at low outdoor temperatures. The lower suction temperature leads to lower superheat at the outlet of the regenerator (low pressure side, T9 in Figure 36). Beside this observation, Figure 37 shows that the compressor temperature ratio (between discharge temperature and suction temperature) is significantly higher at lower outdoor room temperature and a more isothermal compression is achieved when the oil mass fraction increases.

As can be seen in Figure 38, the refrigerant mass flow rate tends to increase with oil injection. It is probably due to lower internal leakage. It can also be due to lower temperatures in the suction chamber (i.e. higher density and therefore higher mass flow rate). The refrigerant mass flow rate also increases with the outdoor air temperature because of higher density at the suction (since the evaporating pressure is higher).

Regarding the compressor power consumption shown in Figure 39, no general trends can be pointed out. Indeed, for $T_{out} = 8.33°C$ and $T_{out} = 1.67°C$, a minimum is reached for an oil mass fraction of approximately 0.1. At low oil mass fraction, the power consumption decreases due to the sealing properties of oil and the higher isentropic and volumetric efficiencies of the compressor. At higher oil mass fraction, the opposite effect occurs since the isentropic efficiency decreases. However, at lower temperature, the same trends cannot be pointed out. For $T_{out} = -8.33°C$, the power consumption decreases until $x_o = 0.25$ and for $T_{out} = -17.78°C$, a maximum is reached around $x_o = 0.05$ and then it decreases.

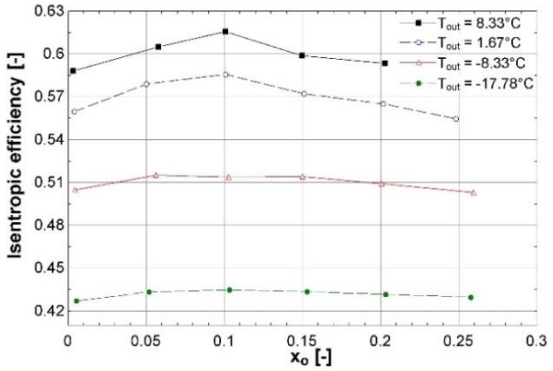

Figure 34: Compressor isentropic efficiency

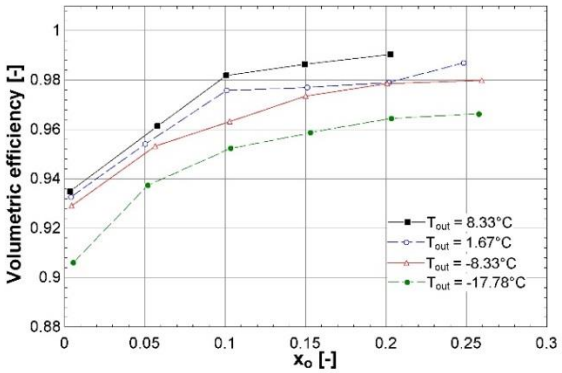

Figure 35: Compressor volumetric efficiency

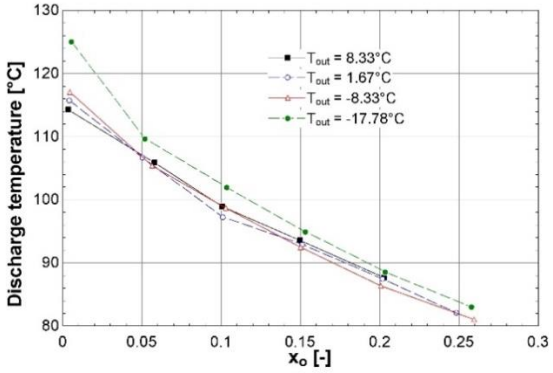

Figure 36: Compressor discharge temperature

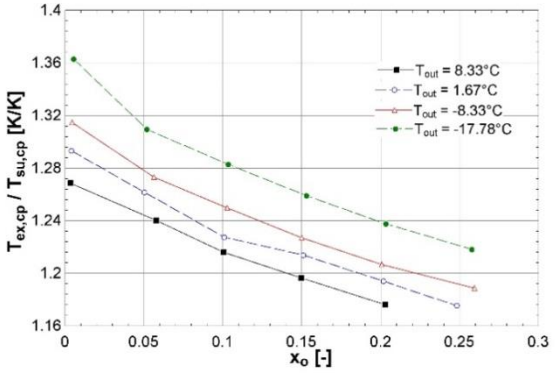

Figure 37: Compressor temperature ratio

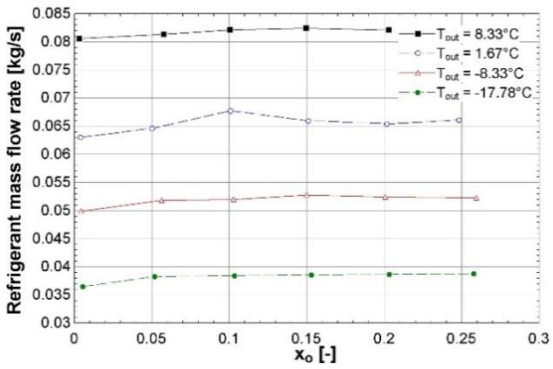

Figure 38: Refrigerant mass flow rate

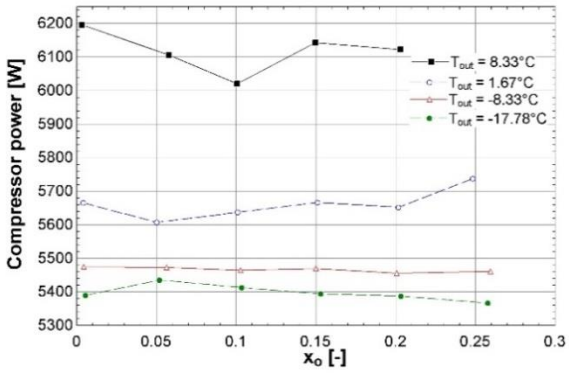

Figure 39: Compressor power

The coefficient of performance of the heat pump in the absence of auxiliary heat is given by:

$$COP = \frac{\dot{Q}_a}{\dot{W}_{cp} + \dot{W}_{in,fan} + \dot{W}_{out,fan}} \tag{6}$$

where $\dot{W}_{in,fan}$ and $\dot{W}_{out,fan}$ are the indoor and outdoor fan power consumption, respectively, and $\dot{Q}_a$ is the heating capacity calculated on the air side. The air-side capacity should also be equal to the sum of the oil cooler capacity, the condenser capacity and the indoor fan power consumption:

$$\dot{Q}_a = \dot{Q}_{o,oc} + \dot{Q}_{r,cd} + \dot{W}_{in,fan} \tag{7}$$

where $\dot{Q}_{o,oc}$ is the heat transfer rate in the oil cooler (oil side) and $\dot{Q}_{r,cd}$ is the heat transfer rate in the condenser (refrigerant side).

Figure 40 shows the effect of oil mass fraction on heating capacity for various outdoor temperatures and a fixed indoor room temperature (21.11°C). It reaches a maximum around $x_o = 0.10 - 0.15$ at high outdoor air temperatures (8.33°C and 1.67°C) and does not reach a maximum even for $x_o = 0.25$ at lower temperatures (-8.33°C and -17.78°C). The increases in maximum capacity due to oil injection compared to $x_o = 0$ are: 1.2% for $T_{out} = 8.33°C$ at $x_o = 0.15$, 5.0% for $T_{out} = 1.67°C$ at $x_o = 0.1$, 4.3% for $T_{out} = -8.33°C$ at $x_o = 0.25$ and 5.7% for $T_{out} = -17.78°C$ at $x_o = 0.25$. At a given outdoor temperature, the condensing temperature does not have a significant dependence on oil mass fraction. When the oil mass fraction is increased, the refrigerant mass flow rate tends to increase, which increases the capacity. But at the same time, the superheat at the inlet of the condenser decreases (which decreases the capacity) because the discharge temperature of the compressor decreases. However, when the oil mass fraction increases, the cooling of oil increases as well, which increases the capacity since more oil is cooled down by the air flow (i.e. the oil cooler capacity is increased). Overall, these opposing effects result in an increase of heating capacity when oil mass fraction is increased.

For the COP, the same trends can be pointed out as shown in Figure 41. For $T_{out} = 8.33°C$ and $T_{out} = 1.67°C$, the COP increases as the oil mass fraction is increased and reaches a maximum for $x_o = 0.1$ before decreasing. The increases in maximum COP associated with oil injection compared to no oil injection are 3.3% and 5.6% for $T_{out} = 8.33°C$ and $T_{out} = 1.67°C$, respectively. The increase in COP with oil mass fraction at low values is because the capacity increases (see Figure 9) and the compressor power consumption decreases (see Figure 8). At higher oil mass fractions, the opposite effect occurs: compressor power consumption increases whereas capacity decreases. At lower outdoor air temperatures ($T_{out} = -8.33°C$ and $T_{out} = -17.67°C$), the COP also increases with oil injection but a maximum is not reached, even for $x_o = 0.25$. This is consistent with the trends that there is no minimum for the compressor power consumption and no maximum for the capacity over the range of oil mass fractions tested. The COP improvements for oil flooding over no flooding (i.e., between $x_o = 0$ and $x_o = 0.25$) are 4.5% and 6.1% for $T_{out} = -8.33°C$ and $T_{out} = -17.67°C$, respectively.

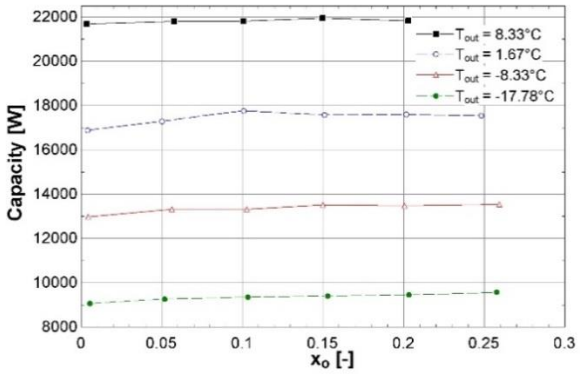

Figure 40: Heating capacity of heat pump

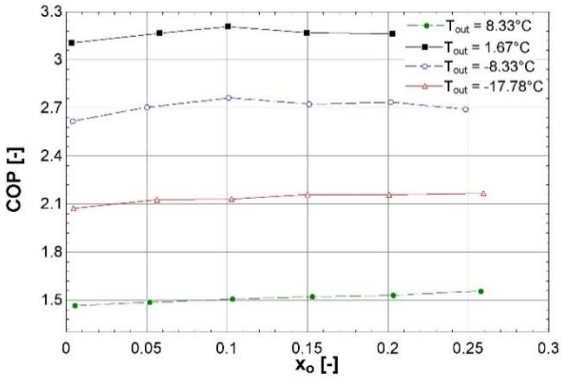

Figure 41: COP of heat pump

Experimental data were recorded at 8.33°C (outdoor temperature) for two different superheats at the outlet of the evaporator: 5°C and 10°C. Figures 42 and 43 show the influence of variations in superheat on COP and heating capacity. It can be seen that the influence is high. Indeed, the COP is decreased by 0.5 (i.e. a decrease of around 15%) between 5°C and 10°C superheat and the heating capacity is decreased by more than 4000 W (i.e. a decrease of around 20%) between 5°C and 10°C superheat. This high influence is due to a large decrease in evaporating temperature (it decreases from -3°C at 5°C superheat to -11°C at 10°C superheat). Indeed, it seems that this lower evaporating temperature hurts the performance much more than the superheat. It must be pointed out

that the capacity is mainly decreased by the refrigerant mass flow rate that decreases from 0.08 kg/s to 0.06 kg/s between -3°C and -11°C evaporating temperature. The opening of the EXV2 (see Figure 2) was approximately 40% open for 5°C superheat and only 25% open for 10°C superheat. The expansion valve opening of 25% lowered the evaporating pressure to balance the flow through its constriction.

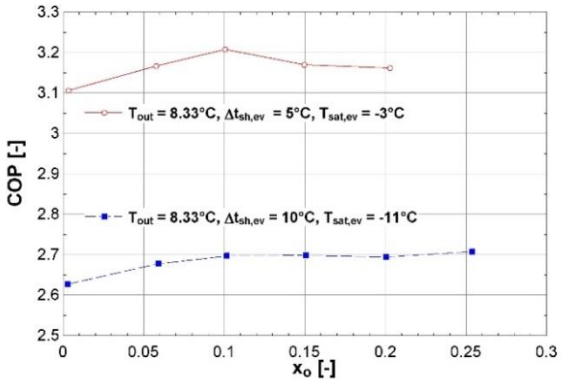

Figure 42: Superheat influence on COP

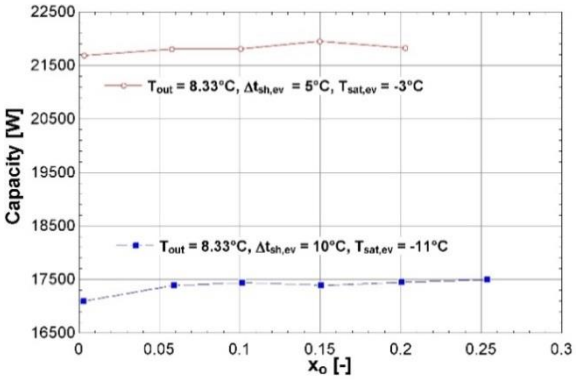

Figure 43: Superheat Influence on heating capacity

In order to compare the performance of the oil-flooded system with regeneration to that of a conventional heat pump system, some tests were run without the regenerator and without oil injection in the oil-flooded compressor. The results obtained with this baseline system were then used to identify the performance improvement by oil-flooding and regeneration. To compare these two systems, the COP improvement is defined as follows:

$$COP_{imp} = \frac{COP_{oil-flooded} - COP_{baseline}}{COP_{baseline}} \tag{8}$$

where $COP_{oil-flooded}$ is the COP of the oil-flooded system with regeneration and $COP_{baseline}$ is the COP of the baseline system (without oil injection and without regeneration). An analogous expression is used for the heating capacity improvements. Using the 4 experimental points available for the conventional heat pump (one point for each outdoor room temperature of the test matrix) and the 23 experimental points available for the heat pump with oil-flooding, the results of Figures 44 and 45 were generated to show the COP and capacity improvements as a function of oil mass fraction. The COP improvements range between 4% and 15% and the capacity improvements are between about 1% and 19%. Most of the experimental points are characterized by a superheat of 5°C at the outlet of the evaporator. However, it must be pointed out that for the baseline system, the test at $T_{out} = 8.33°C$ was carried out with a superheat of 7.5°C (instead of 5°C) at the outlet of the evaporator because without the regenerator, the system could not reach the lower superheat even with the EXV2 fully open (see Figure 44). As explained in previous section, the superheat influences the performance. Therefore, this explains why the capacity and COP improvements are greater for $T_{out} = 8.33°C$. Therefore, the results for the other three operating temperatures are more meaningful and are the focus of additional analysis and discussion.

The three points without oil injection (i.e. $x_o = 0$ in Figure 44 and 45) are analyzed first. It can be seen that even without oil injection, the COP increases (between 4 and 8%) between the conventional heat pump and the heat pump with regeneration, which clearly shows the benefit of the regenerator. Several factors directly or indirectly influence the higher COP with regeneration:

- The condensing temperature is slightly lower (by approximately 2°C) and the evaporating temperature slightly higher with regeneration. Therefore, the pressure ratio is lower with the regenerator.
- The compressor power consumption is lower (by approximately 200 W) with the regenerator. This is due to both a lower refrigerant mass flow rate and a lower pressure ratio through the compressor.
- The heating capacity is higher with regeneration (see Figure 14). The capacity increases with regeneration because the superheat at the inlet of the condenser is higher due to a higher superheat at the inlet of the compressor. However, two opposite effects decrease the capacity: the refrigerant flow rate and the condensing temperature are lower with the regenerator. But in general, the heating capacity was increased for the cases considered.

When oil is injected into the compressor of the system with regeneration, the maximum COP is reached at $x_o = 0.1$ and the COP improvement is 10.3% for $T_{out} = 1.67°C$. For the two lowest outdoor temperatures, the maximum COP is not reached even for an oil mass fraction of $x_o = 0.25$. At this oil mass fraction, the COP improvements are 13.3% and 14.3% at outdoor temperatures of -8.33°C and -17.78°C, respectively.

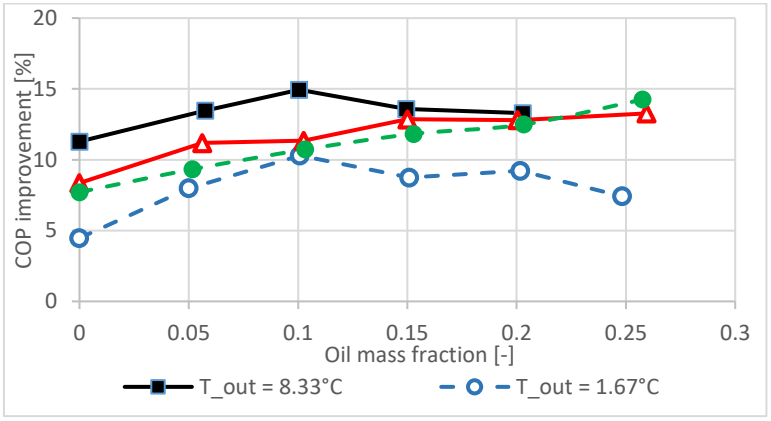

Figure 44: COP improvement between oil-flooded system with regeneration and baseline system

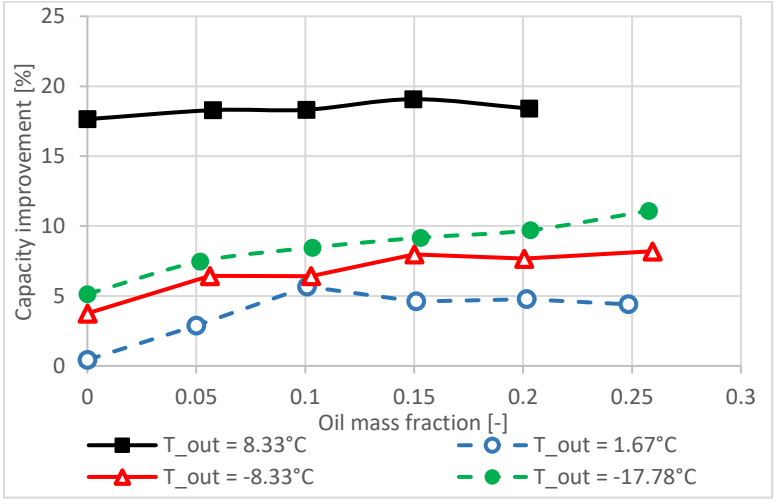

Figure 45: Capacity improvement between oil-flooded system with regeneration and baseline system

5 SINGLE-STAGE ASHP WITH TWO PARALLEL COMPRESSORS

Research at ORNL investigated several different ASHP cycle configurations to identify those with potential to meet the heating capacity degradation target limit listed in Table 5. Two-capacity compressor, variable speed compressor, and dual, parallel single speed compressor (tandem compressor) systems were investigated. Nine of the system options investigated are listed in Table 8 along with a baseline conventional single speed compressor ASHP.

Table 7: ASHP design and sizing options

#	Equipment Sizing Scenarios
1	Single speed heat pump having rated HSPF of 9.6: sized such that rated cooling capacity matches building design cooling load [BASELINE].
2	Single heat pump, having a two-stage scroll compressor: sized such that rated high-stage (100%) cooling capacity matches building design cooling load.
3	Single heat pump, having a two-stage scroll compressor: sized such that rated low-stage (67%) cooling capacity matches building design cooling load.
4	Single heat pump, having a variable speed scroll compressor: sized such that rated cooling capacity at 2700 rpm matches building design cooling load.
5	Single heat pump, having a variable speed scroll compressor: sized such that rated cooling capacity at 3600 rpm matches building design cooling load.
6	Single heat pump, having a variable speed scroll compressor: sized such that rated cooling capacity at 4500 rpm matches building design cooling load.
7	Single heat pump, having a two-stage scroll compressor: sized such that 80% of rated cooling capacity matches building design cooling load.
8	Single heat pump, having a tandem scroll compressor pair: sized such that rated cooling capacity with one compressor matches building design cooling load.
9	Single heat pump, having a single speed VI scroll compressor: sized such that rated cooling capacity matches building design cooling load.
10	Two identical single speed heat pumps, having rated HSPF of 9.6: sized such that rated cooling capacity of one unit matches building design cooling load; both units used for heating.

Note: All variable speed compressor system options have a speed range of 1800 - 7200 rpm; option 8, tandem compressor pair contains two identical compressors; the two-stage compressor options include one compressor having two capacity levels, i.e. 100%/67%.

Table 9 lists the heating capacity ratio and the heating COPs at 8.3°C and -25°C for each of the systems in Table 8. Four of the options (4, 5, 8, and 10) have estimated capacity ratios near the target level noted in Table 1 (≥75%). COPs at -25°C for these options range around 45-55% of the nominal COPs at 8.3°C. Estimated HSPF ratings are calculated based on the method prescribed in AHRI Standard 210/240 (AHRI, 2008) for U.S. region IV (mildly cold climate). The VS compressor-based designs offered somewhat greater low temperature capacity capability while the tandem compressor designs were somewhat less complex and had almost as much capacity capability.

Table 8: Predicted ASHP system performance indices

Options	COP @ 8.3°C (47°F)	Heating Capacity Ratio @ -25°C (-13°F)	COP @ -25°C (-13°F)	Region IV HSPF Rating (per AHRI Standard 210/240-2008)
	[W/W]	[-]	[W/W]	[W/W (Btu/Wh)]
1.	3.58	40%	1.92	2.80 (9.55)
2.	3.79	42%	2.09	2.92 (9.96)
3.	3.78	57%	2.09	2.92 (9.98)
4.	4.30	94%	1.89	3.40 (11.61)
5.	4.14	74%	1.89	3.43 (11.71)

Options	COP @ 8.3°C (47°F)	Heating Capacity Ratio @ -25°C (-13°F)	COP @ -25°C (-13°F)	Region IV HSPF Rating (per AHRI Standard 210/240-2008)
6.	3.80	61%	1.89	3.40 (11.59)
7.	3.79	52%	2.09	2.95 (10.05)
8.	4.38	75%	1.98	3.31 (11.31)
9.	3.75	43%	2.12	2.96 (10.09)
10.	3.58	80%	1.92	N/A

Based primarily on its relatively simple cycle concept (Figure 46), the tandem approach appeared to offer a relatively more cost-effective approach compared to VS compressor based approaches (Shen et al., 2014). So the following experimental investigations were based on the tandem compressor concept for several reasons.

1. The system refrigerant flow cycle is very similar to that of conventional ASHPs (Figure 26); the major difference is replacement of one large compressor with two equal-size, smaller compressors.
2. Equal tandem, single-speed compressors generally have larger operation envelope than a VS compressor of the same maximum capacity, in terms of pressure ratio and discharge temperature.
3. A VS compressor is usually optimized at one speed level. When moving away from the optimum speed level, especially at maximum and minimum speeds, the VS compressor tends to have some efficiency degradation.
4. A two-capacity heat pump using tandem compressors is easily adaptable to a wide range of 2-stage thermostats available on the market.

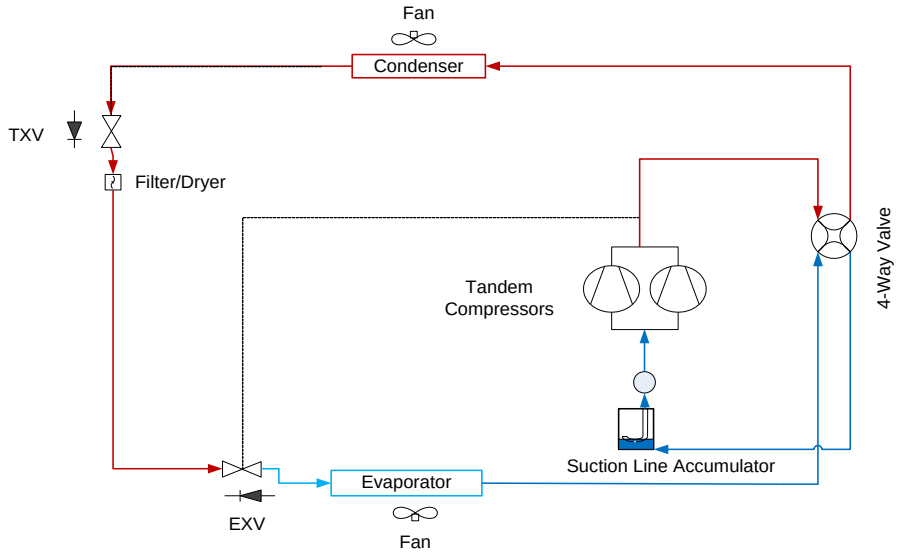

Figure 46: CCHP using tandem, single-speed compressors and an EXV for discharge temperature control in heating mode

The laboratory prototype was built by modifying a 17.5 kW (~60,000 Btu/h or 5-ton) rated cooling capacity, single-speed, conventional ASHP, having a factory rated seasonal heating COP (SCOPh) of about 2.5 (seasonal heating seasonal performance factor, or HSPF of about 8.5 Btu/Wh). A pair of equally sized (10.6 kW or 3-ton nominal cooling capacity), single-speed compressors were used to replace the existing compressor. Parallel compressor CCHP systems using three different scroll compressor designs were evaluated in the lab: 1) conventional scroll compressor optimized for space cooling operation; 2) scroll compressors optimized for space heating operation; and 3) VI scroll compressors. For all cases the compressors were insulated and placed outside the outdoor air flow stream to minimize the compressor shell heat losses. Testing data confirmed that the insulation layer

reduced the compressor heat loss by 50%, and boosted the capacity and COP at -25°C (-13°F) by more than 5%. For the lab test system an electronic expansion valve (EXV) was added for refrigerant flow control in the space heating mode to optimize the compressor discharge temperature based on the outdoor air temperature. Refrigerant flow control for space cooling (air-conditioning) used the existing thermostatic expansion valve (TXV) supplied with the base ASHP. The two heat exchangers, indoor blower (2-speed), and outdoor fan (1-speed) were unchanged. Figure 47 shows the indoor air handler section of the prototype. An air flow monitor (pitot tube array) was used to measure the indoor air flow rate at the exit of the indoor air handler. Averaging thermocouple grids were used to measure the return and supply air temperatures for the indoor section as well as the air temperature entering the outdoor coil section. Watt transducers were used for the electric power of the compressors, blower and outdoor fan individually. Pressure transducers and insertion probe thermocouples were used to measure the refrigerant conditions around the system.

Figure 47: Lab Prototype – Indoor Air Handler

The sections which follow introduce the CCHP lab prototypes investigated using tandem single-speed or VI compressors. All the prototypes used R410A refrigerant.

5.1 'More Cost-Effective' Option - Equal Tandem, Single-Speed Compressors

The lab test system evaluated for this option is shown in Figure 46. The design considerations are summarized as below:

1. Two types of equal size, single-speed compressors: conventional scroll compressor design optimized for space cooling operation and a special heating-optimized pair with design features, allowing them to operate at discharge temperatures up to 138°C [280°F]. This enables the CCHP system to operate down to extremely low ambient temperatures.
2. Current two-capacity heat pumps on the market use a single, two-capacity compressor having a displacement volume split ratio of 100% to 67%. In comparison, the equal-size tandem compressor approach provides a volume split ratio of 100% to

50%, yielding a larger over-capacity potential in heating mode when only the lower capacity was used in cooling mode. This enabled the prototype to reach the >75% heating capacity target at -13°F (-25°C).

3. The CCHP is sized to match an assumed 10.5 kW (36,000 Btu/h or 3-ton) building design space cooling load using only one of the tandem compressors. Since the system retained the heat exchangers of the base 17.5 kW (5-ton) heat pump, the heat exchangers are unloaded when only one compressor is operating (for space cooling or space heating at mild outdoor temperatures). This yields higher system efficiency at these conditions and is the key that enabled the CCHP lab prototypes to reach a nominal rated COP > 4.0 at 8.3°C (47°F).
4. For the prototypes, the compressors were well insulated and placed outside the outdoor air flow stream (shown in Figure 48) to minimize the shell heat losses at very low ambient heating operation. Adding the insulation impairs the cooling performance somewhat by loading the condenser more; however, this effect is mitigated since only one compressor is used for space cooling; e.g. the condenser (outdoor heat exchanger) oversized for cooling.
5. Heating mode discharge temperature control, which uses an EXV, coupled with a suction line accumulator, is intended to optimize the active charge in the system over an extensive operation range. This mitigates the typical charge imbalance problem between cooling and heating modes. A standard thermostatic expansion valve (TXV) is used for cooling mode.

Figure 48: Insulated tandem compressors

As noted earlier, the lab prototype CCHP used the original two-speed indoor blower from the base single-speed ASHP. At high speed the air flow rate was 0.83 m^3/s (1750 CFM) with a power consumption of 460 W; at low speed the air flow and power consumption were 0.67 m^3/s (1420 CFM) and 270 W, respectively. The outdoor fan was fixed-speed, consuming 300 Watts. We evaluated two samples of tandem compressors – one pair optimized for space cooling mode (typical design practice for conventional ASHPs) and a specially-made pair optimized for heating mode.

Figures 49 and 50 show measured capacity and COP vs. ambient temperature, respectively for the CCHP prototype using the cooling-mode optimized compressor pair. These lab test results indicate that this system met the heating capacity target, achieving 77% of the nominal rated capacity at -25°C (-13°F). COP at -25°C was ~1.9, and the rating point COP (at 8.3°C or 47°F) was 4.1.

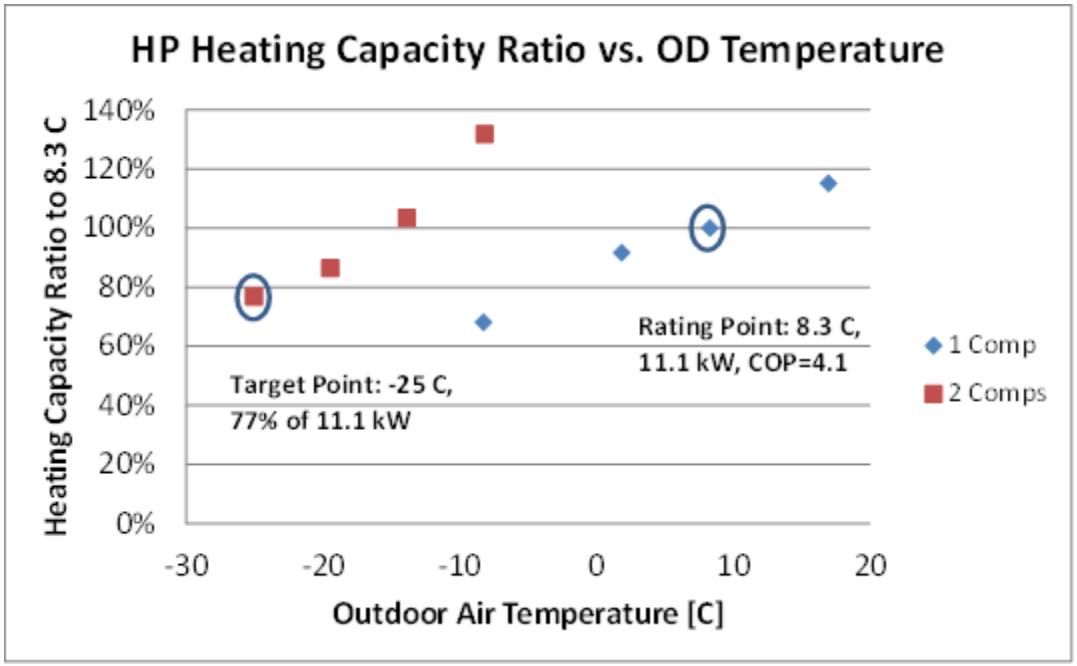

Figure 49: Lab prototype heating capacity ratio with cooling-optimized compressors (relative to capacity at the nominal 8.3°C (47°F) rating point, with one compressor)

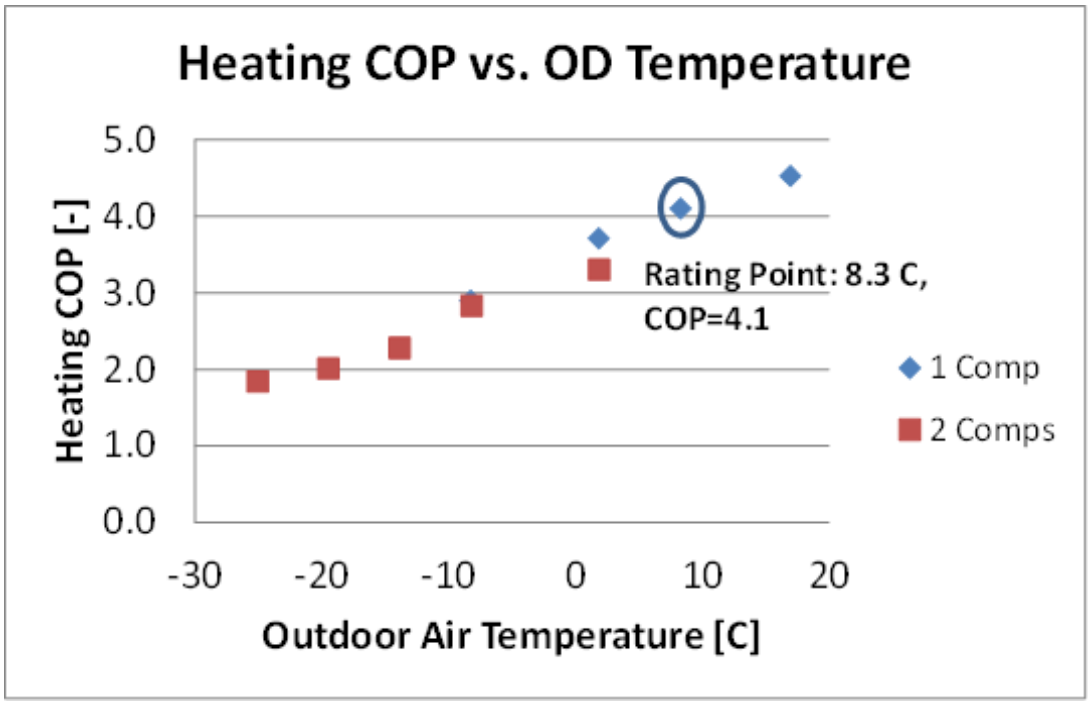

Figure 50: Lab prototype heating COP with cooling-optimized compressors

Space heating performance was somewhat better at all ambient temperature test conditions using the heating-mode-optimized tandem compressor pair. Table 10 shows the lab-measured performance indices at 8.3°C, -8.3°C, and -25°C (47°F, 17°F and -13°F) outdoor temperature conditions with one or two compressors. Table 11 shows SCOPhs (HSPFs) as calculated per AHRI Standard 210/240 in Region IV and V climates. The DHR_{min} and DHR_{max} building load levels are generally representative of a very tight and well insulated house and a rather poorly insulated house, respectively. The dropoff in seasonal efficiencies going from Region IV to the colder Region V climate is about 10.5% and 15.5% for the DHRmin and DHRmax load lines, respectively. It is also notable that the drop in SCOPh for the heating

optimized tandem design between the min and max heating load lines is 1.3% in Region IV. This indicates that this design maintains seasonal performance well over the full range of house performance levels. By comparison, the single-speed baseline loses 23% in seasonal performance in Region IV between the DHRmin (rated) and DHRmax heating load lines. The SCOPh robustness of the tandem design is also in contrast to recently tested variable-speed designs which lose 10 to 20% SCOPh in Region IV for representative heating loads approximately halfway between DHRmin and DHRmax levels (Rice et al, 2016). A similar performance robustness advantage is realized in Region V at higher heating load lines for the parallel tandem design, due to the boosted performance at -8.3°C (17°F) and below.

Table 9: Performance indices of CCHPs using tandem single-speed compressors

	Ambient/Comp(s)	**8.3°C, 1 Comp**	**-8.3°C, 2 Comp**	**-8.3°C, 1 Comp**	**-25°C, 2 Comp**
Optimized for cooling mode	COP [-]	4.09	2.76	2.89	1.85
	Capacity, kW (Btu/h)	11.1 (37,960)	14.8 (50,455)	7.6 (25,860)	8.8 (30,040)
	Capacity Ratio vs. 8.3°C	100%	133%	68%	79%
	Discharge Temperature, °C [°F]	50.0 (122)	83.4 (183)	55.0 (131)	125.0 (257)
Optimized for heating mode	COP [-]	4.24	2.80	2.97	1.94
	Capacity, kW (Btu/h)	11.6 (39,717)	14.9 (50,921)	7.6 (25,917)	8.9 (30,245)
	Capacity Ratio vs. to 8.3°C	100%	128%	65%	76%
	Discharge Temperature, °C [°F]	51.1 (124)	82.8 (181)	51.1 (124)	100.6 (213)
%COP Increment		3.7%	1.4%	2.8%	4.9%

Table 10: Heating Seasonal Performance Factors of CCHPs using tandem single-speed compressors

Load	**SCOPh (HSPF, Btu/Wh) cooling optimized**	**SCOPh (HSPF, Btu/Wh) heating optimized**
	Heating Season Ratings, Region: IV	
DHRmin	3.24 (11.04)	3.29 (11.21)
DHRmax	3.19 (10.90)	3.21 (10.95)
	Heating Season Ratings, Region: V	
DHRmin	2.90 (9.90)	2.94 (10.03)
DHRmax	2.69 (9.18)	2.71 (9.26)

One noticeable advantage of the heating-optimized tandem pair is that they achieved improved performance at -25°C (-13°F) with a much lower discharge temperature than the cooling-optimized pair. This indicates that the heating-optimized compressor design can operate at very low ambient temperatures without approaching the discharge temperature limit of 138°C, and have potential to provide larger heating capacities at extremely low ambient temperatures.

Figures 51 and 52 show the variation in space heating COP and capacity (air-side measurements), respectively, vs. compressor discharge temperature for the -25°C ambient condition. The blue symbols represent performance with the heating-optimized tandem compressors and the red symbols represent that with the cooling-optimized compressors. One can see that the prototype with the heating-optimized compressors achieves its maximum COP at a much lower discharge temperature than the system using the cooling-optimized compressors; about 101°C (213°F) vs. 125°C (257°F). Looking at the heating capacity data (Figure 31) it can be seen that the heating-optimized compressors experience much less sensitivity to discharge temperature. Increasing the discharge temperature from

about 93°C to 127°C (200°F to 260°F) results in only about a 3% capacity increase with the heating-optimized compressors versus about a 9% increase for the cooling-optimized compressors. Therefore, there is less benefit in using the EXV for discharge temperature control (Figure 26) with the heating-optimized compressors. So the refrigerant cycle could potentially be simplified further to use a TXV for refrigerant flow control (based on evaporator exit superheat) in both heating and cooling operation.

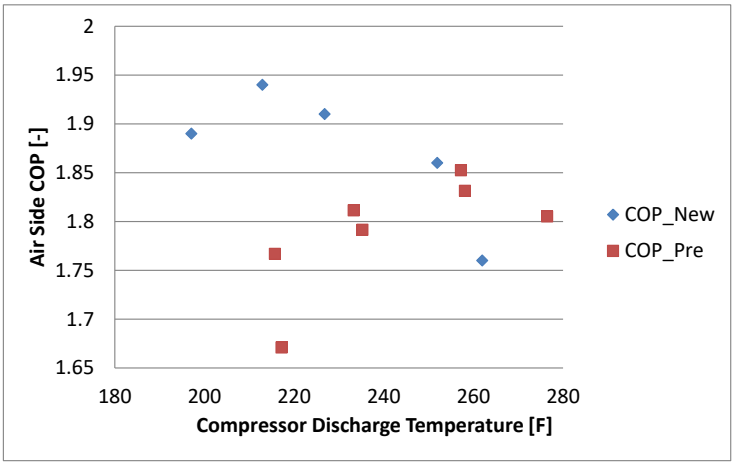

Figure 51: Prototype CCHP air-side heating COP vs. compressor discharge temperature for heating-optimized (new) and cooling-optimized (pre) compressors at -25°C outdoor temperature

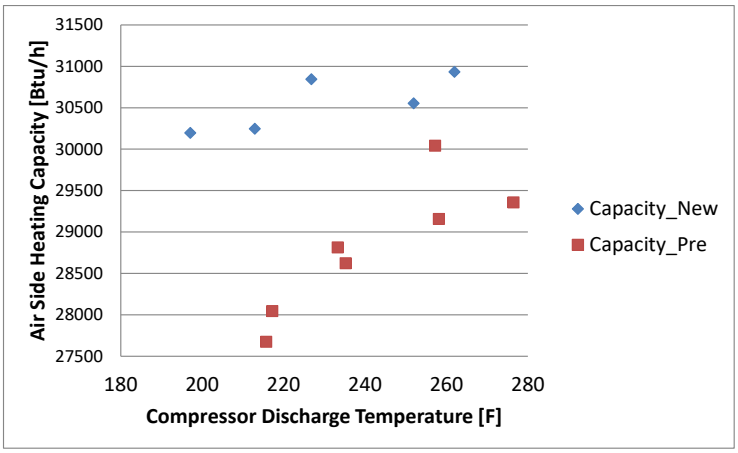

Figure 52: Prototype CCHP air-side heating capacity vs. compressor discharge temperature for heating-optimized (new) and cooling-optimized (pre) compressors at -25°C outdoor temperature

Field Test Site and Equipment Setup

An occupied, single-story ranch home in central Ohio (shown in Figure 53), was selected to host a field test of a tandem, single-speed compressor CCHP prototype. The prototype system replaced the original home HVAC system – an ASHP with rated cooling capacity of ~10.0 kW (34000 Btu/h) at 35°C (95°F) and heating capacity of ~10.3 kW (35000 Btu/h) at 8.3°C (47°F), equipped with a 19.5 kW supplemental resistance heater for second stage heating.

Figure 53: Field testing home

A two-capacity ASHP of nominal 17.6 kW (5-ton) cooling capacity was modified to create the field test prototype CCHP by replacing its original 2-capacity compressor with a heating-optimized tandem scroll compressor pair and adding controls needed to stage the compressors. For the field test, the original 2-capacity ASHP control was retained and re-wired with a relay enable calling the second compressor for second stage heating. A standard commercially available 24 VDC, 2-stage thermostat (wi-fi enabled) was used. Its Y1 signal calls the first stage (one compressor, and low speed indoor blower) and its Y2 signal calls the second stage (two compressors and high speed indoor blower). The outdoor fan ran at a constant speed in both stages. The thermostat can be programmed manually to prevent running the second stage, and this was done for cooling operation. The original 2-capacity unit had a demand defrost control that measures the outdoor air coil surface temperature and refrigerant temperature to initiate the defrosting cycle. During defrosting, the prototype operated both compressors to minimize defrost time. The thermostat was set up as follows to initiate first or second stage heating operation:

- If the zone air temperature is <0.6°C (1.0°F) below the thermostat set point, the first stage (single-compressor) is enabled;
- If the zone air temperature is >0.6°C (1.0°F) below the thermostat set point, the second stage (two compressors) is enabled;
- If the zone air temperature falls to >1.1°C (2.0°F) below the thermostat set point, supplemental resistance heat will be activated.

As illustrated above in Figure 52, the performance of the heating-optimized compressors is relatively insensitive to discharge temperature. In addition, after placing the tandem compressors in the outdoor unit, there was hardly any room left to install any other components, as indicated in Figure 54. Based on these observations, and discussion with Emerson/Copeland engineers (compressor manufacturers and partner in the tandem CCHP system development R&D effort) it was decided to simplify the refrigerant flow control to more conventional suction superheat control using a TXV with optimized system charge for heating mode (Figure 55, below). The recommended charge for the base 2-capacity ASHP, optimized for cooling mode, was 7.6 kg (17 lbs) of R-410A. The charge for the CCHP prototype, optimized for heating mode, was 9% lower, 6.9 kg (15.5 lbs). With this charge, condenser subcooling degree in cooling mode at 27.8°C (82°F) was 1.7K (3R) with one compressor. In heating mode subcooling was around 11.1 K (20 R) at -8.3°C (17°F) with both compressors. Figure 54 shows the outdoor unit of the prototype as installed at the test home, and one can see the compressors were wrapped by a thermal insulation layer. Figure 56 illustrates the indoor air handler and data acquisition system, which were located in the basement.

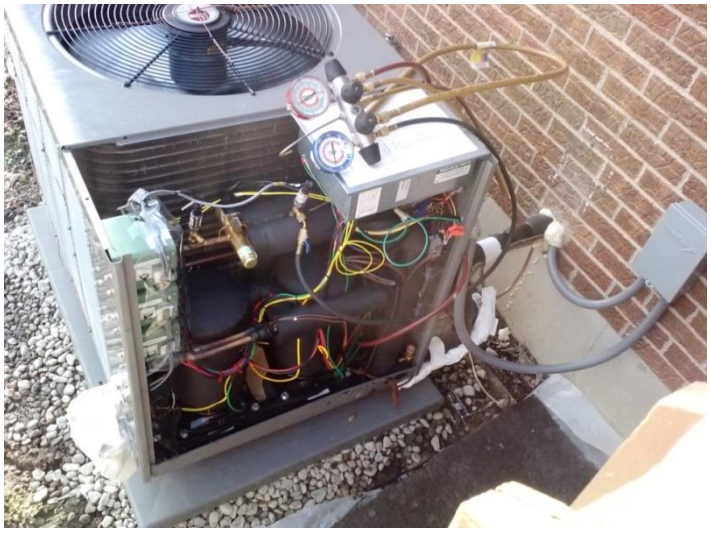

Figure 54: Outdoor unit of field investigation

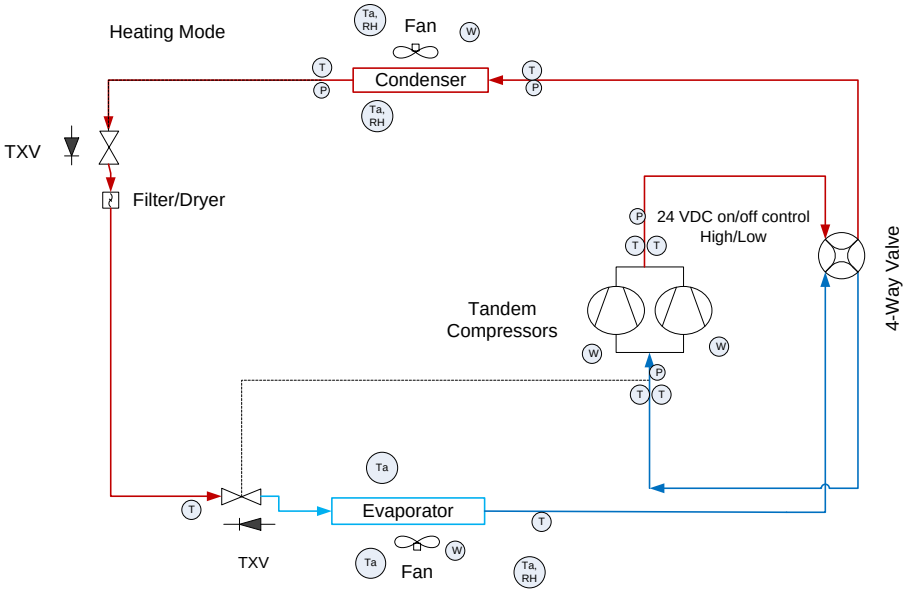

Figure 55: System diagram of field testing HP and instrumentation

Figure 56: Indoor air handler and data acquisition system

Field Data Acquisition and Measurement System

Since the field test was in an occupied home, a wireless data acquisition (DAQ) system was designed to eliminate wire connections between the indoor and outdoor units of the prototype, and minimize interruptions on the home owner. As illustrated in Figure 57, the DAQ controller and measurement devices were used to monitor the outdoor unit with data relayed to the indoor host computer via wireless communication. The host computer and other measurement devices were used to monitor the indoor unit. Data was transmitted through Dropbox via an internet connection back to ORNL for analysis.

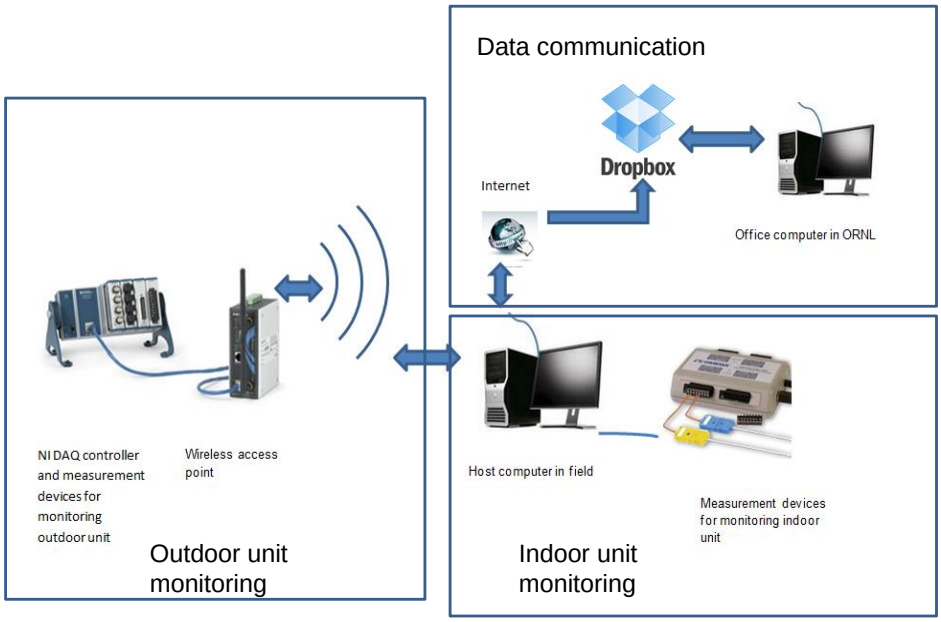

Figure 57: Data acquisition system schematic for CCHP field test

Figure 55 describes the system diagram and instrumentation. Air temperature entering and leaving the outdoor coil were measured using T-type thermocouples. Outdoor humidity was monitored using a Relative Humidity sensor. Three thermocouples were evenly placed at the entrance of the indoor unit to measure the average return air temperature, and a RH sensor was used to measure the return RH. At the exit of the indoor coil, and upstream of the blower, three thermocouples and a RH sensor were used to monitor the supply air state. Thermocouples were soldered on refrigerant tube walls and well insulated to measure the refrigerant temperatures entering and leaving the indoor coil and suction and discharge temperatures of each compressor. Four pressure transducers were used to measure the refrigerant pressures entering and leaving the indoor coil and the compressors. Four Watt transducers were used to measure the outdoor fan, indoor blower and compressor power, individually. Another Watt transducer was used to measure the total power consumption of the outdoor unit. The total outdoor power consumption was determined using the larger of the total power measurement or sum of the individual power measurements. An additional thermocouple was placed in the air duct downstream of the indoor unit to indicate operation of the electric supplemental heater. The DAQ system scanned all the sensors and recorded the data every half minute.

The field testing was conducted using the test home's existing ductwork system. To minimize the interruption on the home owner, no air flow monitor was installed in the duct. Instead, a "true flow grid" was used to perform measurements of the air flow rates once during the heating season and again during the cooling season. As shown in Figure 58, the "true flow grid" is composed of a grid of pitot tubes. It is usually used in the air filter slot of

indoor air handlers, to provide one time air flow measurement during field installation and diagnosis.

Figure 58: True flow grid air flow monitor

For heating mode, the measured air flow rates are given below:

1. For single-compressor operation heating mode with low fan speed setting - measured reading was 0.53 m^3/s (1120 CFM) with True Flow meter (or about 7% less than indicated by the air handler product literature for cooling operation with the same setting), at a blower power of 230 W.
2. For two-compressor operation in heating mode with high fan speed setting - measured reading was 0.64 m^3/s (1350 CFM) with True Flow meter (or about 10% lower than indicated by the air handler product literature for cooling operation with the same setting), at a blower power of 430 W.

One reason for the lower measured air flow in heating mode compared to the product literature is that the latter correspond to cooling operation. Converting the product literature flows to heating operation and assuming the blower drives the same CFM at its exit, a scale factor for heating flow vs. cooling flow can be computed based on the ratio of supply air density in heating vs. that in cooling mode. The computed scale factor was 0.92, indicating an 8% lower air flow for heating operation. Therefore, the “True flow grid” measured indoor air flow rates were considered credible and were used for the entire heating season. The measured blower power was used to indicate which flow rate was applicable, i.e. for blower power <350 W, the air flow rate was assumed as 0.53 m^3/s; for blower power >350 W, the air flow rate was assumed 0.64 m^3/s.

Measurement of the duct external static pressure indicated that the existing duct system was relatively restrictive at high speed blower operation, resulting in larger blower power consumption than the manufacturer’s data indicated. The indoor blower used an ECM motor and was able to maintain a constant volumetric flow rate at the blower exit, regardless of the external static pressure.

Field Heating Performance

2015 heating season operation was monitored from the beginning of February to the end of April 2015 for three full months. During that period the coldest day saw the field temperature drop to -25°C (-13°F).

Figure 59 illustrates runtime fractions for two compressor operation, and total compressor run time (either one or two compressors operating), versus ambient temperature bins (decreasing in temperature from left to right). It can be seen that the second compressor

operated more at the lower ambient temperatures as expected. At the lowest temperature of -25°C, total compressor run time was 100% but the second compressor still cycled at an 80% rate. This indicates that the CCHP prototype still had some extra heating capacity capability even at this extreme condition.

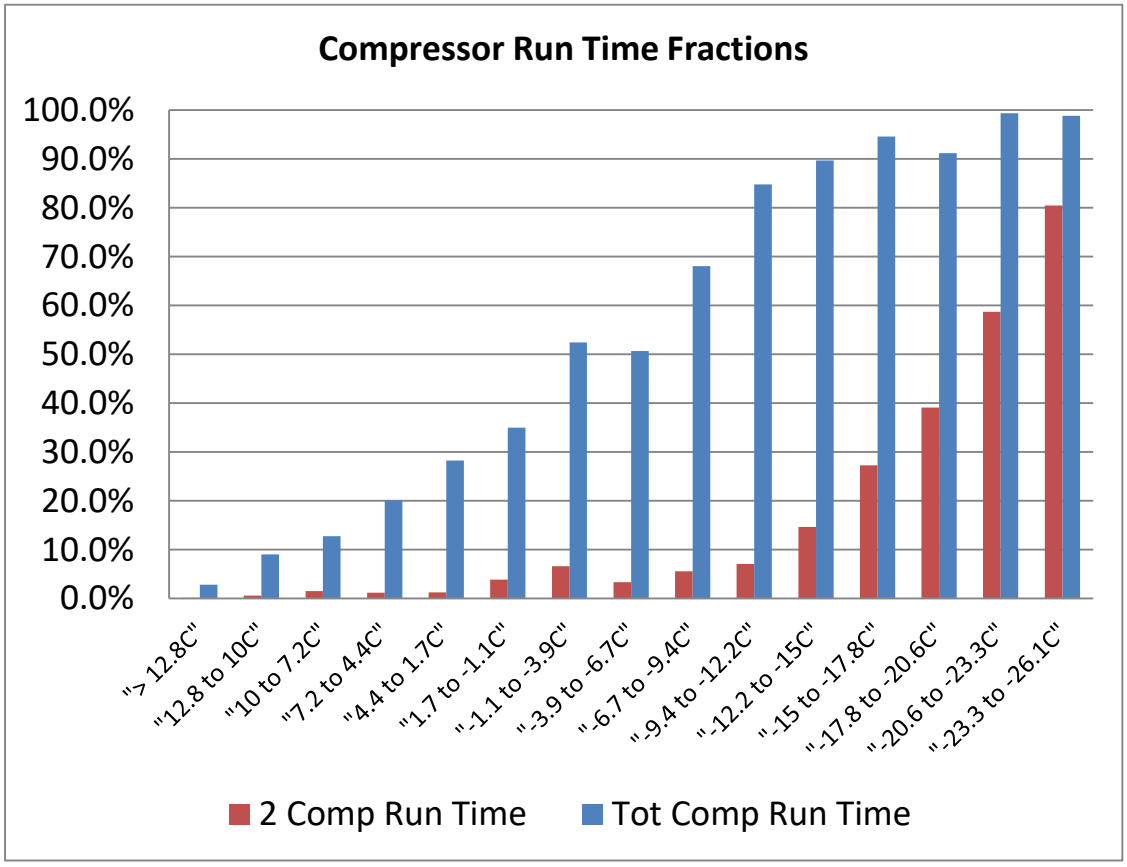

Figure 59: Compressor run time fractions during 2015 winter

Figure 60 shows delivered heating capacities for one- and two-compressor operation, in comparison to the total delivered heating load line. It can be seen that the second compressor was needed when the ambient temperature fell below -12.2°C (-10°C). At the -25°C condition, the CCHP delivered 8.9 kW (30,416 Btu/h) of heating, which is 75% of the rated capacity of 11.6 kW (39,717 Btu/h), as measured in the lab (see Table 6).

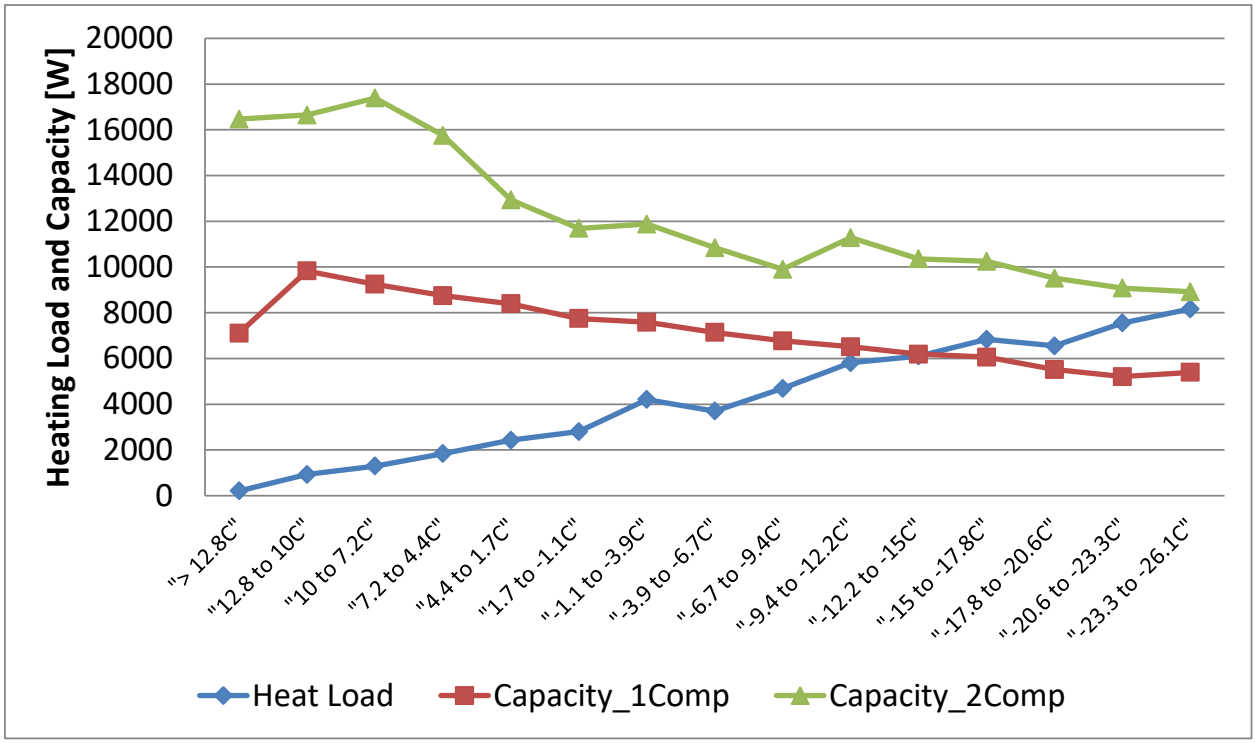

Figure 60: Delivered heat capacities and measured building heating load line

Figure 61 illustrates percentage of supplemental resistance heat use to the total energy use in each temperature bin. Overall resistance heat use was negligible, with most of the usage traceable to either system control issues or occupant behavior. (No defrost tempering resistance heat was used at the engineer homeowner's request.) At -25°C, the resistance energy use was 3.2% of the total even though the second compressor still cycled at 80%. This means that the heat pump responded slower than needed at this condition allowing space temperature to fall below the 1.1 K dead band limit and activate the supplemental heater. Much of the resistance heat use seen during the test period could have been eliminated by changing the control to prevent running only one compressor below a certain ambient temperature. The resistance heat usage at moderate ambient temperatures (between 7.2°C to -6.7°C) was mainly due to the thermostat setback operation by the homeowner. When the homeowner left for extended periods the thermostat set point would be lowered and then raised back up when the homeowner returned. At times this resulted in temperature setting being increased by more than the 1.1K resistance heat trigger point. Modifying the control to lock out the supplemental heater above a set outdoor temperature could eliminate most of this inadvertent usage.

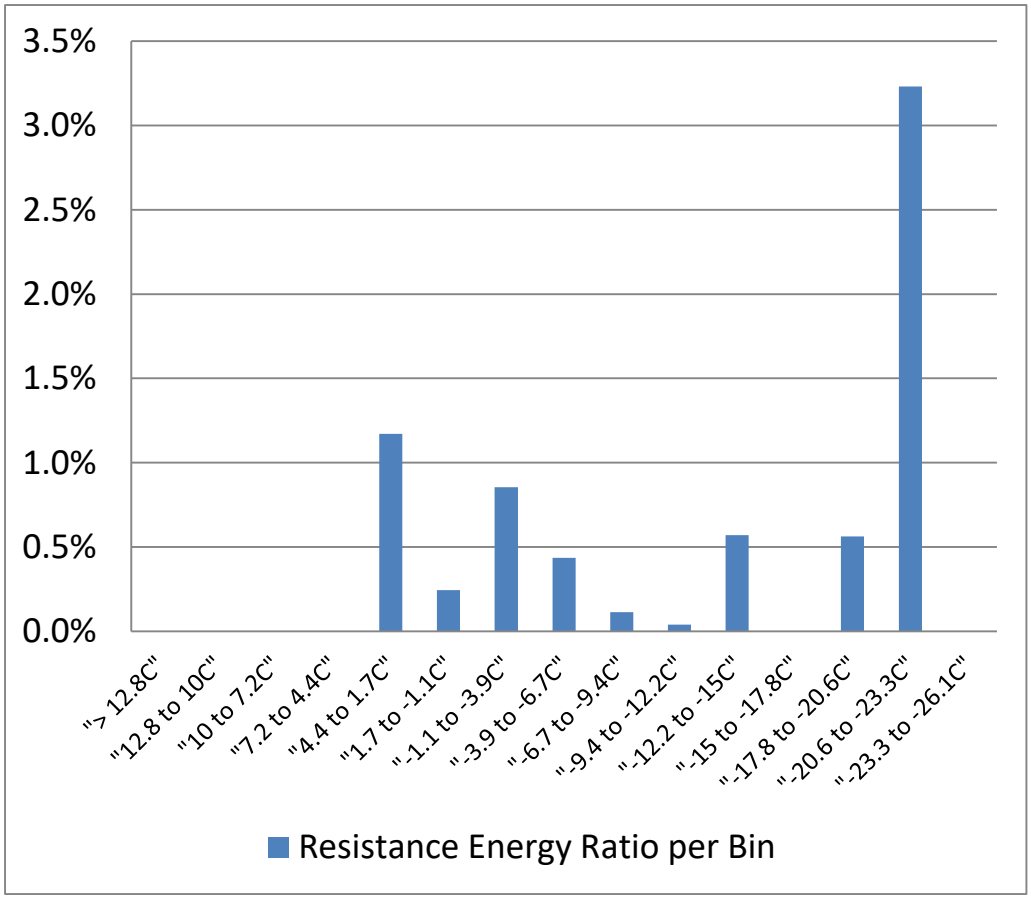

Figure 61: Supplemental resistance heat uses

Figure 62 shows the return and supply air temperatures. The return temperature profile indicates that the homeowner set the thermostat at 20°C during the majority of time when the heat pump was operating. At -25°C, the heat pump was able to deliver supply air at 30°C out of the indoor blower before the resistance heater, with the high air flow rate of 0.64 m^3/s. It should be mentioned that we allowed the indoor air flow rate to change with the compressor staging without consideration of the ambient temperature, due to the desire to simplify the control during the field testing.

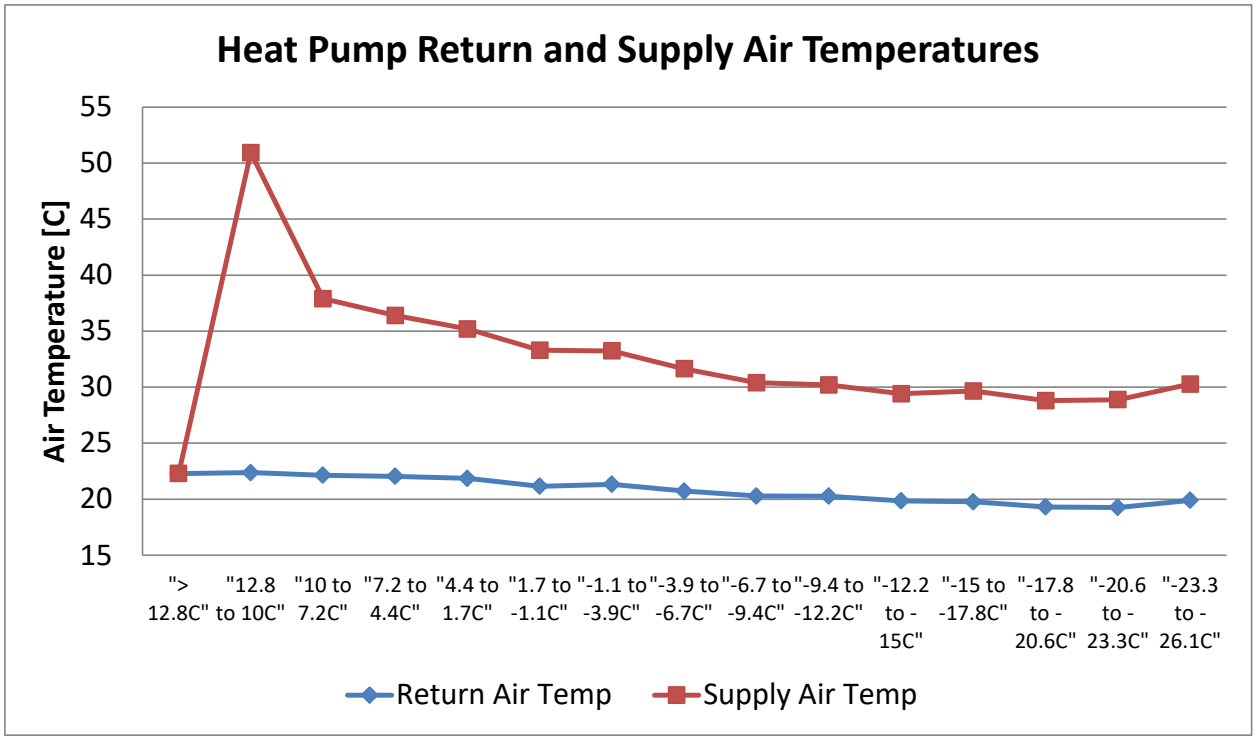

Figure 62: Return and supply air temperatures

Figure 63 presents the defrost runtime fraction (time ratio) and the ratio of the added heating load due to defrost to the total heating energy (load ratio) delivered in each temperature bin. It was concluded that defrost frequency and resultant energy losses were minimal for the CCHP for two reasons. First, when operating in the outdoor temperature range where the outdoor coil is most prone to frost build-up (roughly -5°C to 5°C), generally only one compressor was running leading to slow frost formation because the outdoor HX was relatively oversized and evaporating temperature higher than for typical ASHP systems. Secondly, when two compressors were needed at low ambient temperatures, the outdoor humidity level was generally very low and hardly any moisture condensed on the outdoor coil.

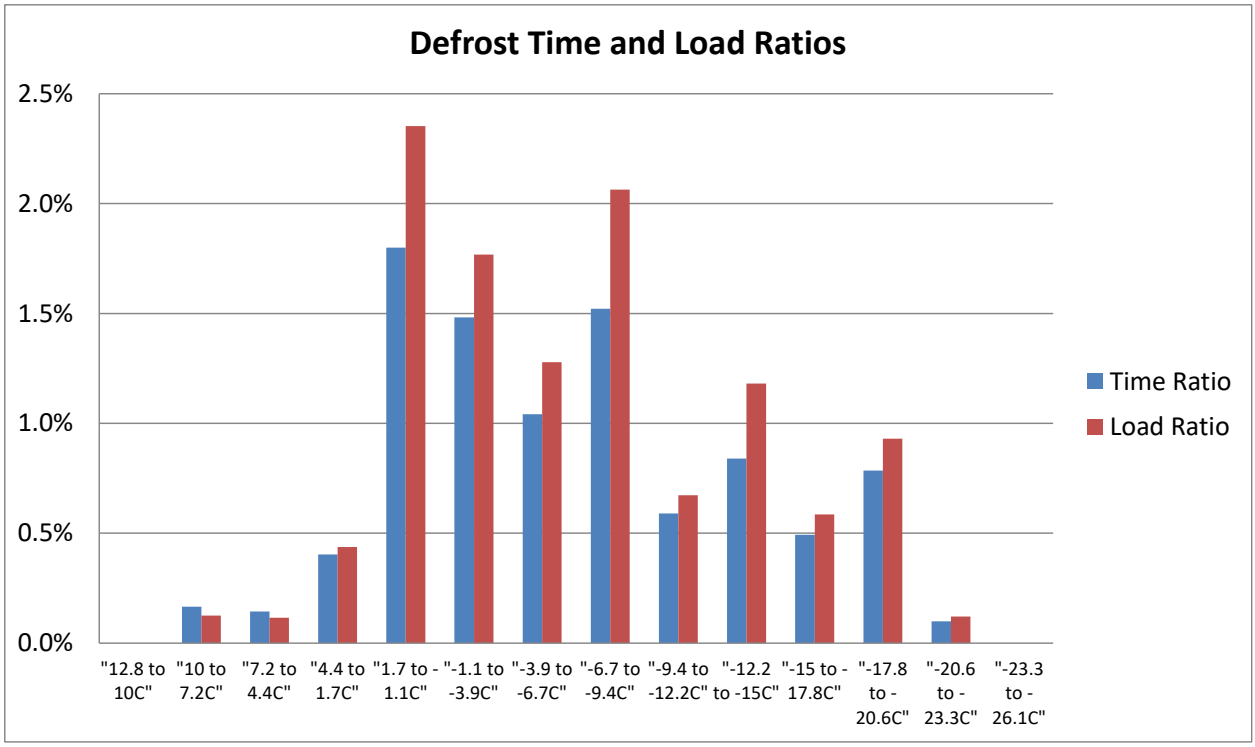

Figure 63: Defrost time ratio and load relative to capacity delivered in each bin

Figure 64 shows field-measured COPs by outdoor temperature bin for single-compressor and two-compressor operation as well as a "total" COP. The total COP was calculated by the total energy delivery divided by the total energy consumed and includes the impacts of cycling losses, supplemental resistance heat use, frosting/defrosting losses, and losses due to switching between one- and two-compressor operation. For the 7.2°C to 10°C bin, the single-compressor COP was 4.05 while the total COP was 3.83 (lower because of cycling losses and occasional two-compressor operation). It should be mentioned that a control modification to prevent two-compressor operation above a set outdoor temperature would allow the total COP at moderate heating conditions to much more closely follow the single compressor COP curve.

It is encouraging to see that, at -25°C, the total COP was 2.2 i.e. 120% more efficient than resistance heating. The field COP at -25°C is higher than that measured in the lab (1.94 given in Table 6) mainly because the field return air temperature is 1.1 to 2.2°C lower than the controlled value in the lab. In addition, the field COP was also boosted a bit due to the small amount of one-compressor operation.

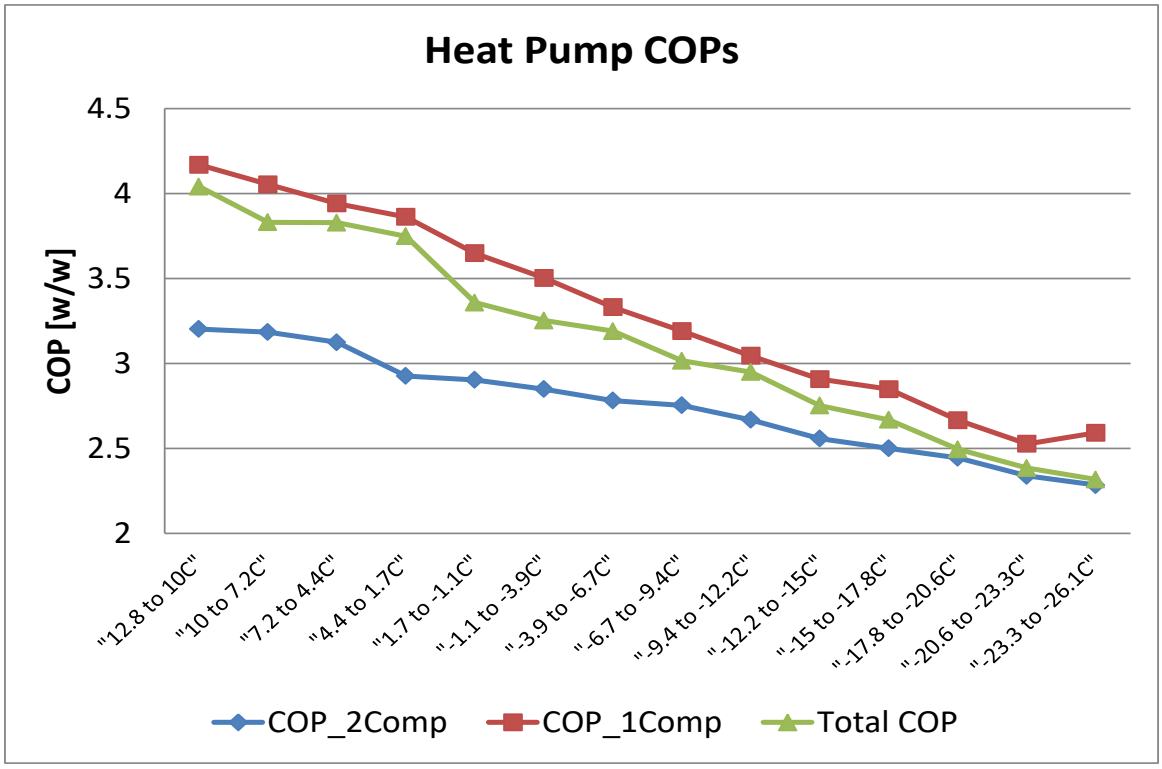

Figure 64: Field COPs in heating mode

In the three months of heating operation in 2015, the overall average field-measured COP was 3.16, compared to the 3.29 to 3.21 predicted ratings value for the AHRI 210/240 DHRmin and DHR-max load lines, respectively. Figure 65 compares heat energy delivered per temperature bin from the 2015 winter field data with that for a house having the AHRI 210/240 load characteristic in region IV. It can be seen that the test home in 2015 had a higher percentage of the total heating energy delivered at lower ambient temperatures because the 2015 winter in Ohio was much colder than usual.

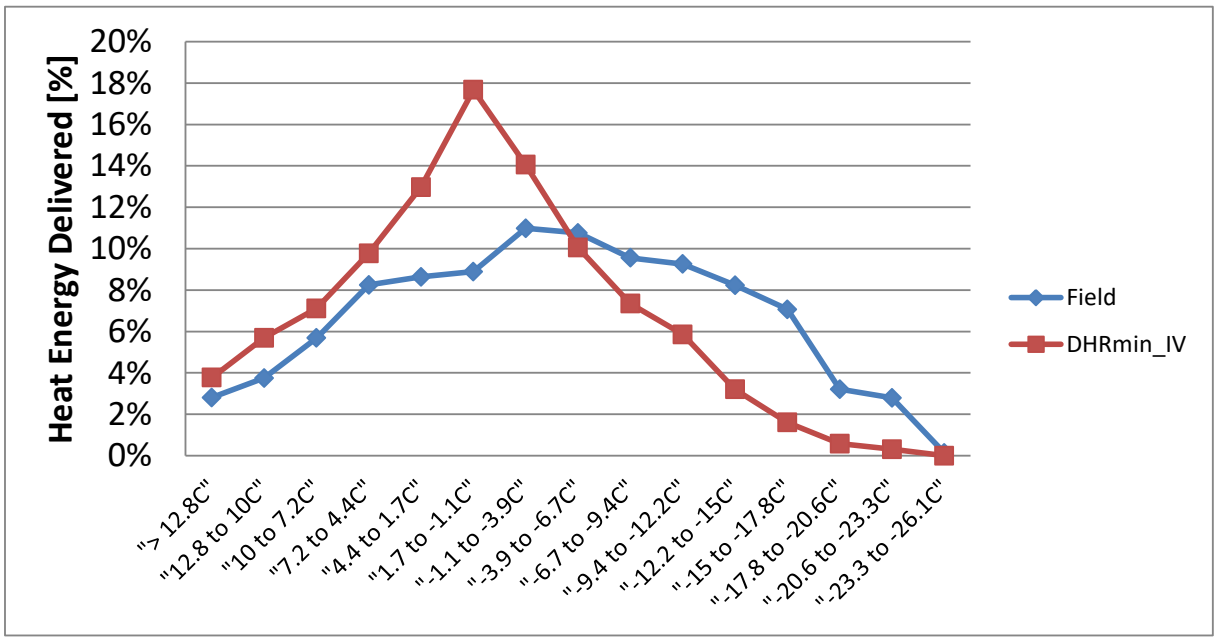

Figure 65: Field-measured heat energy delivered by bin in 2015 vs. AHRI 210/240 house load

Field Cooling Performance

Cooling season data for the CCHP prototype was recorded from June through August of 2015. Prior to the start of the cooling season the control board was adjusted to allow only single compressor operation with low-speed indoor blower operation. One-time measurement of the cooling mode indoor air flow rate using the "True Flow Grid" indicated an air flow quantity of 0.65 m^3/s (1380 CFM). This is in excellent agreement with the rated airflow of 0.65 m^3/s (1375 CFM) given in the air handler product literature.

Figure 66 shows average, delivered cooling capacities per outdoor temperature bin (air-side measurement). As the outdoor temperature increased from 15.6 to 23.9°C the cooling capacity increased due to the reduced cycling losses. As the temperature increased further the cooling capacity decreased due to increasing condensing temperature. For the 32.2°C to 35°C temperature bin, the field average capacity was right at 10.6 kW (3-ton).

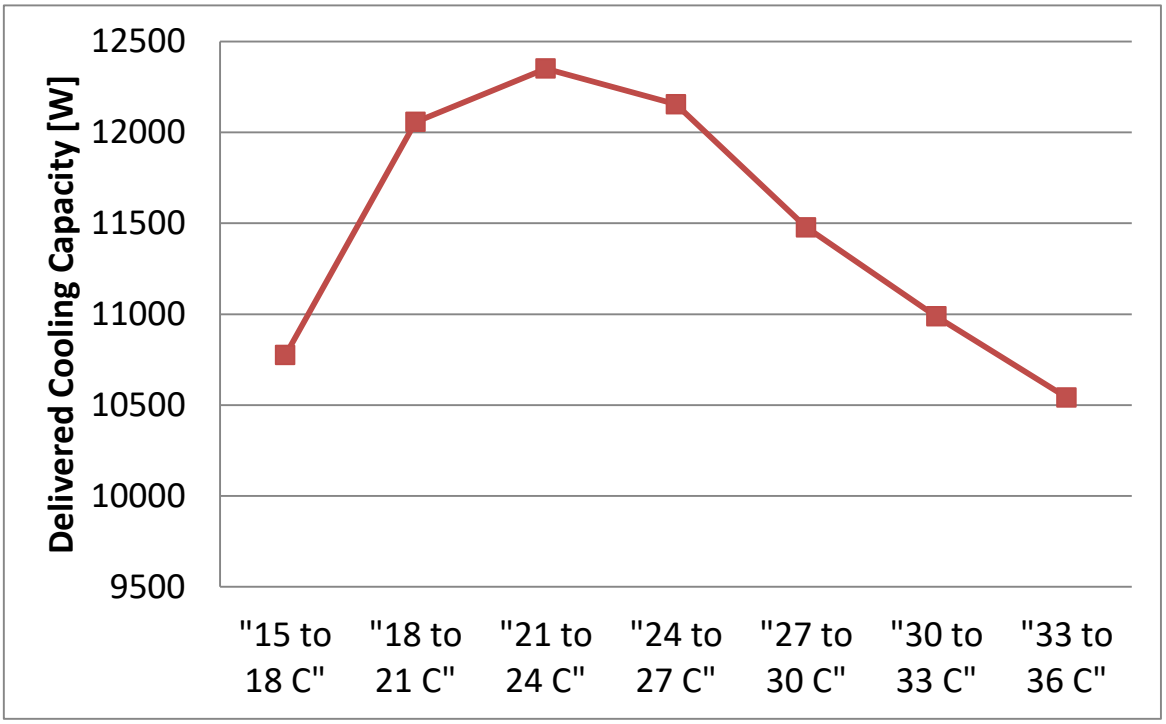

Figure 66: Delivered cooling capacities

As noted earlier, during the cooling season only single-compressor operation was permitted for the CCHP prototype. In this case, the indoor and outdoor heat exchangers, sized for the base 17.5 kW ASHP were oversized for the single compressor, thus leading to superior cooling performance. The averaged field measured COP over the test period was 5.2, with the return air temperature varying from 21.1 to 25.6°C, and an average ambient temperature of 25.6°C (78°F). Figure 67 below shows the field measured average COPs per temperature bin. It can be seen that for the highest temperature bin), the average field COP is 4.1.

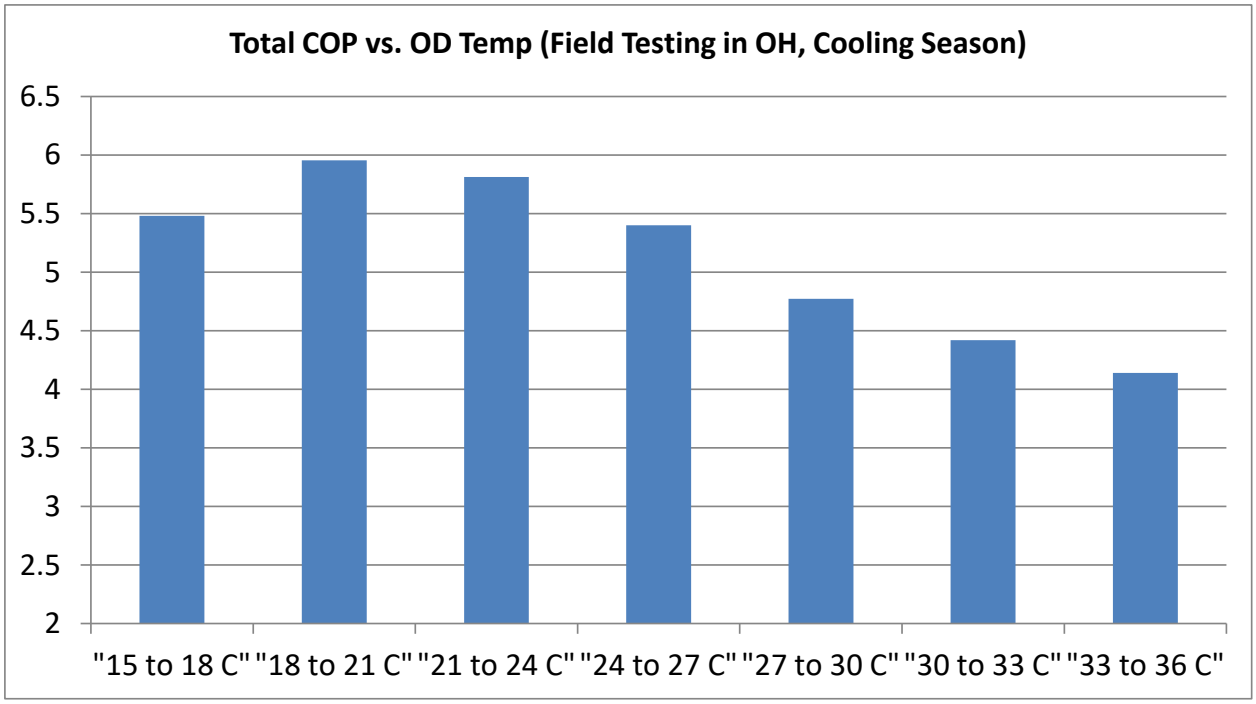

Figure 67: Field COPs in cooling mode

Comparison of Utility Billing Data before and After Installing the CCHP

Figure 68 compares monthly electricity billing data for about two years before and one year after installation of the prototype CCHP. Note here that the kWh from the electric bills has had 800 kWh in "base" consumption (due to lights, water heater, appliances, etc.) subtracted so that it represents the heat pump usage only. As shown in Figure 48 below, in comparison to the previous single-speed ASHP in the same house, >40% energy reduction was achieved during the coldest months with similar monthly average temperatures (around -6 to -7°C).

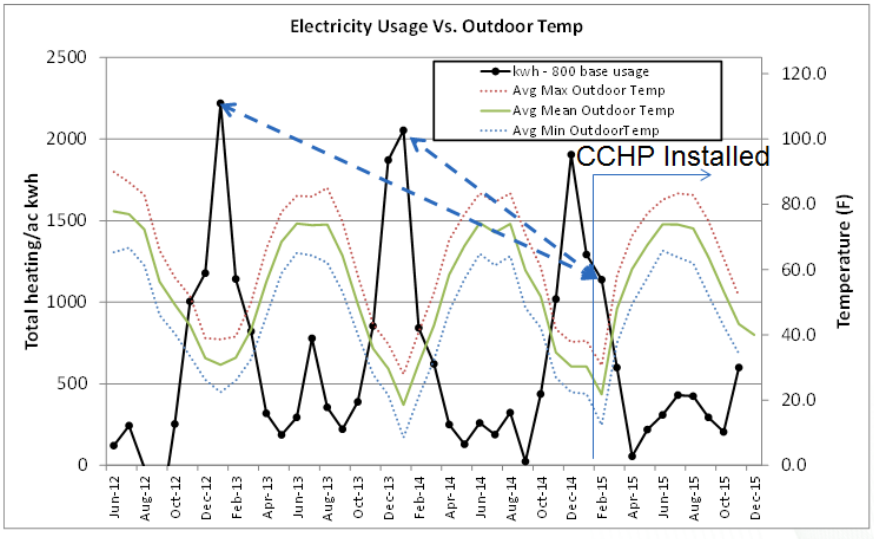

Figure 68: Comparing electric bills of the field testing home before/after installing the CCHP with tandem single-speed compressors.

Figure 69 compares the field measured kwh/day vs. outdoor temperature with similar data extracted from the monthly billing statements. It can be seen that the field data is very close to that from the two monthly electricity bills when the CCHP prototype was operating, which

indicates good field measurement accuracy. The field data indicate that the CCHP unit has lower average daily energy use at all temperatures with the savings increasing as the temperature drops.

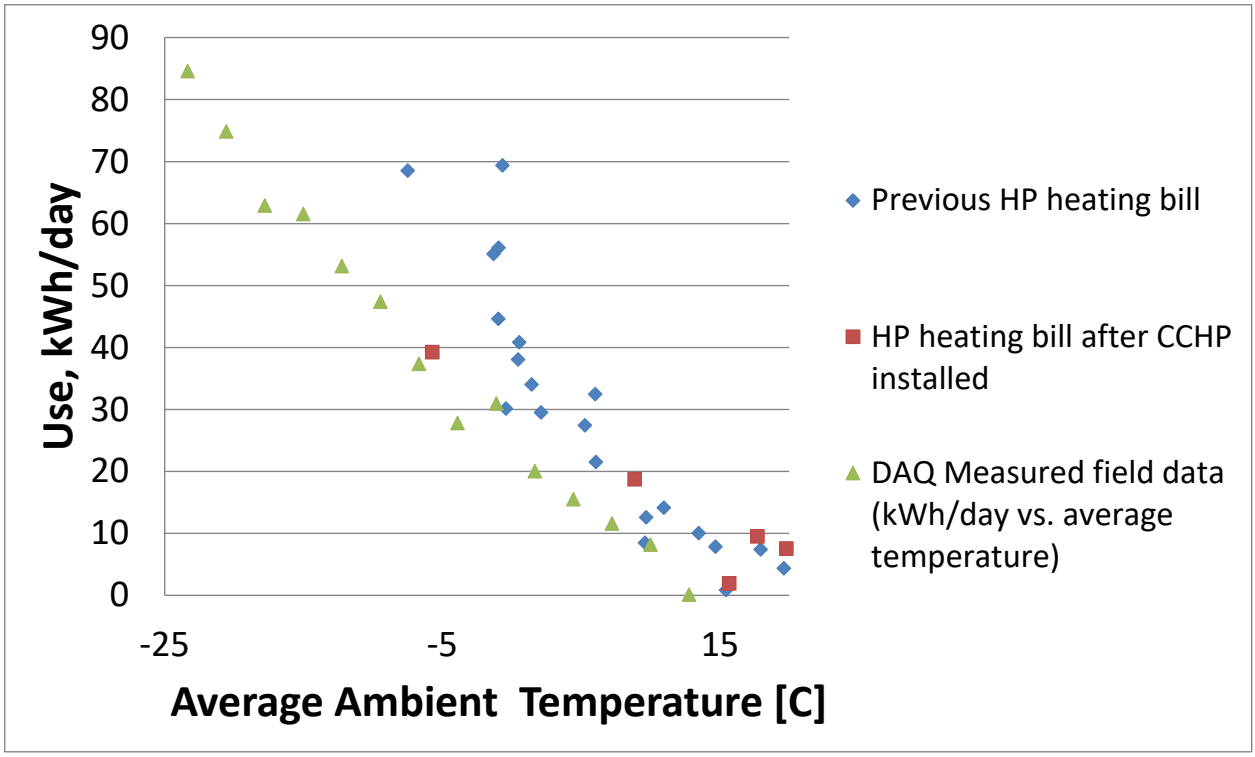

Figure 69: Overlay of the field testing data with the electricity bills

In Figure 68, it can also be seen that there are no apparent energy savings in the cooling months. This was due to a change in the family situation change --- the home owners had a new baby in the 2015 summer. So they set the thermostat to a lower temperature than they had used in previous summers and the heat pump ran more frequently.

Sensitivity Study of Field Heating Performance – Feb. – Apr. 2015 vs. Dec. 2015 – Jan. 2016

Before the project ended another set of heating data from December 2015 through January 2016 was collected. For this period the homeowner adopted a higher thermostat setting of 21.7°C, about 1.7°C higher than the previous heating season due to the new family member. In addition an outdoor new temperature controller was added to the CCHP system to prevent the second compressor from running when the ambient temperature was above -12.2°C.

Due to the higher thermostat setting, the return air temperatures to the CCHP in 2016 were consistently 4°F (2.2°C) higher than those in 2015 (Figure 70) leading to bigger heating loads per temperature bin in 2016, as illustrated in Figure 71. Consequently, the second compressor ran more frequently in 2016. As shown in Figure 72 in the temperature bin from -20°C to -17.8°C, the second compressor run time fraction was 88% in 2016 vs. ~40% in 2015 (Figure 59). On the other hand, the resistance heat did not operate in 2016. Thus, the prototype CCHP was able to fully meet the building heating load with the higher temperature setting.

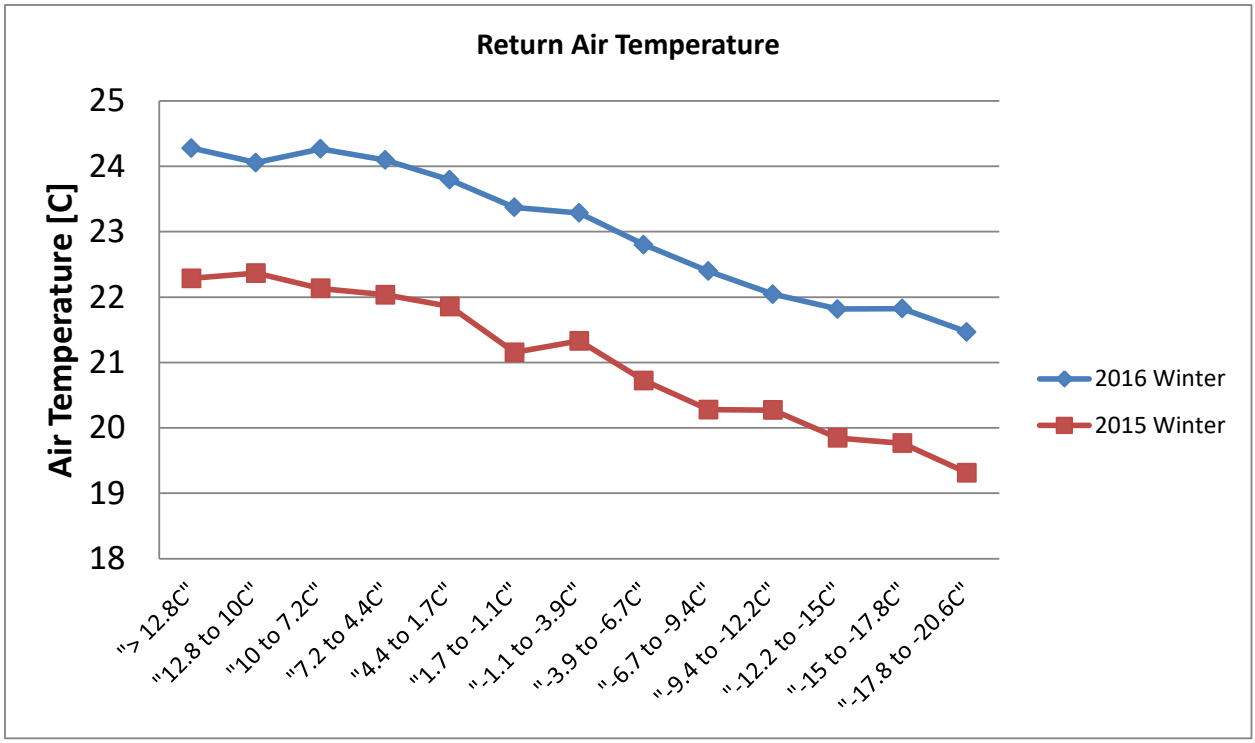

Figure 70: Return air temperatures in 2015 and 2016 heating seasons

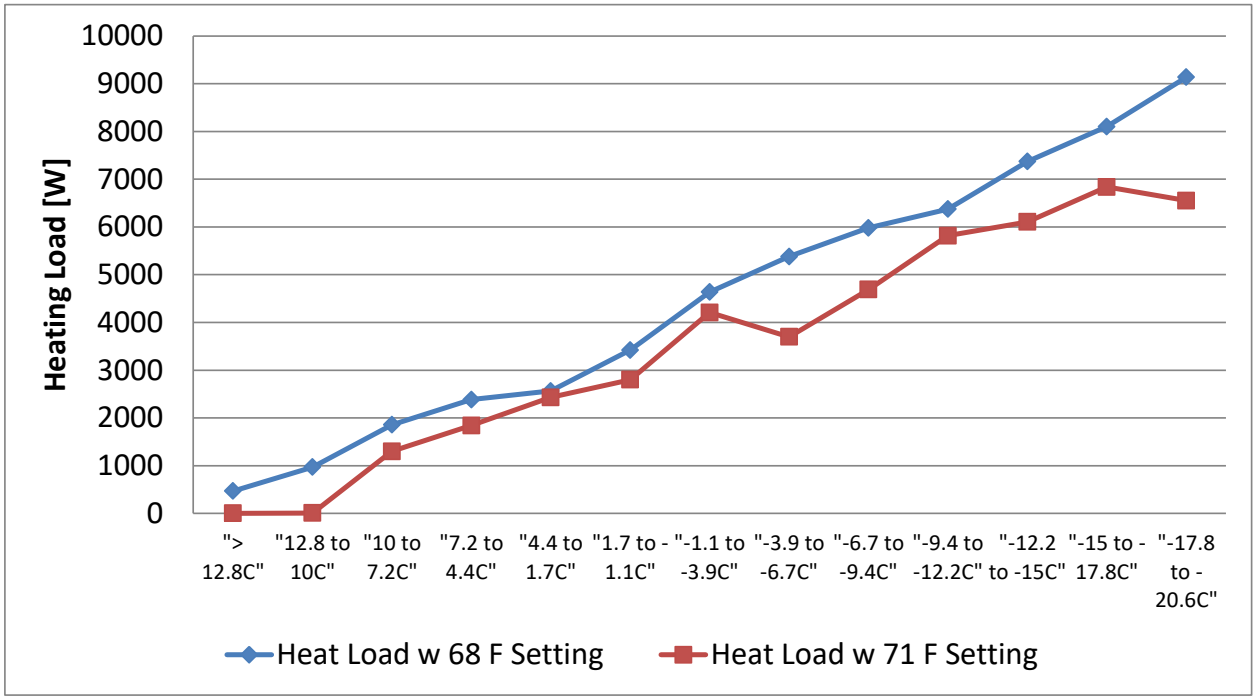

Figure 71: Comparing building heating loads in 2015 and 2016

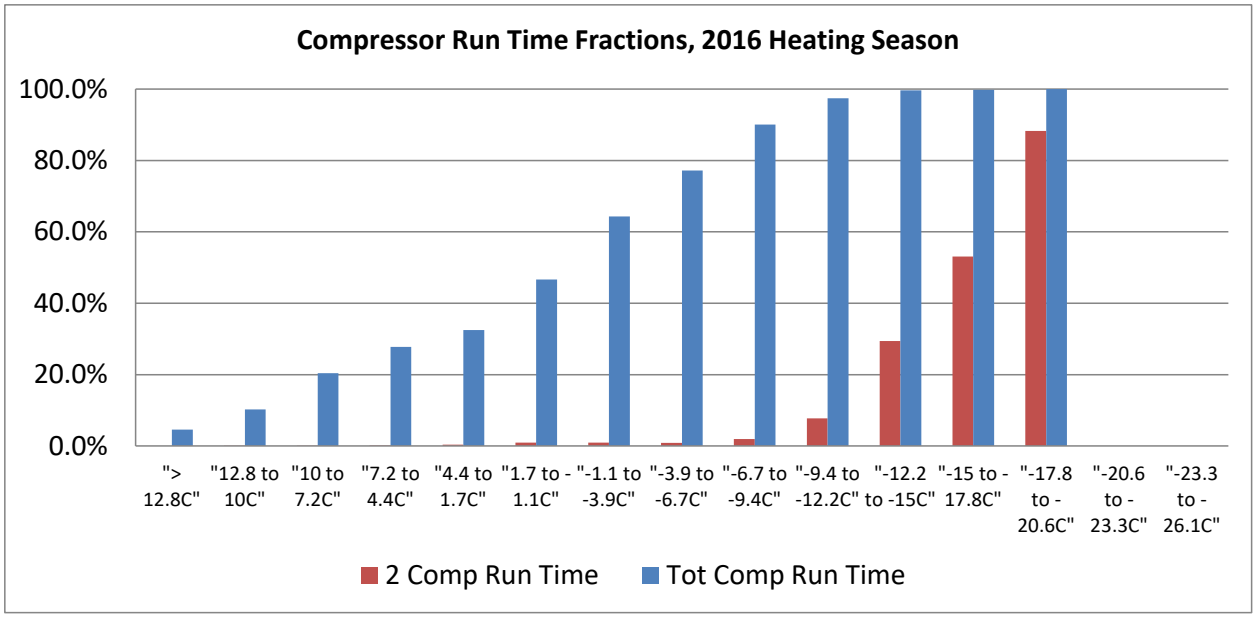

Figure 72: Compressor runtime fractions for the 2016 heating season

Figure 73 compares the average heat pump COPs per temperature bin for the 2015 and 2016 heating test periods. Because of the higher temperature setting and the ~2.2°C higher return air temperature to the CCHP, the heat pump heating COPs of 2016 are 10% to 15% lower than those of 2015. The field measured, averaged COP in 2016 was 2.84, or about 10% lower than the 2015 average of 3.16. For both test seasons combined, the overall average measured seasonal COP was about 3.00.

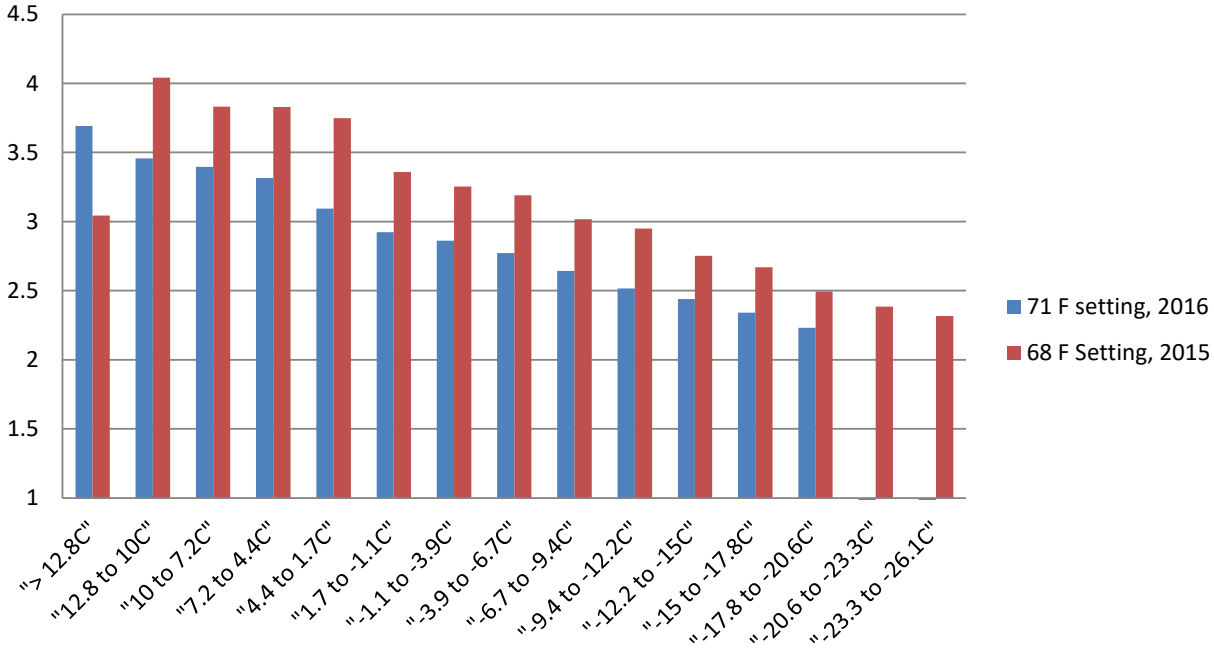

Figure 73: Average total COPs in 2015 and 2016

5.2 'Premium' Option - Equal Tandem, VI Compressors

It has been shown that application of vapor injection (VI) technology to a compressor can yield increased heating capacity and efficiency. A sample pair of tandem VI compressors was obtained from Emerson Climate Technologies and the performance evaluated in the

same breadboard unit as used for the 'more cost-effective' configuration. The tandem VI compressors were investigated in three scenarios. The first used a TXV to control the evaporator exit superheat (similar to the approach used in the field test tandem system discussed previously in Figure 55); the second (Figure 74) used an EXV to control the compressor discharge temperature; the third (Figure 75) coupled the discharge temperature control with a suction line heat exchanger (SLHX).

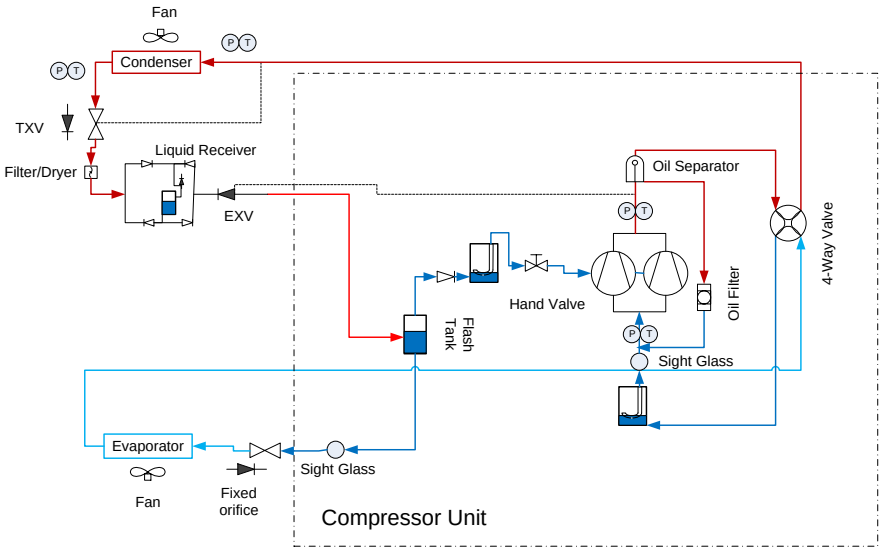

Figure 74: CCHP using tandem VI compressors and an EXV for discharge temperature control in heating mode

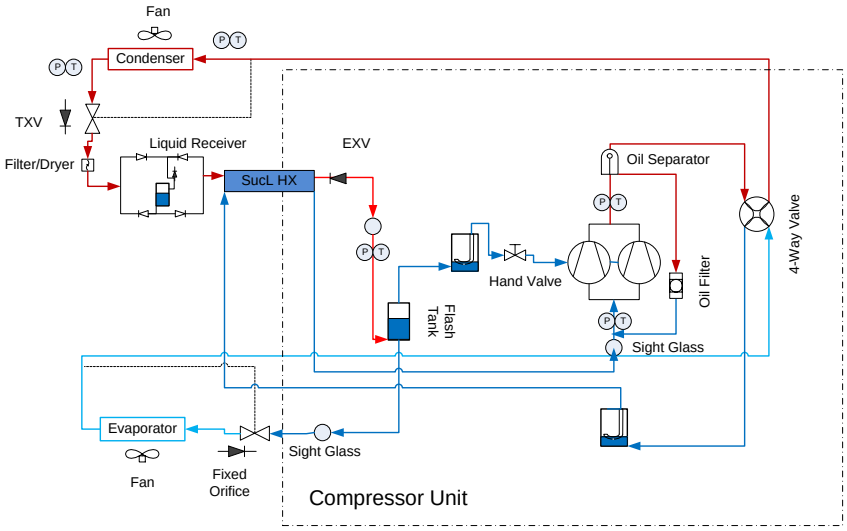

Figure 75: CCHP using tandem VI compressors, discharge temperature control and suction line heat exchanger

It was observed that the discharge temperature control approach led to better performance with the VI tandem pair than compressor suction superheat control. Tests of the lab breadboard prototype with and without the SLHX indicated no net improvements in COP or heating capacity. Use of an SLHX was observed to increase the compressor suction superheat degree and discharge temperature, which increased the heating capacity per unit refrigerant mass flow rate. However, the increased suction superheat also decreased the suction density, and reduced the compressor mass flow rate. In addition, the compressor efficiency appeared to decrease due to elevated suction and discharge temperatures. Consequently, neither capacity nor efficiency gain was observed with the SLHX so it was not considered further for the final design VI tandem prototype design.

The tandem VI compressor system configuration of Figure 74 achieved 5% better COPs than the tandem, single-speed heating-optimized system configuration of Figure 35 at various ambient conditions. It achieved an 88% heating capacity ratio and 2.0 COP at -25°C, and a 4.4 COP and 11.7 kW (40,000 Btu/h) capacity at the 8.3°C nominal rating condition. Figure 76 compares the heating capacities of the tandem single-speed compressors (heating optimized) and the tandem VI compressors, at two speed levels, as a function of the ambient temperature. Figure 77 compares the heating COPs. In Figure 76, DHRmax and DHRmin house load lines for the DOE Region V climate (e.g., U. S. cold region) are overlaid on the VI prototype capacity data. These indicate the potential for the CCHP prototypes to eliminate supplemental electric heat use in tight, well-insulated homes (aka DHRmin) in Region V.

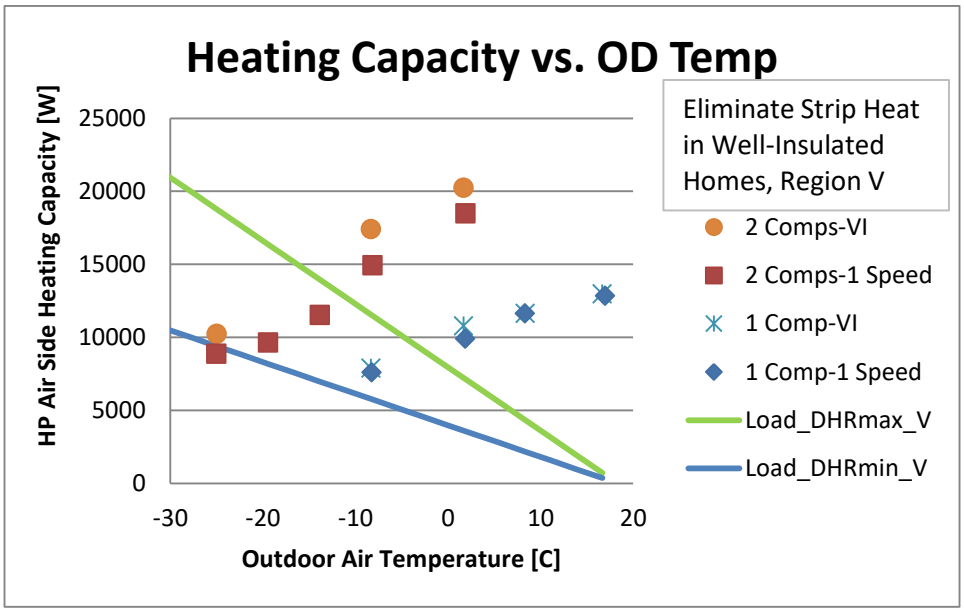

Figure 76: Heating capacity vs. ambient temperature, for tandem single-speed compressors and tandem VI compressors versus Region V house load lines

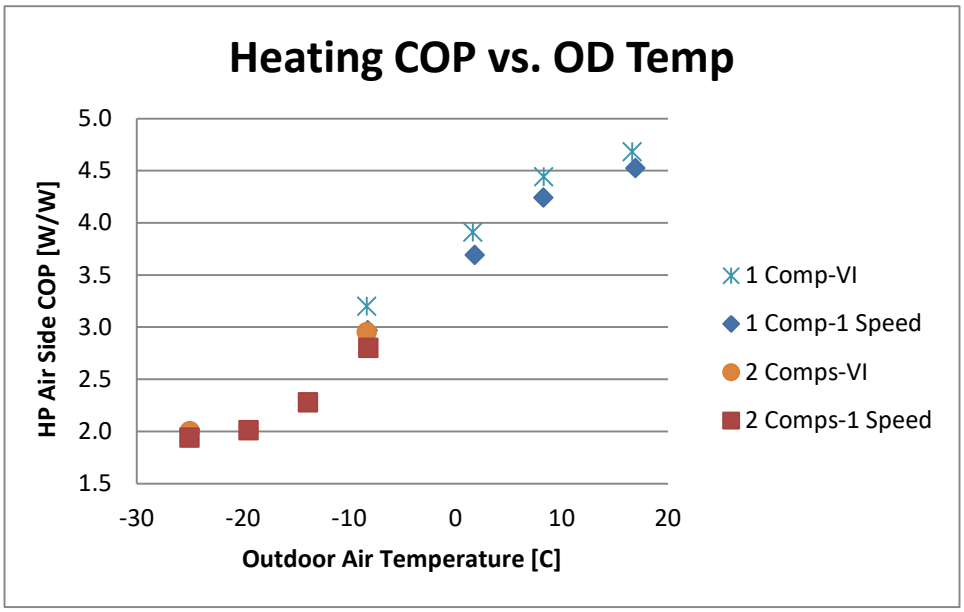

Figure 77: Heating COP vs. ambient temperature, for tandem single-speed compressors and tandem VI compressors

Table 12 reports the calculated SCOPhs (HSPFs) from the lab-measured data for the tandem VI compressor CCHP lab prototype with discharge temperature control for DOE climate regions IV and V. It is especially notable that the drop in SCOPh for the VI tandem design between the min and max heating load lines is less than 1% in Region IV and 5.4% in Region V. This indicates that this design maintains seasonal performance extremely well over the full range of house performance levels. As noted earlier, this performance is in contrast to much larger drops with higher heading loads for current ducted variable-speed units tested at ORNL (Rice et al, 2016). Figure 78 shows supply air temperature as a function of the ambient temperature. For this figure in the case of the tandem single-speed compressor system, the indoor air flow rate was set to Low for one-compressor operation. For two-compressor operation the indoor air flow rate was set to High when the ambient temperature ≥-8.3°C, and it was set to low, with the ambient temperature <-8.3°C, as to maintain a more comfortable supply air temperature. However, for the tandem VI compressor system, since it had higher heating capacity, the indoor air flow was always set at High when running two compressors. It can be seen that down to -25°C, both the tandem single-speed compressors and VI compressors were able to maintain supply air temperature higher than 31.7°C (89°F).

Table 11: Heating Seasonal Performance Factors of CCHPs using tandem VI compressors and discharge temperature control (per AHRI Standard 210/240)

Load	SCOPh (HSPF, Btu/Wh)
	Heating Season Ratings, Region: IV
DHRmin	3.47 (11.84)
DHRmax	3.46 (11.80)
	Heating Season Ratings, Region: V
DHRmin	3.13 (10.68)
DHRmax	2.96 (10.10)

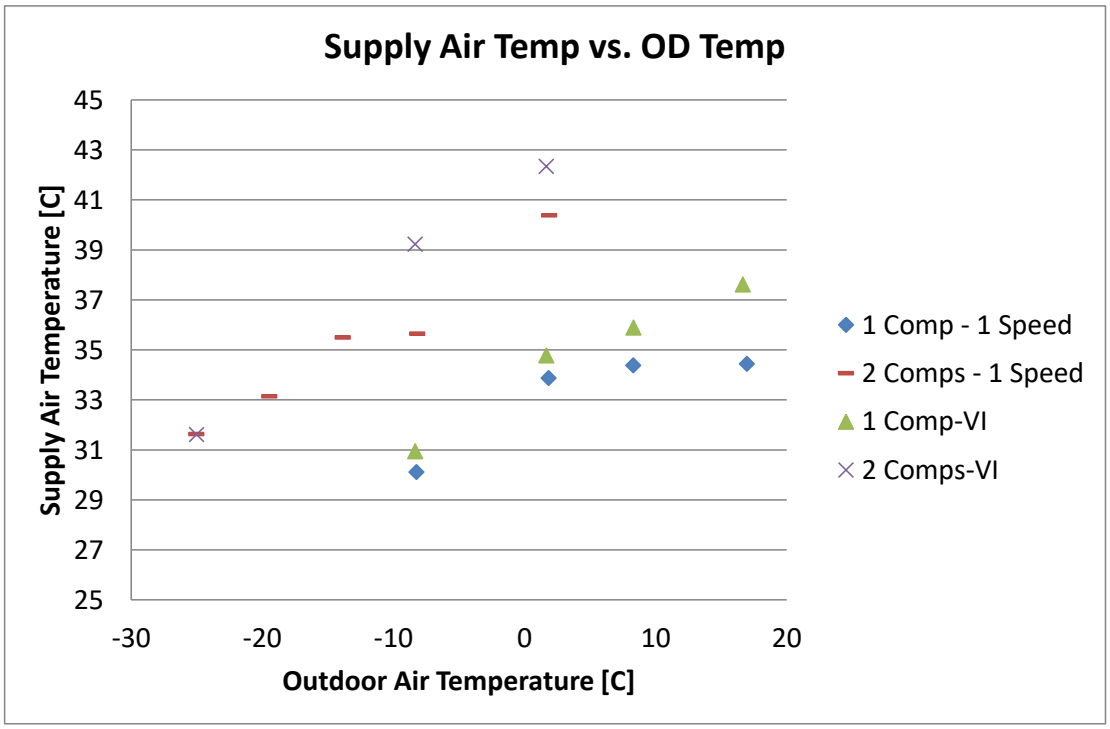

Figure 78: Supply air temperature vs. ambient temperature, for tandem single-speed compressors and tandem VI compressors

A second CCHP field test prototype system has been constructed based on the tandem VI compressor lab prototype design of Figure 74 starting from a baseline 17.5 kW single-speed ASHP. It was installed at the Cold Climate Housing Research Center in Fairbanks, AK in May 2016 and field testing began in June 2016. Shortly after testing began it became apparent that the electric power supply system experienced a number of power outages causing loss of data. After installing an uninterruptible power supply (UPS) system and monitoring, further computer loss of data was minimized.

The 2016/2017 heating season began in the latter part of August. For August through September the unit ran in low stage (one compressor) almost exclusively, matching the building heating load adequately. Outdoor temperatures ranged from 15.6°C down to -9.4°C (60°F to 15°F). It was observed that this CCHP required almost no defrost operation during this period (defrost accounting for <1% of the total heat pump run time). With only one compressor in operation, the outdoor heat exchanger is oversized leading to slow frost accumulation.

In October, however, when ambient temperatures went down to 0°F, two-compressor operation occurred more frequently. A fault occurred in the defrost control algorithm so that defrost operation failed to initiate and frost covered the entire outdoor coil. After applying a fix to the algorithm, the system operated normally in all modes. Figure 79 shows average heating COPs for each temperature bin for September 2016 through March 2017 with minimum outdoor temperatures as low as -34.4°C (-30°F). The CCHP demonstrated average COPs >1.8 with space heating capacity >75% of the rated capacity (10.6 kW @ 8.33°C).

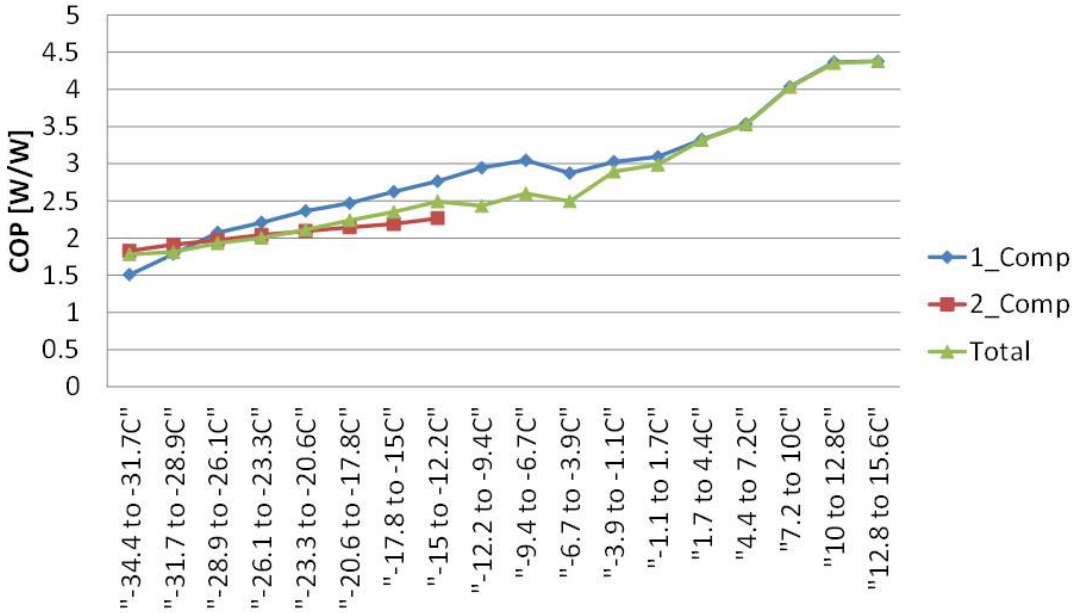

Figure 79: Field-measured average space heating COP vs. ambient temperature bin, for tandem VI compressor CCHP field test unit

Figure 80 shows the field-measured average delivered heating capacities for each outdoor temperature bin for both single and dual-compressor operation. At the lowest temperatures bin of -34.4°C to -31.7°C (about -30°F to -25°F), with two compressors, the average delivered capacity was 7.9 kW (27000 Btu/h). This is 75% of the nominal rated heating capacity (36000 Btu/h (10.6 kW)) of the “starting point” heat pump unit at 8.3°C (47°F). Note that the average bin heating capacity decreases as the ambient temperature drops to ~15°C (only one compressor operating for majority of the time). As the outdoor temperature decreased from -15°C to -35°C, two-compressor operation took place for an increasing

portion of the time with the average bin operating heating capacity (rate) increasing with temperature as the run time for the second compressor increased as needed to match the increasing building load.

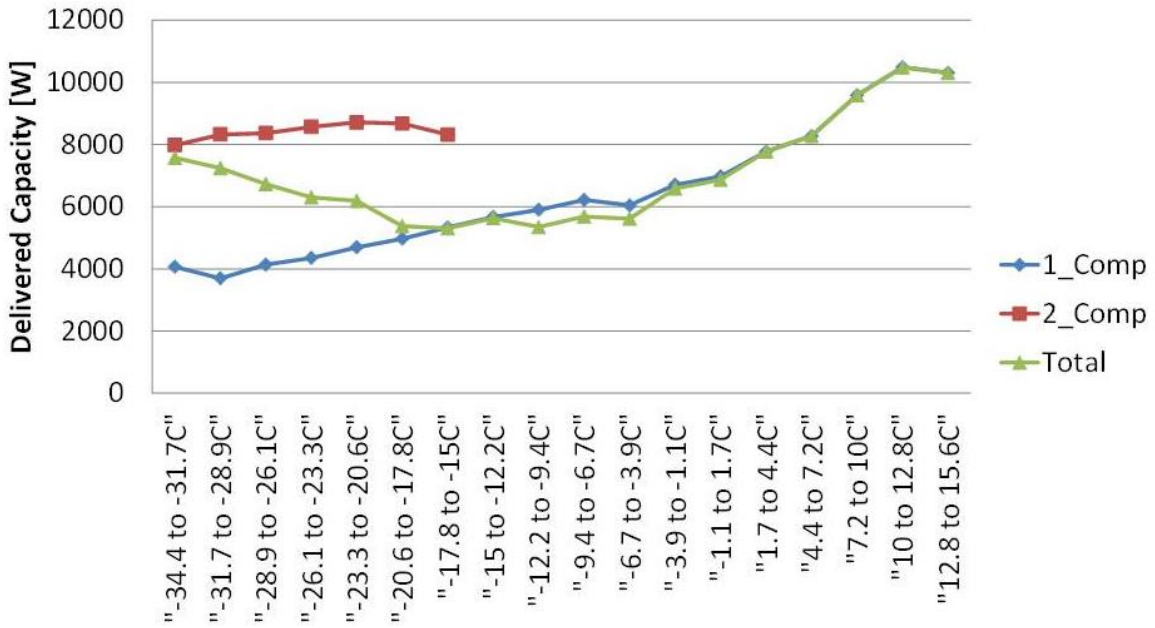

Figure 80: Field-measured average delivered space heating capacity vs. ambient temperature bin, for tandem VI compressor CCHP field test unit

Full monitored field performance results for the VI tandem system will be reported after the planned one-year field test is concluded.

6 REFERENCES

AHRI 2008. ANSI/AHRI Standard 210/240-2008, "Performance Rating of Unitary Air-Conditioning and Air Source Heat Pump Equipment," Air-Conditioning, Heating, and Refrigeration Institute, Arlington, VA, USA.

Baxter, V. D., E. A. Groll, O. A. Abdelaziz, B. Shen, G. C. Groff, K. Sikes, and G. Khowailed. 2013. IEA HPP Annex 41 – Cold Climate Heat Pumps: Task 1 Report – Literature and Technology Review – United States, Oak Ridge National Laboratory, Report Number - ORNL/TM-2013/472, October.

Bell I. H., E. A. Groll, and J. E. Braun. 2011. "Performance of Vapor Compression Systems with Compressor Oil Flooding and Regeneration," *International Journal of Refrigeration*, Vol. 34, No. 1, pp. 225-233.

Bertsch S. S. and E. A. Groll. 2006. "Air Source Heat Pump for Northern Climates Part I: Simulation of Different Heat Pump Cycles," Proceedings of the 11th International Refrigeration and Air Conditioning Conference at Purdue.

Bertsch S. S. and E. A. Groll. 2008. "Two-stage air-source heat pump for residential heating and cooling applications in northern US climates," *International Journal of Refrigeration*, Vol. 31(7), pp. 1282-1292.

Caskey S. L. 2013. "Cold Climate Field Test Analysis of an Air-Source Heat Pump with Two-Stage Compression and Economizing," Master's Thesis, Purdue University, Ray W. Herrick Laboratories, West Lafayette, IN.

Liegeois O., Winandy E., 2008: Scroll Compressors for Dedicated Heat Pumps: Development and Performance Comparison, International Compressor Engineering Conference at Purdue University, Paper 1906, July 14 – July 17, 2008.

Ramaraj, S., Braun, J.E., Groll, E.A, and Horton, W.T. (2016). “Performance analysis of liquid flooded compression with regeneration for cold climate heat pumps,” Int’l J. Refrigeration, Vol. 68, August 2016, Pages 50–58.

Rice, C. K., B. Shen, and S. S. Shrestha, 2016. *Revised Heating Load Line Analysis: Addendum to ORNL/TM-2015/281*, ORNL/TM-2016/293, UT-Battelle LLC, Oak Ridge National Laboratory, July.

Shen, B., O. A. Abdelaziz, and C. K. Rice. 2014. “Compressor Selection and Equipment Sizing for Cold Climate Heat Pumps,” paper no. P.6.11 in the Proceedings of the 11th IEA Heat Pump Conference 2014, May 12-16 2014, Montréal (Québec) Canada.

Yang, B., Blatchley, T., Bach, C.K., Braun, J.E., Horton, W.T., and Groll, E.A., “Application of Oil Flooded Compression with Regeneration to a Packaged Heat Pump System,” Proc. of the 15th Int’l Refrig. and Air Cond. Conf. at Purdue, Paper 2631, Purdue University, West Lafayette, IN, July 14-17, 2014, 10 pages.